Electronic Thesis and Dissertation Repository

8-11-2020 1:00 PM

Foliage Type Controls Mercury Input, Storage, and Release in the Boreal Forest

Madelaine J R Anderson, *The University of Western Ontario*

Supervisor: Branfireun, Brian A., *The University of Western Ontario*
Joint Supervisor: Lindo, Zoē, *The University of Western Ontario*
A thesis submitted in partial fulfillment of the requirements for the Master of Science degree in Biology
© Madelaine J R Anderson 2020

Follow this and additional works at: https://ir.lib.uwo.ca/etd

Part of the Biochemistry Commons, and the Forest Biology Commons

Abstract

Mercury (Hg) is a naturally occurring element with a complex biogeochemical cycle. Forests act as net sinks for both carbon (C) and Hg as foliage accumulates Hg with time. Litterfall represents a main input of C and Hg into forest soils. My aim was to investigate how foliage type (coniferous, deciduous) governs the input of Hg into forests with a field-based study that measured Hg accumulation over a growing season, and then investigate the storage and release of Hg from foliar tissues into soil with a laboratory-based incubation experiment. Results from the field-based study demonstrate deciduous leaves have more linear Hg uptake rates than conifer needles after the first growing season. Results from the incubation study suggest that Hg release is a function of decomposition influenced by litter type. Understanding how vegetation influences Hg cycles in forests is important for understanding how climate change will impact forest Hg cycles.

Keywords

Summary for Lay Audience

Mercury (Hg) is a metal that can be found everywhere in the natural environment. The atmosphere transports gaseous Hg globally, which can then be incorporated into foliage. As such, Hg accumulates in vegetation (e.g. leaves and needles) over time, and enters the soil system when this plant tissues die or senesce, such as during autumn litterfall events. The overall goal of my thesis was to investigate the controls on Hg input, storage, and release in tree vegetation in the boreal forest. My thesis first investigated the rates of Hg accumulation in two common boreal forest tree types representing conifer needles (black spruce) and deciduous leaves (white birch). The deciduous leaves accumulated Hg relatively linearly over the growing season, however the conifer needles did not, probably because deciduous leave display a more continuous growth pattern. My second objective was to investigate how Hg is released from leaves and needles into soil during decomposition and the influence of temperature on this release. I conducted a laboratory-based experiment to monitor Hg concentrations that were released from the leaves and needles for three months. My results suggest that litter type controls decomposition and subsequent Hg release rates from leaves and needles. Overall, because of a higher rate of Hg accumulation, larger annual litter inputs, and more rapid release from the tissues, deciduous leaves cycle Hg through forest systems at different rates than coniferous needles. Understanding Hg flux (uptake and release) in forest systems based on dominant vegetation type is important for forecasting how Hg cycles will change and lead to better predictions for the recovery times of contaminated watersheds. My results are significant because the dominate tree type in forests is changing as deciduous tree ranges shift northward under climate warming. Coupled with an increase in temperature, the implication is a greater Hg flux (uptake and release) in the boreal forest in the near future.

Co-Authorship Statement

The two experimental chapters (Ch. 2, Ch. 3) of this thesis are planned manuscripts for submission to peer-reviewed journals. Both chapters 2 and 3 were developed by Madelaine Anderson, Dr. Zoë Lindo, and Dr. Brian A. Branfireun. Manuscripts from this thesis will be developed by Anderson, Lindo, and Branfireun.

Acknowledgments

Table of Contents

List of Tables

List of Figures

List of Appendices

Chapter 1

1 Introduction

1.1 Mercury as a global pollutant

Mercury (Hg) is a trace element that is found ubiquitously in air, soil, water and biota, and is the only metal that can be found in all three phases at standard temperature and pressure. In solid, liquid, and gaseous phases it can be found in three oxidation phases: Hg(0), Hg(I), and Hg(II) (Krabbenhoft *et al.*, 2005). Mercury enters and circulates in the atmosphere in its gaseous form from both natural and anthropogenic sources. Natural sources of gaseous Hg include volcanos, volatilization from mercuriferous minerals, and forest fires. Since the industrial revolution, anthropogenic sources of Hg have increased concentrations in the atmosphere by between two and three times (United Nations Environment Programme [UNEP], 2018), with main sources historically being coal combustion, metal smelting, incinerators, and cement production (UNEP, 2018). The fugitive release (i.e. unintentional release) of gaseous Hg from artisanal small-scale gold mining is now the largest anthropogenic source of Hg to the atmosphere (UNEP, 2018).

North American background atmospheric Hg concentrations are generally in the range of 1.2-1.3 ng m^{-3} (Zhang *et al.*, 2016). Speciation of Hg in the atmosphere is complex, and an important control on its residence time and deposition pathway. The dominant species is gaseous elemental Hg (GEM, Hg(0)$_g$), which generally makes up over 95% of total gaseous Hg in the atmosphere (Schroeder and Munthe, 1998, Driscoll *et al.*, 2013). With a residence time of 6-9 months, Hg(0)$_g$ can circulate hemispherically, making Hg truly a global pollutant (Lindberg *et al.*, 2007). Other forms of Hg in the atmosphere including gaseous oxidized Hg (GOM, Hg(II)$_g$) and particle bound Hg (PBM, Hg(II)$_s$) are more rapidly deposited, usually associated with local emission sources, and make up a much smaller fraction of total atmospheric Hg (Schroeder and Munthe, 1998, Driscoll *et al.*, 2013).

1.2   Mercury accumulation and sequestration in forests

As Hg cycles in the atmosphere it can be deposited on surfaces including on vegetation and soils. Forests as a whole are considered net sinks for atmospheric Hg as the metal accumulates in both soil and vegetation (Stamenkovic *et al*., 2008, Obrist *et al*., 2011, Demers *et al*., 2013). Foliage in forests present large surface areas with high aerodynamic resistance compared to other environments like open fields making the canopy a significant sink for atmospheric Hg (Zhang *et al*., 2009). Some Hg deposition is in the form of $Hg(II)_s$ or $Hg(II)_g$, which are deposited on the cuticle of leaves, although both of these forms are associated with local sources and in pristine locations contribute to a small portion of overall atmospheric Hg and subsequent Hg in leaf tissues (Millhollen *et al*., 2006, Wright *et al*., 2016). Due to the prevalence of $Hg(0)_g$ in the atmosphere and uptake processes, most Hg in leaves is $Hg(0)_g$ in origin (Millhollen *et al*., 2006, Wright *et al*., 2016). Processes such as stomatal uptake are responsible for the exchange and subsequent incorporation of Hg into foliage tissues (Stamenkovic and Gustin, 2009). While some of this Hg is incorporated into leaf tissue as Hg(II), reduced back to Hg(0), and then reemitted to the atmosphere (Yuan *et al*., 2019), overall Hg accumulates in foliage tissues with time (Grigal, 2002, Rea *et al*., 2002, Assad *et al*., 2016).

There are strong seasonal trends in atmospheric $Hg(0)_g$ concentrations with the highest concentrations found in winter and lowest occurring in the summer months in the northern hemisphere. Previous hypotheses to explain this attributed increased fossil fuel combustion and energy consumption in winter (a main Hg source to the atmosphere) and increased oxidation of $Hg(0)_g$ in summer, but a recent study linked the seasonal growth of vegetation with $Hg(0)_g$ concentrations (Jiskra *et al*., 2018). Jiskra *et al*. (2018) concluded terrestrial vegetation acts as a global pump for $Hg(0)_g$, which contributes not only to lower levels during the summer growing season but has also contributed to an overall reduction in atmospheric concentrations over the last 20 years due to forest growth. Therefore, the future of global carbon (C) stocks may be intimately linked to Hg atmospheric concentrations (Obrist, 2007, Jiskra *et al*., 2018).

At the end of the growing season for deciduous tree species and on variable yearly cycles for conifers, senescence of foliage that has accumulated Hg ensues. Timing of senescence

depends on many factors including species, climate, and geography, and it can be triggered by both endogenous and exogenous factors (Lim *et al.*, 2007). During senescence plants resorb nutrients from the leaf to put towards other processes like seed development. This resorption is coupled with the turnover of chlorophyll pigment that causes many green leaves to turn yellow and brown (Kikuzawa and Lechowicz, 2011). While the cycling of nutrients in plants is understood, what remains unclear is the fate of the Hg in leaf tissue during these degenerative processes. Following senescence, leaves and needles abscise from the branch and the collective process is called litterfall. Different biomes experience peaks in litterfall at different times of the year with the boreal forest experiencing a peak in autumn (Zhang *et al.*, 2014). This litterfall event is mainly triggered by declining solar radiation (Zhang *et al.*, 2014) and lower temperatures characteristic of northern latitudes (Kramer *et al.*, 2000).

The boreal zone covers approximately 1.890 billion hectares globally, of which approximately 28% is located in Canada (Brant *et al.*, 2013). The boreal ecozone has been defined as the broad, circumpolar vegetation zone that occurs at northern latitudes, covered primarily with forests and other wooded lands (Brandt, 2009). Due to its northern latitudes, this ecozone is projected to experience more intense climate warming than biomes at southern latitudes (Price *et al.*, 2013). The majority of research focusing on forest Hg cycles has been conducted in forests that have atmospheric Hg concentrations several times higher than the boreal forest (e.g. Zhou *et al.*, 2019 and Du *et al.*, 2019 in China; Barquero *et al.*, 2019 in Spain) and in other forest types (e.g. Ma *et al.*, 2017 in subtropical forest; Demers *et al.*, 2007 in temperate forest) that experience different climates and species composition, and thus different patterns of carbon cycling. Because of the higher overall Hg concentrations and larger portion of atmospheric Hg made up of $Hg(II)_s$ and $Hg(II)_g$ present in studies conducted in these areas, and because of differing C cycling patterns, it is difficult to determine how the processes of Hg cycling the boreal forest differs from other forest systems. These factors around atmospheric Hg variation and C cycling make understanding present Hg cycling in the boreal forest important to contribute to current gaps in the literature as well as understanding how this the Hg cycle for this expansive zone will be impacted by climate change.

1.3   Decomposition and mercury inputs to soil systems

Mercury's complex biogeochemical cycle is tightly linked with C cycling in catchments, as Hg in forest ecosystems is largely sequestered with organic matter. Litterfall is the main input of C and nutrients to forest soils and plays an important role in global C cycling (Cornwell *et al*., 2008). Because foliage accumulates Hg over time, in the autumn when leaves and some needles drop from trees, litterfall also represents a major input of Hg into forest soils (Grigal, 2002, Rea *et al*., 2002, Assad *et al*., 2016). The input of both C and Hg into the organic horizons and the soil pool is governed by decomposition processes that break down organic matter. General trends in decomposition processes are observed on global scales across different biomes, and these provide models with estimations of decomposition rates although there are still considerable knowledge gaps surrounding decomposition. Similarly, while litterfall is understood to be a main input of Hg into forest soils there is little research into its release from litter tissues into soil organic matter (SOM). Overall, climate exerts a large control on decomposition rate at broad geographic scales, while litter quality, commonly reported as C to nitrogen (N) ratio (C:N), N content, and lignin content, better explains rate variation at a forest stand level (Berg *et al*., 1993).

Decomposition processes occur over a range of timescales, but follow defined phases as fresh, plant materials are incorporated into the soil system. It remains unclear if it is a continuous process, or at what point Hg is released from litter tissues. Carbon compounds can be lost from the soil system via heterotrophic respiration of the microbial community, leaching, and erosion, while N compounds can similarly be lost through leaching and denitrification. Carbon compounds can become stabilized (i.e. material that resists further transformation and decreases loss of C) in soils through microbial processing and through the formation of organo-mineral complexes (Cotrufo *et al*., 2013, Lehmann and Kleber, 2015). However, soil C can also be destabilized (increase in losses of C) during decomposition (Sollins *et al*., 1996), and there remains uncertainty around the specific factors that govern whether or not plant-derived C is directed into the stable SOM pool or is re-mineralized into carbon dioxide. Different models propose decomposition and SOM formation at different time scales and rates (Lehmann and Kleber, 2015), and also link

the above ground (plants) and below ground (microbes) communities, and their interactions, to these controls on decomposition (Wardle, 2004). Studies that have examined Hg concentration and distribution based on soil horizon have consistently observed the highest Hg concentrations in the upper litter and organic horizons (e.g. Juillerat *et al*., 2012, Obrist *et al*., 2012, Blackwell and Driscoll, 2015), suggesting the Hg is derived from foliage and can be flushed from the litter pool before migrating to lower horizons.

The accumulation of SOM in soil depends not only on input amounts but also the quality of the input and rate of decomposition (Berg *et al*., 2001). As foliage type influences Hg accumulation before litterfall, organic tissues fall to the ground with different Hg concentrations. Litter type is then a main control of decomposition and likely influences the rate and overall amount of Hg released from these tissues. Ultimately, the processes that dominate in a system are influenced by many direct (such as microbial activity or soil particle aggregation) and indirect controls (such as pH or temperature) (Sollins *et al*., 1996). Together, with the accessibility of the compounds and their recalcitrance, these factors dictate the interactions between C compounds and the microbial community that ultimately breaks downs litter into SOM (Sollins *et al*., 1996). Dissolved organic matter (DOM) (i.e. soluble organic molecules < 0.45 μm) is also a product of decomposition and plays a major role in the transport of pollutants, including Hg, which Hg binds strongly to (Kalbitz *et al*., 2000, Ravichandran, 2004, Jiang *et al*., 2015). Conditions that results in enhanced mineralization and production of DOM (i.e. decomposition) could facilitate the transport of Hg from forest soil pools to downstream environments.

It is well established that litterfall is a main input of Hg into forest soils (Demers *et al*., 2007, Bushey *et al*., 2008, Du *et al*., 2019) but overall Hg dynamics within the forest ecosystem have knowledge gaps. The most mechanistic Hg flux model at a forest stand scale is Demers *et al*. (2007) who attempted to track Hg fluxes in deciduous and coniferous Adirondack forests. Demers *et al*. (2007), as others (e.g. Rea *et al*., 2000, Risch *et al*., 2012), found throughfall — deposited Hg on leaves that is washed off during precipitation events and then falls to the ground — to be the other major input of Hg into forest soil. Demers *et al*. (2007) also found throughfall to be more important in

coniferous dominated forests, highlighting a need for further research in different forest types. This is consistent with a 2012 study by Fisher and Wolfe that found throughfall to have greater Hg concentrations in conifer-dominated forests. While throughfall and litterfall are the major sources of Hg to soil system, there is a gap in the literature on the processes governing accumulation before litterfall and the subsequent storage and release of Hg from litter into forest soils.

1.4   Climate change implications for forest mercury cycles

Finally, both Hg and C cycling will be widely impacted by a changing climate. Increased atmospheric temperatures are expected to weaken global atmospheric Hg circulation and because the majority of anthropogenic Hg emissions are distant from the boreal forest, atmospheric concentrations are likely to change (Krabbenhoft and Sunderland, 2013, UNEP, 2018). Land use, technology, and energy industry change will also alter anthropogenic emissions Hg cycles, with estimates of Hg emissions projected to either increase or decrease by 2050 depending largely on the future energy sector in Asia (Streets *et al*., 2009, Krabbenhoft and Sunderland, 2013). There are also projected to be additional inputs from increases in forest fires and increased Hg evasion from the ocean further complicating Hg emissions forecasts (Krabbenhoft and Sunderland, 2013). These contribute to uncertain feedbacks on the fate of Hg globally as well as in forest ecosystems (Obrist *et al*., 2018).

Similarly, shifting plant communities and predicted increased rates of decomposition will alter C and Hg cycling. Specifically, for the boreal forest, it is widely anticipated that climate change (i.e. increased global temperatures) will lead to a plant species composition shift as deciduous trees expand their range northward (Cramer *et al*., 2001, McKenney *et al*., 2007, 2011). As Hg uptake rates in foliage are different depending on tree type and species this could change Hg and C inputs into the soil. A shift to deciduous dominated species would also change the quantity and quality of annual litter inputs into forest soils, which the fate of Hg is closely related to. Finally, decomposition rates will change with increasing temperatures and changing precipitation regimes in the boreal forest (Trumbore, 1997, Soja *et al*., 2007) so the residence time of Hg in the soil may be impacted.

1.5 Thesis objectives and rationales

Because Hg is intimately linked with vegetation, decomposition processes and soil C, it is important to understand the relationship between soil C and SOM-bound Hg, and how climate change will impact C and Hg cycling together. There remains uncertainty around the accumulation of Hg in foliage as well as the patterns of Hg release from litter into forest soils, especially for the boreal zone as much of the literature of Hg cycling in forests are in other ecozones. In this thesis I investigate Hg accumulation in tree needle and leaf tissues over a summer growing season, and the subsequent dynamics of Hg release from coniferous and deciduous tissues into soils for the southern boreal forest. The objectives of my thesis were to:

1. Quantify plant tissue Hg accumulation patterns over one growing season based on tree type (deciduous; coniferous) and to determine whether foliar uptake of $Hg(0)_g$ is an active or passive process by comparing tissue levels to established passive air samplers for atmospheric Hg (Chapter 2),

2. Determine the influence of tree litter type (deciduous and coniferous) and temperature on Hg release from forest litter (Chapter 3).

To address objective one, I conducted a field based observational study (Chapter 2) examining Hg accumulation in deciduous species (white birch, *Betula papyrifera* Marshall) and coniferous (black spruce, *Picea mariana* Mill. (L.)) foliage over one growing season. To address objective two, I conducted a laboratory-based incubation experiment examining Hg release from different boreal forest litter types (white birch) and coniferous needles (black spruce and jack pine, *Pinus banksiana* Lamb.) into soils at different temperatures.

1.6 References

Assad, M., Parelle, J., Cazaux, D., Gimbert, F., Chalot, M., Tatin-Froux, F., 2016. Mercury uptake into poplar leaves. Chemosphere 146, 1–7.

Barquero, J.I., Rojas, S., Esbrí, J.M., Garcia-Noguero, E.M., Higueras, P. 2019. Factors influencing mercury uptake by leaves stone pine (*Pinus pinea* L.) in Almaden (central Spain). Environmental Science and Pollution Research 26, 3129–3137.

Berg, B., Berg, M.P., Bottner, P., Box, E., Breymeyer, A., Calvo De Anta, R., Couteaux, M., Escuardo, A., Gallardo, A., Kratz, W., Madeira, M., Mälkönen, E., McClaugherty, C., Meenetemeyer, V., Muñoz, F., Piussi, P., Remacle, J, Virzo De Santo, A., 1993. Litter mass loss rates in pine forests of Europe and eastern United States: Some relationships with climate and litter quality. Biogeochemistry 20, 127–159.

Berg, B., McClaugherty, C., Virzo De Santo, A., Johnson, D., 2001. Humus buildup in boreal forests: effects of litter fall and its N concentration. Canadian Journal of Forest Research 31, 988–998.

Brandt, J.P., 2009. The extent of the North American boreal zone. Environmental Reviews 17, 101–161.

Brandt, J.P., Flannigan, M.D., Maynard, D.G., Thompson, I.D., Volney, W.J.A., 2013. An introduction to Canada's boreal zone: ecosystem processes, health, sustainability, and environmental issues. Environmental Reviews 21, 207–226.

Bushey, J.T., Nallana, A.G., Montesdeoca, M.R., Driscoll, C., 2008. Mercury dynamics of a northern hardwood canopy. Atmospheric Environment 42, 6905–6914.

Cornwell, W.K., Cornelissen, J.H.C., Amatangelo, K., Dorrepaal, E., Eviner, V.T., Godoy, O., Hobbies, S.E., Hoorens, B., Kurokawa, H., Pérez-Harguindeguy, N., Quested, H.M., San-tiago, L.S., Wardle, D.A., Wright, I.J., Aerts, R., Allison, S.D., Van Bodegom, P., Brovkin, V., Chatain, A., Callaghan, T.V., Díaz, S., Garnier, E., Gurvich, D.E., Kazakou, E., Klein, J.A., Read, J., Reich, P.B., Soudzilovskaia, N.A., Viaeretti, M.V., Westoby, M., 2008. Plant species traits are the predominant control on litter decomposition rates within biomes worldwide. Ecology Letters 11, 1065–1071.

Cotrufo, F.M., Wallenstein, M.D., Boot, C.M., Denef, K., Paul, E., 2013. The microbial efficiency-matrix (MEMS) framework integrates plant litter decomposition with soil organic matter stabilization: do labile plant inputs form stable organic matter? Global Change Biology 19, 988–995

Cramer, W., Bondeau, A., Woodward, F.I., Prentice, I.C., Betts, R.A., Brovkin, V., Cox, P.M., Fisher, V., Foley, J.A., Friend, A.D., Kuckarik, C., Lomas, M.R., Ramankutty, N., Sitch, S., Smith, B., White, A., Young-Molling, C., 2001. Global response of terrestrial ecosystem structure and function to CO2 and climate change: results from six dynamic global vegetation models. Global Change Biology 7, 357–373.

Demers, J.D., Driscoll, C.T., Fahey, T.J., Yavitt, J.B., 2007., Mercury cycling in litter and soil in different forest types in the Adirondack region, New York, USA. Ecological Applications 17, 1341–1351.

Demers, J.D., Blum, J.D., Zak, D.R., 2013. Mercury isotopes in a forested ecosystem: implications for air-surface exchange dynamics and the global mercury cycle. Global Biogeochemical Cycles 27, 222–238.

Driscoll, C.T., Mason, R.P., Chan, H.M., Jacob, D.J., Pirrone, N., 2013. Mercury as a global pollutant: sources, pathways, and effects. Environment Science & Technology 47, 4967–4983.

Du, B., Zhou, J., Zhou, L., Fan, X., Zhou, J., 2019. Mercury distribution in the foliage and soil profiles of a subtropical forest: process for mercury retention in soils. Journal of Geochemical Exploration 205, 106337.

Fisher, L.S., Wolfe, M.S., 2012. Examination of mercury inputs by throughfall and litterfall in the Great Smoky Mountains National Park. Atmospheric Environment 47, 554–559.

Grigal, D.F., 2002. Inputs and outputs of mercury from terrestrial watersheds: a review. Environmental Reviews 10, 1–39.

Jiang, T., Skyllberg, U., Wei, S., Wang, D., Lu, S., Jiang, Z., Flanagan, D.C., 2015. Modeling the structure-specific kinetics of abiotic, dark reduction of Hg(II) complexed by O/N and S functional groups in humic acids while accounting for time-dependent structural arrangement. Geochimica et Cosmochimica Acta 154, 151–167.

Jiskra, M., Sonke, J.E., Obrist, D., Bieser, J., Ebinghaus, R., Lund Myhre, C., Pfaffhuber, K., Wängberg, I., Kyllönen, K., Worthy, D., Martin, L., Labuschagne, C., Mkololo, T., Ramonet, M., Magand, O., Dommergue, A., 2018. A vegetation control on seasonal variations in global atmospheric mercury concentrations. Nature Geoscience 11, 244–250.

Juillerat, J.I., Ross, D.S., Bank, M.S., 2012. Mercury in litterfall and upper soil horizons in forested ecosystems in Vermont, USA. Environmental Toxicology and Chemistry 31, 1720–1729.

Kalbitz, K., Solinger, S., Park, J., Michalzik, B., Matzner, E., 2000. Controls on the dynamics dissolved organic matter in soils: A review. Soil Science 165, 277–304.

Kikuzawa, K., Lechowicz, M.J., 2014. Ecology of Leaf Longevity, first ed. Springer Verlag, Tokyo.

Krabbenhoft, D.P., Branfireun, B.A., Heyes, A., 2005. Biogeochemical cycles affecting the speciation, fate, and transport of mercury in the environment. In Parsons, M.B. and Percival, J.B. (Eds.), Mercury: Sources, measurements, cycles and effects. Short course series volume 34, 139−156. Halifax, Nova Scotia: Mineralogical Association of Canada.

Krabbenhoft, D.P., Sunderland, E.M., 2013. Global change and mercury. Science 341, 1457.

Kramer, K., Leinonen, I., Loustau, D., 2000. The importance of phenology for the evaluation of impact of climate change on growth of the boreal, temperate and

Mediterranean forests ecosystems: an overview. International Journal of Biometeorology 44, 67–75.

Lehmann, J., Kleber, M., 2015. The contentious nature of soil organic matter. Nature 528, 60–68.

Lim, P.O., Kim, H.J., Nam, H.G., 2007. Leaf senescence. Annual Review of Plant Biology. 58, 115–136.

Lindberg, S., Bullock, R., Ebinghaus, R., Engstrom, D., Feng, X., Fitzgerald, W., Pirrone, N., Pretsbo, E., Seigneur, C., 2007. A synthesis of progress and uncertainties in attributing the sources of mercury in deposition. Ambio 36, 19–32.

Ma, M., Du, H., Wang, D., Sun, T., Sun, S., Yang, G., 2017. The fate of mercury and its relationship with carbon, nitrogen and bacterial communities during litter decomposing in two subtropical forests. Applied Geosciences 86, 26–35.

McKenney, D.W., Pedlar, J.H., Lawrence, K., Campbell, K., Hutchinson, M.F., 2007. Potential impacts of climate change on the distribution of North American trees. Bioscience 57, 939–948.

McKenney, D.W., Pedlar, J.H., Rood, R.B., Price, D., 2011. Revisiting projected climate shifts in the climate envelopes of North American trees using updated general circulation models. Global Change Biology 17, 2720–2730.

Millhollen, A.G., Gustin, M.S., Obrist, D., 2006. Foliar mercury accumulation and exchange for three tree species. Environment Science & Technology 40, 6001–6006.

Obrist, D., 2007. Atmospheric mercury pollution due to losses of terrestrial carbon pools? Biogeochemistry 85, 119–123.

Obrist, D., Johnson, D.W., Edmonds, R.L., 2012. Effects of vegetation type on mercury concentrations and pools in two adjacent coniferous deciduous forests. Journal of Plant Nutrition and Soil Science 175, 68–77.

Obrist, D., Johnson, D.W., Lindberg, S.E., Luo, Y., Hararuk, O., Bracho, R., Battles, J.J., Dail, D.B., Edmonds, R.L., Monson, R.K., Ollinger, S.V., Pallardy, S.G., Pregitzer, K.S., Todd, D.E., 2011. Mercury distribution across 14 U.S. forests. part I: spatial patterns of concentration in biomass, litter and soils. Environment Science & Technology 45, 3974–3981.

Obrist, D., Kirk, J.L., Zhang, L., Sutherland, E.M., Jiskra, M., Selin, N.E., 2018. A review of global environmental mercury processes in response to human and natural perturbations: changes of emissions, climate, and land use. Ambio 47, 116–140.

Parton, W., Silver, W.L., Burke, I.C., Grassens, L., Harmon, M.E., Currie, W.S., King, J.Y., Adair, E.C., Brandt, L.A., Hart, S.C., Fasth, B., 2007. Global-scale similarities in nitrogen release patterns during long-term decomposition. Science 315, 361–364.

Price, D.T., Alfaro, R.I., Brown, K.J., Flannigan, M.D., Fleming, R.A., Hogg, E.H., Girardin, M.P., Lakusta, T., Johnston, M., McKenney, D.W., Pedlar, J.H., Stratton, T., Sturrock, R.N., Thompson, I.D., Trofymow, J.A., Venier., L.A., 2013. Anticipating the consequences of climate change for Canada's boreal forest ecosystems. Environmental Reviews 21, 322–65.

Ravichandran, M., 2004. Interactions between mercury and dissolved organic matter – a review. Chemosphere 55, 319–331.

Rea, A.W., Lindberg, S.E., Keeler, G.J., 2000. Assessment of dry deposition and foliar leaching of mercury and selected trace elements based on washed foliar and surrogate surfaces. Environment Science & Technology 34, 2418–2425.

Rea, A.W., Lindberg, S.E., Scherbatskoy, T., Keeler, G.J., 2002. Mercury accumulation in foliage over time in two northern-hardwood forests. Water, Air, and Soil Pollution 133, 49–67.

Risch, M.R., DeWild, J.F., Gay, D.A., Zhang, L., Boyer, E.W., Krabbenhoft, D.P., 2017. Atmospheric mercury deposition to forests in the eastern USA. Environmental Pollution 228, 8–18.

Schroeder, W.H., Munthe, J., 1998. Atmospheric mercury – an overview. Atmospheric Environment 32, 809–822.

Soja, A.J., Tchebakova, N.M., French, N.H.F., Flannigan, M.D., Shugart, H.H., Stocks, B.J., Sukhinin, A.I., Parfenova, E.I., Chapin III, F.S., Stackhouse Jr., P.W., 2007. Climate-induced boreal forest change: predictions versus current observations. Global and Planetary Change 56, 274–296.

Sollins, P., Homann, P., Caldwell, B.A., 1996. Stabilization and destabilization of soil organic matter: mechanisms and controls. Geoderma 74, 65–105.

Stamenkovic, J., Gustin, M.S., Arnone, J.A., Johnson, D.W., Larsen, J.D., Verburg, P.S.J., 2008. Atmospheric mercury exchange with a tallgrass prairie ecosystem housed in mesocosms. Science of the Total Environment 406, 227–238.

Stamenkovic, J., Gustin, M.S., 2009. Nonstomatal uptake versus stomatal uptake of atmospheric mercury. Environment Science & Technology 43, 1367–1372.

Streets., D.G., Zhang, Q., Wu, Y., 2009. Projections of global mercury emissions in 2050. Environment Science & Technology 43, 2983−2988.

Trumbore, S.E., 1997. Potential responses of soil organic carbon to global environmental change. Proceedings of the National Academy of Science 94, 8284−8291.

United Nations Environment Program, 2018. Global Mercury Assessment 2018. UNEP Chemicals Branch, Geneva, Switzerland, 2018, 1–258.

Wardle, D.A., Bardgett R.D., Klironomos J.N., Setälä H., van der Putten W.H., Wall D.H., 2004. Ecological linkages between aboveground and belowground biota. Science 304, 1629–1633.

Wright, P.L., Zhang, L., Marsik, F.J., 2016. Overview of mercury dry deposition, litterfall, and throughfall studies. Atmospheric Chemistry and Physics 16, 13399–13416.

Yuan, W., Sommar, J., Lin, C., Wang, X., Li, K., Liu, Y., Zhang, H., Lu, Z., Wu, C., Feng, X., 2019. Stable isotope evidence shows re-emission of elemental mercury vapor occurring after reductive loss from foliage. Environment Science & Technology 53, 651−660.

Zhang, H., Yuan, W., Dong, W., Liu, S., 2014. Seasonal patterns of litterfall in forest ecosystems worldwide. Ecological Complexity 20, 240−247.

Zhang, L., Wright, L.P., Blanchard, P., 2009. A review of current knowledge concerning dry deposition of atmospheric mercury. Atmospheric Environment 43, 5853–5864.

Zhang, Y., Jacob, D.J., Horowitz, H.M., Chen, L., Amos, H.M., Krabbenhoft, D.P., Slemr, F., St. Louis, V.L., Sunderland, E.M., 2016. Observed decrease in atmospheric mercury explained by global decline in anthropogenic emissions. Proceedings of the National Academy of Science 113, 526–531.

Zhou, J., Du, B., Shang, L., Wang, Z., Cui, H., Fan, X., Zhou, J., 2020. Mercury fluxes, budgets, and pools in forest ecosystems of China: a review. Critical Reviews in Environmental Science and Technology, 50, 1411-1450.

Chapter 2

2   Foliage type controls mercury accumulation over the growing season

2.1   Introduction

Mercury (Hg) is emitted to and circulates in the atmosphere in predominantly gaseous forms. Gaseous elemental Hg (GEM, $Hg(0)_g$) generally makes up over 95% of total Hg in the atmosphere (Schroeder and Munthe, 1998, Driscoll *et al*., 2013). Other forms of Hg in the atmosphere including gaseous oxidized Hg (GOM, $Hg(II)_g$) and particle bound Hg (PBM, $Hg(II)_s$), are more rapidly deposited closer to emission sources, and are a smaller fraction of total atmospheric Hg (Schroeder and Munthe, 1998, Driscoll *et al*., 2013).

Mercury is constantly being exchanged between the atmosphere and the Earth's surface, including soils and vegetation, with $Hg(II)_g$ rapidly stripped from the atmosphere by condensation and wet deposition and $Hg(II)_s$ adsorption to leaf surfaces (Millhollen *et al*., 2006). The Hg on the leaf cuticle can be volatilized to its gaseous elemental form and re-emitted (Schroeder and Munthe, 1998, Yuan *et al*., 2019). Despite re-emissions, undisturbed forests are a net sink for Hg as Hg is sequestered in both soil and vegetation (Stamenkovic and Gustin, 2009, Obrist *et al*., 2011, Demers *et al*., 2013). The forest canopy sequesters atmospheric Hg because of the large surface area and high aerodynamic resistance (Zhang *et al*., 2009).

Research has shown that much of this sequestration in vegetation is not solely due to surface deposition and sorption but also uptake processes by which Hg is incorporated into the foliar tissue. The application of natural abundance stable Hg isotope techniques has demonstrated that the incorporation of $Hg(0)_g$ is the dominant fraction of Hg in leaves of various tree species rather than Hg(II) deposited on the surface (Yuan *et al*., 2019). The most well understood pathway is stomatal exchange (Stamenkovic and Gustin, 2009). Through this process Hg is taken into the leaf when the stomata are open to facilitate gas exchange and incorporated into leaf tissues, predominantly in stomatal and epidermal cell walls (Millhollen *et al*., 2006, Stamenkovic *et al*., 2008, Stamenkovic and Gustin, 2009). While stomatal uptake is identified as the main pathway for gaseous Hg

uptake in foliage (Stamenkovic and Gustin, 2009, Assad *et al*., 2016), there have been fewer experiments investigating incorporation of Hg into conifer needle tissues. Mercury can also be assimilated into foliar tissues through non-stomatal uptake although these pathways are not well defined (Stamenkovic and Gustin, 2009, Arnold *et al*., 2018). Laacouri *et al*. (2013) suggested that for deciduous species, Hg(0) uptake is predominantly through the stomata while the leaf cuticle is responsible for uptake of ionic forms of Hg as the cuticle has both polar and non-polar routes that could potentially transport both non polar Hg(0) and polar Hg(II), although the authors note this requires further study. Additional observations of Hg exchange between tissues with the atmosphere in darkness when stomatal conductance is low (Stamenkovic and Gustin, 2009), and similar accumulation rates between species with different stomatal conductance (Frescholtz and Gustin, 2004) suggests non-stomatal uptake processes play an important role in Hg uptake.

Several studies have investigated potential translocation of Hg from soils into plant biomass through roots, but evidence indicates that this is not an important pathway. Experiments have been conducted that have grown a range of plant species (e.g. Frescholtz *et al*., 2003 [aspen and pine trees]; Niu *et al*., 2011 [maize and wheat]; Assad *et al*., 2016 [poplar trees]; and Arnold *et al*., 2018 [pine trees]) in growing media spiked with Hg. None of these studies found any significant correlation between foliage tissue and growing media Hg concentrations. From these studies, coupled with low Hg concentrations in xylem (Bishop, 1998), uptake of Hg has been established to be almost exclusively through atmospheric pathways (Bishop, 1998, Assad *et al*., 2016).

Mercury accumulates in foliage tissue over the growing season (Grigal, 2002, Rea *et al*., 2002, Assad *et al*., 2016), but the Hg accumulation rate varies among tree types (Graydon *et al*., 2008) and is influenced by meteorological factors as well as atmospheric Hg concentrations (Yuan *et al*., 2019). Coniferous needles often have higher Hg concentration as a result of the increased exposure to the atmosphere because of a multi-year turnover time (Niu *et al*., 2011, Blackwell and Driscoll, 2015), although the leaves of deciduous species may play a more active role in gaseous Hg exchange due to greater stomatal conductance and/or larger leaf specific area resulting in more rapid Hg

accumulation (Millhollen *et al.*, 2006). Vertical gradients of Hg have been observed in the canopy, and within-tree variation of Hg concentration in leaf tissues indicates that there are both regional and local scale factors that influence Hg concentrations and leaf accumulation (Stupple, 2009, Siwik *et al.*, 2009).

Since atmospheric Hg concentrations are an important control on foliar Hg concentrations (Graydon *et al.*, 2006), knowing background Hg concentrations is critical to understanding Hg uptake. There has been interest and research into whether organic tissues (e.g. Kang *et al.*, 2019 investigated tree rings) can act as effective passive air samplers (PAS) because until recently with the development of the Mercury Passive Air Sampler (Tekran® MerPAS), atmospheric monitoring of Hg was expensive, and required a reliable electricity source and trained personnel to operate the instruments (McLagan *et al.*, 2016a). The MerPASs require minimal investment comparatively. They can be deployed virtually anywhere, not needing a power source, extensive training or constant monitoring, and only require laboratory analysis after retrieval. While the MerPASs only measure $Hg(0)_g$, this species makes up the majority of atmospheric Hg and because both $Hg(II)_s$ and $Hg(II)_g$ are not readily transported long distances (Schroeder and Munthe, 1998, Driscoll *et al.*, 2013), the use of MerPAS is especially appropriate in remote, pristine areas. Finally, as stable isotopes have demonstrated that $Hg(0)_g$ is the dominant source of Hg in foliage tissue (Yuan *et al.*, 2019), MerPASs are an ideal comparison for foliar uptake.

Another factor contributing to the potentially more important role of deciduous vegetation in the Hg cycle is annual senescence. This is a highly regulated series of both degenerative processes and recycling processes whereby nutrients are resorbed by trees from leaves to put towards other processes like seed development (Gan and Amasino, 1997). Senescence can be triggered by both endogenous factors such as fruiting, as well as exogenous, environmental factors (e.g. drought, temperature, photoperiod) (Gan and Amasino, 1997). One of the main physiological changes that occurs early in senescence is the breakdown of the chloroplasts (Lim *et al.*, 2007). A significant portion of nitrogen (N) in a leaf is in the chloroplasts so with the onset of senescence, N is resorbed from the leaf (Makino and Osmond 1991, Gan and Amasino, 1997). During senescence the plant

resorbs N and other nutrients from the leaf to put towards other processes, and this resorption is coupled with the turnover of chlorophyll pigment that causes many green leaves to turn yellow and brown (Kikuzawa and Lechowicz, 2011). Immediately following senescence, abscission (the separation of the leaf from the plant) occurs, and when this occurs on a large scale the collective process is known as litterfall.

Litterfall comprises a major input of soil Hg (Grigal, 2002, Rea *et al*., 2002, Assad *et al*., 2016) via the delivery of Hg to soils during leaf tissue decomposition. Some of the deposited Hg on foliage is washed off during precipitation events and then falls to the ground as throughfall, which is the other major input of Hg into forest soils (Rea *et al*., 2000, Demers *et al*., 2007, Risch *et al*., 2012). Demers *et al*. (2007) concluded that throughfall was a more important pathway of Hg to the forest floor in conifer dominated forests and more work was needed comparing Hg uptake between leaves and needles and their subsequent Hg inputs to the forest floor.

Studies have observed the accumulation of Hg in leaf tissue in the field although this has largely been observed on a broad scale with few time points or with the collection of fallen litter. To date there has not been high definition sampling for leaves and needles to investigate Hg uptake, and there is considerably less literature on Hg uptake in conifer needles. Similarly, there is a knowledge gap in comparing Hg uptake in leaves and needles to determine if uptake in foliage approximates passive uptake. The objectives of this study were to:

1) Quantify spatial patterns (vertical in canopy and laterally across multiple plots) of foliar Hg concentrations and accumulation rates in two common boreal deciduous and coniferous tree species over a full growing season from leaf out to senescence;

2) Compare these Hg accumulation rates in foliage to that of a verified $Hg(0)_g$ Passive Air Sampler (PAS) to determine if Hg concentration approximates passive uptake in leaves and needles;

3) Compare changing Hg concentrations in foliage with percent C and percent N content by mass and changing C:N ratios to determine the relationship between

foliage quality with Hg accumulation and how these relationships change during senescence.

These data will provide insights into Hg cycling patterns in the boreal forest. The data will provide comparison in accumulation rates of Hg between dominant boreal tree species and how they relate to different foliage quality. It will also provide insights to what happens to the Hg that accumulates in foliage during senescence before the foliage falls to the ground and can enter the soil pool. These data will contribute to understanding the controlling factors on the Hg inputs to forest soils.

2.2 Methods

2.2.1 Study site

The study site was located at 48.349381° N; 85.353414° W in the southern boreal forest near White River, ON. This site is mixed broad leaf deciduous and coniferous forest, approximately 70 years since regeneration after fire, adjacent to several wetlands (McLaughlin, 2009). The dominant tree species in the mixed wood forest are white birch (*Betula papyrifera*), balsam fir (*Abies balsamea* Mill.), and black spruce (*Picea mariana*). The soil is Typic Haplorthod based on USDA-NRCS classification, which are common to the boreal forest and found under deciduous and coniferous tree stands (McLaughlin, 2009). There are no identified point Hg sources in the region that would influence ambient atmospheric Hg concentrations.

2.2.2 Experimental design and vegetation sampling

In the summer of 2019, a 12 m aluminum scaffolding tower was erected in the forest stand. The tower had an internally framed ladder system to four platform heights: lower (3.7 m), mid-lower (5.8 m), mid-upper (7.9 m), and upper (10 m). The location of the tower was selected to maximize access to each of the dominant tree species of the site. I sampled black spruce needles from each platform height, and white birch leaves at the upper three levels. There were no branches with white birch leaves at the lower (3.7 m) height that were close enough to the tower to sample as the trees adjacent to the tower were more mature and their canopy started higher up. To evaluate the degree of

local-scale spatial variability in leaf Hg in the two tree species, four additional sampling locations were established ~30 m from the tower in each cardinal direction (hereafter referred to as the 'radial' sites). The radial sites captured a range of canopy density/maturity in the forest stand. The North Site was on the edge of the forest stand and had an open canopy relative to the other sites. The East Site and South Site were in denser forest with a closed mature upper canopy, and the West Site was near to the forest edge with an intermediate canopy cover. At each of these radial sites, white birch and black spruce were sampled at a height of approximately 3.7 m above the ground. As there was no scaffold installation at the radial sites, this was the maximum height possible to sample from the ground using a pruning rod with stainless steel blades.

Leaves (white birch) and new needles (black spruce) were sampled weekly at each tower height and radial site. Collection began in early June just after bud phase such that only new needles from this year and leaves starting in bud form were collected. Because needle emergence varied more than white birch leaf emergence, the first sample of needles started a week after the white birch samples were collected at the radial sites. All vegetation was collected wearing gloves, cut with a stainless-steel knife or extendable clippers, placed in a clean, sealed bag and frozen until analysis.

As there are many senescence cues, absolute timing of senescence in this forest varies yearly. At a forest stand level its timing is influenced by both short-term (e.g. daily minimum temperature) and longer-term environmental conditions (e.g. summer rainfall and tree drought stress conditions). Color and quality (thinner leaves with reduced luster) changes in leaves began at the end of August in 2019. For the final two vegetation samples (September 15 and September 20), I cut fully yellow leaves and still fully green leaves at each tower height and the radial sites. Coniferous needles, which do not undergo senescence and abscission on the same cycle as deciduous leaves or based on the same environmental cues, were sampled as previously described at each site.

At the same time, during the mid-September sampling, I placed litterfall traps (approximately 1.5 m by 2 m) at the base and top of the tower for four days to capture litterfall representative of the true fresh litter Hg input to the forest floor early in the

senescence period (as opposed to litter accumulated in a trap and left for days to weeks as is common in many litterfall studies). Traps were made of clean fabric and emptied each day wearing gloved hands. Only white birch litter was retained, and the traps were cleared daily. A litter trap was again deployed at the base of the tower in early October for three days to collect litterfall during late-mid period senescence. See Table 2.1 for sampling dates.

Table 2.1 Sampling dates of fresh foliage (white birch leaves and black spruce needles) and litterfall (white birch leaves) over 2019 summer growing season and deployment times of MerPASs at tower and radial sites. Fresh leaves were collected at three tower heights and four radial sites. Fresh needles were collected at four tower heights and four radial sites.

Date	Foliage Sampled	Samples
June 13	Leaves and needles at tower. Leaves at radial sites.	11
June 20	Leaves and needles at tower and radial sites	15
June 27	Leaves and needles at tower and radial sites	15
July 4	Leaves and needles at tower and radial sites	15
July 10	MerPASs deployed at tower and radial sites	
July 20	Leaves and needles at tower and radial sites	15
July 25	Leaves and needles at tower and radial sites	15
August 1	Leaves and needles at tower and radial sites	15
August 8	Leaves and needles at tower and radial sites	15
August 14	Leaves and needles at tower and radial sites	15
August 22	Leaves and needles at tower and radial sites	15
August 29	Leaves and needles at tower and radial sites	15
Sept. 15	Green and yellow on-tree leaves and needles at tower and radial sites	22
Sept. 16	Litterfall trap deployed at base and top of tower	
Sept. 17	Litterfall traps collected	2
Sept. 18	Litterfall traps collected	2
Sept. 19	Litterfall traps collected	2
Sept. 20	Green and yellow on-tree leaves and needles at tower and radial sites	
	Litterfall traps collected	24
	MerPASs collected from all sites	
Oct. 6	Litterfall trap collected from 2-day deployment	1
Total		214

2.2.3 Environmental Monitoring

The tower was equipped with two Gill 3-cup Anemometers (RM Young®), one at the upper level and one at the mid-lower level that extended approximately 1.25 m off the north side of the tower to measure continuous wind speed across the site. Two SP Lite Pyranometers (Kipp & Zonen®) were also installed on mounting arms approximately 1.5 m off the north-west side of the tower at the upper and mid lower tower levels to measure incoming solar radiation. Additionally, a CS500 Temperature and Relative Humidity Probe (Campbell Scientific®) was mounted to the tower at the mid-lower level to monitor air temperature in the canopy. These sensors took measurements every five seconds and were compiled into hourly and daily averages over the sampling period using a Campbell Scientific CR-1000x datalogger. Open field wind speed was measured at a weather station set up in an open peatland adjacent to the forest (approximately 500 m north of tower).

2.2.4 Atmospheric mercury monitoring

Mercury passive air samplers (Tekran® MerPAS) were deployed July 10, 2019 on the scaffolding system at each tower height adjacent to the trees, and at each of the radial sites at approximately 3.7 m at the same height as foliage sampling to correlate atmospheric Hg to leaf samples. The MerPAS are small (height =7.6 cm, diameter =7.2 cm) blue plastic (polyethylene terephthalate) jars with a lid at the bottom to allow airflow with a thin mesh plastic (polytetrafluoroethylene) to prevent animals or debris from getting inside the sampler. Within the plastic jar, bituminous, coal-derived sulfur-impregnated activated C that acts as a sorbent is housed inside a protective mesh stainless steel cylinder that protects the sampler from wind and precipitation (McLagan *et al*., 2016b). McLagan *et al*. (2016b) provide a comprehensive validation of the use of MerPASs for environmental monitoring. The MerPASs were retrieved September 20, 2019 (total duration of deployment = 72 days). During collection, MerPASs were removed from the tower or trees they were attached to, capped to stop air exchange and placed in two clean bags before being returned back to the laboratory for analysis.

2.2.5 Laboratory analyses

To prepare foliage for Hg concentration analysis, and percent C (%C) and percent N (%N) by mass analysis, black spruce needles were handpicked from the selected cut branches and the petioles of the white birch leaves were separated using a stainless-steel blade cleaned after each sample. All leaves and needles were rinsed with 18.2 MOhm deionized water, freeze dried, and homogenized using a stainless-steel knife mill (Retsch® GM200) cleaned between each sample. Samples were ground for approximately 45 seconds or longer for larger samples until the sample was fully homogenized.

Mercury analysis took place in the ISO 17025 accredited Analytical Services Laboratory (Western University London, ON). Mercury concentration of the leaves and needles were determined using a using a Milestone® Tri-Cell DMA-80 analyzer following standard method US EPA 7473 (1998). Briefly, in the instrument the sample is heated to 750°C in an oxygenated decomposition furnace, then dried and chemically and thermally decomposed to free the Hg from the sample before the gold amalgamator selectively traps Hg from the remaining decomposition products. The amalgamator is flushed with oxygen gas and then heated to 750 °C, releasing Hg vapor that is carried with oxygen through absorbance cells a single wavelength atomic absorbance spectrophotometer where absorbance is measured at 253.7 nm as a function of Hg concentration. The instrument was calibrated daily with analytical blanks confirmed under the method reporting limit, and certified standard checks for each absorbance cell confirming Hg concentration within 10% of target. After daily calibration, analytical blanks, duplicates, matrix spikes, matrix spike duplicates, and a certified-reference material (CRM) (freeze dried fish protein, DORM 4) were run every ten samples. The CRM used, required by EPA 7473, had a relatively low Hg concentration such that absorbance occurred within the same absorbance cell of the instrument as for the foliage samples. Percent recovery was within 10% for initial check standards and 20% for matrix spikes and CRM in the sample runs. Reported percent differences for duplicates were all within 20% (as required by the method), if any checks failed these standards, samples were further homogenized and re-run.

The MerPASs were analyzed by Dr. Carl Mitchell's laboratory at University of Toronto, Toronto, ON who developed the MerPASs. The subsamples of sulfur-impregnated activated C to which the atmospheric Hg is sorbed was analyzed using a Nippon® MA-3000 direct Hg analyzer. The average sampling rate (SR) for atmospheric Hg (cm^3 day^{-1}) was determined using the formula described by Restrepo *et al.* (2015) and McLagan *et al.* (2016b):

$$SR = m / (Ct)$$

where *m* is the amount of analyte collected by the MerPAS (nanograms of Hg), C is the mean of actively measured Hg concentration over sampling period, and *t* is deployment time (days) for each MerPAS. Linear uptake by the MerPAS is assumed and the average uptake per day calculated by dividing the total amount of Hg sorbed to the C by the deployment time (72 days). Similarly, I calculated average white birch leaf and black spruce needle uptake rates at different points in the growing season by subtracting the average June 13 concentration and then dividing the Hg concentration by the number of days since June 13. I then calculated the percent difference in uptake between the MerPASs uptake and the uptake in white birch leaves and black spruce needles to determine the efficacy of using foliage tissues as PAS by comparing uptake rates.

Percent C and %N by mass in all leaves and needles were measured by purge and trap chromatography using an Elementar Isotope Cube® CHSNO elemental analyzer on approximately 5 to 10 mg of homogenized freeze-dried sample. After initial daily factor checks with sulfanilamide that fell within 10% of target, blanks, duplicates, and CRM were run every ten samples. The CRM for needle and leaf samples was Birch Leaf Standard (CatNo. B2166). All duplicates and recovery values were within 20% and all reported percent differences were <20%; if a sample exceeded these values the samples were further homogenized and re-run.

2.2.6 Statistical analyses

All statistical analyses were performed using Statistica 7 (StatSoft. Inc., 2004) or R version 3.6.1 using the base statistics package unless otherwise noted (R Core Team,

2019). Spearman's correlations were used to examine the relationship between Hg concentration and %C, %N, and C:N in the foliage. Linear models (separate for white birch and black spruce) were used to compare Hg accumulation, %N, %C, and C:N, at different heights over the growing season using the nmle package in R (Pinheiro *et al.*, 2019). A repeated-measures (RM) analysis of variance (ANOVA) was used to compared Hg concentration between white birch and black spruce foliage over the growing season and separate RM-ANOVAs were run on white birch and black spruce Hg concentrations to analyze the effect of time on Hg concentrations. A multivariate ANOVA (MANOVA) was run to compare %N, %C and C:N by mass in white birch and black spruce over the growing season and separate MANOVAs were run for %C and %N by mass for white birch and black spruce to analyze change over the growing season for these variables. A one-way ANOVA was used to compare Hg concentration between yellow and green leaves for the September white birch samples using color as a main effect. A MANOVA was used to analyze differences in %C, %N, and C:N of yellow and green white birch leaves for the September samples.

2.3 Results

2.3.1 Mercury accumulation in leaves and needles

As expected, Hg concentrations increased in white birch leaves over the growing season (Fig. 2.1). There was a significant difference in Hg concentration over the growing season influenced by time ($F_{11,110}$=71.4, P<0.001) and tree type ($F_{1,10}$=17.8, P=0.002). Initial foliage Hg concentrations were low but were higher in fresh needles than in new leaves (5.10 ng g^{-1} and 1.53 ng g^{-1}, respectively). Accumulation was more linear in white birch leaves and increased steadily with time ($F_{12,60}$=117, P<0.001). Concentrations in both leaves and needles increased more with the onset of senescence that occurred during the last two sampling points (Fig. 2.1). Concentrations in white birch leaves increased through senescence as the leaves turned yellow and abscised from the tree.

Unlike the deciduous leaves, the black spruce needle Hg concentration remained relatively stable with time but increased slightly overall ($F_{11,66}$=8.84, P<0.001), slightly declining mid-season (Fig. 2.1). Like for white birch, the Hg concentrations in black

spruce needles were highest for the last two sampling points (9.36 ng g^{-1} and 9.50 ng g^{-1}, respectively), which was when the needles visually appeared to be fully grown. Because I sampled only 2019 emergent needles, they did not contribute to any litterfall in 2019. See Table 2.2 for summary.

There were no clear trends in different Hg concentrations in white birch leaves ($F_{1,35}$=0.55, P=0.462) or the black spruce needles ($F_{1,47}$=0.080, P=0.779) at the different tower heights and the Hg concentrations from the tower all were within the range of the replicate, radial sites (Table 2.2). Overall, the black spruce needles demonstrated slightly greater variation in Hg concentration across the growing season but there were no consistent trends over time by height or across the radial sites. As a result, all radial sites and tower heights were grouped together for analyses between white birch leaves and black spruce needles and to show aggregate variation over the growing season (Fig. 2.1).

Table 2.2 Summary of statistical analyses of Hg concentration, %N by mass, %C by mass, and C:N ratios in white birch leaves and black spruce needles over 2019 growing season.

Tree	Effect	Hg	%N	%C	C:N
white birch	Time	$F_{12,60}=117$ **P<0.001**	$F_{12,72}=24.9$ **P<0.001**	$F_{12,72}=w35.1$ **P<0.001**	$F_{12,72}=22.0$ **P<0.001**
	Height	$F_{1,35}=0.55$ P=0.462	$F_{1,35}=3.07$ P=0.088	$F_{1,35}=0.95$ P=0.338	$F_{1,35}=24.5$ P=0.877
	Height × Time	$F_{3,35}=0.06$ P=0.801	$F_{3,35}=0.19$ P=0.667	$F_{3,35}=0.25$ P=0.6205	$F_{3,35}=0.03$ P=0.874
	[Hg] correlation		$R=-0.63$ **P<0.001**	$R=0.82$ **P<0.001**	$R=0.62$ **P<0.001**
black spruce	Time	$F_{11,66}=8.84$ **P<0.001**	$F_{11,33}=13.4$ **P<0.001**	$F_{11,33}=25.2$ **P<0.001**	$F_{11,33}=10.3$ **P<0.001**
	Height	$F_{2,47}=4.53$ P=0.782	$F_{2,42}=2.31$ P=0.136	$F_{2,42}=2.19$ P=0.146	$F_{2,42}=3.59$ P=0.065
	Height × Time	$F_{1,47}=0.08$ P=0.779	$F_{3,42}=0.05$ P=0.825	$F_{3,42}=0.05$ P=0.945	$F_{3,42}=0.45$ P=0.507
	[Hg] correlation		$R=0.18$ P=0.080	$R=0.02$ P=0.860	$R=-0.23$ **P=0.028**
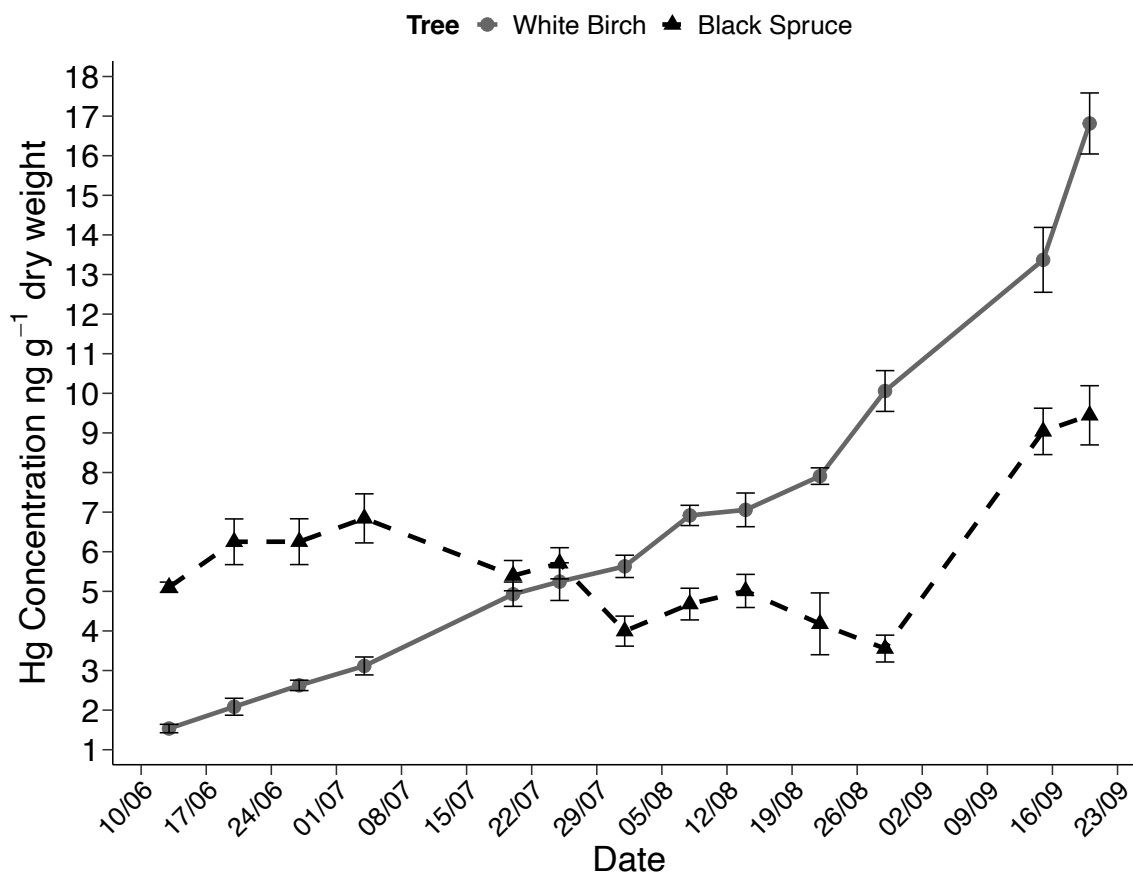
Figure 2.1 Hg concentrations (ng g^{-1}) over 2019 growing season in white birch leaves and black spruce needles. Points are mean ± SE (n=7 for white birch and n=8 for black spruce).

2.3.2 Foliage as mercury passive air samplers

Average temperature over the growing season measured on the tower was 11.9 °C. As expected, wind speed was greater at the upper tower than the mid tower but still less than open field air speed across the sampling period (Fig. 2.2A). Similarly, light penetration was reduced by the canopy cover and solar radiation was consistently greater at the upper tower level than the mid tower (Fig. 2.2B). Despite the differences in wind and light penetration there were no clear trends in atmospheric Hg measured by the MerPAS (Table 2.3). This is consistent with the lack of clear trends in the Hg concentrations of the needles and leaves with height.
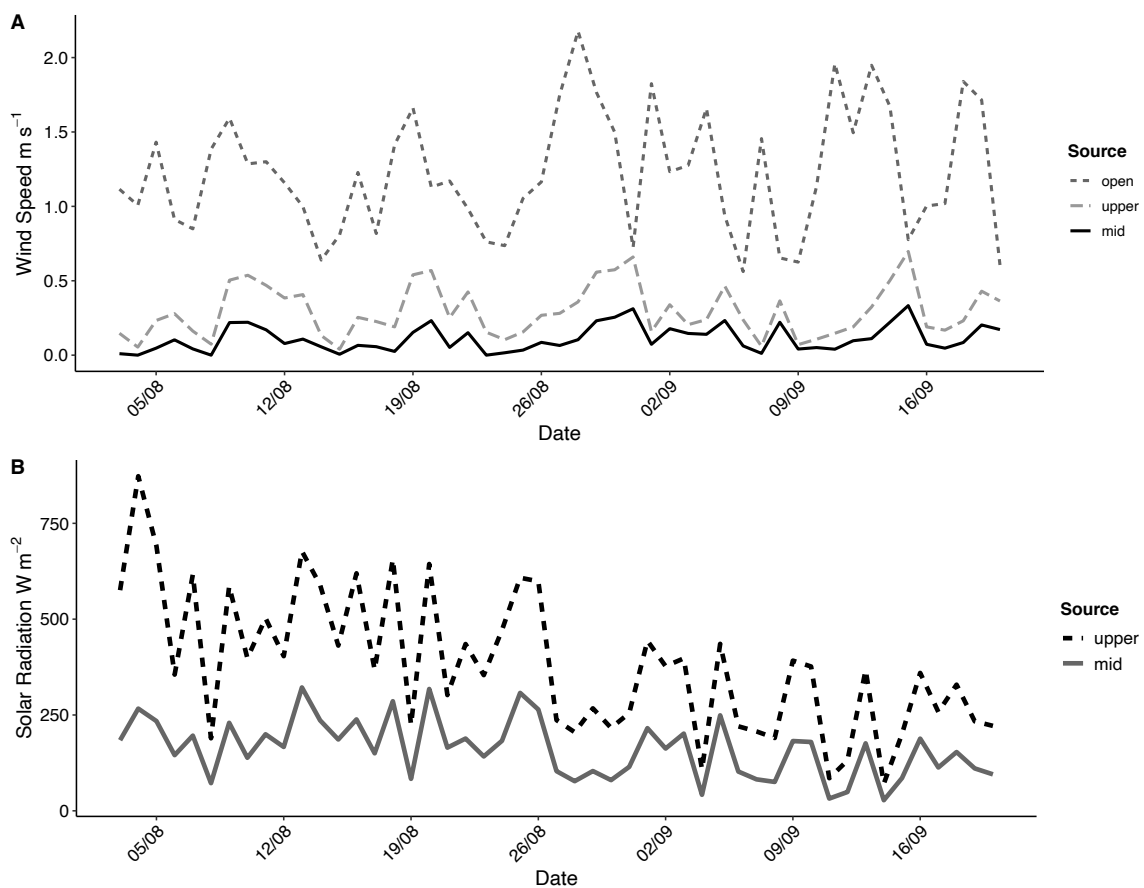
Figure 2.2 A: Wind speed (m s⁻¹) over growing season measured at an open field from weather station 500 m north of the tower, the upper tower level (10 m), and mid tower level (5.8 m). B: Solar radiation (W m⁻²) over growing season measured at upper tower and mid tower levels.

Table 2.3 Average Atmospheric Hg Concentration (ng m^{-3}), uptake rates of MerPASs (ng g^{-1} day^{-1}), and uptake rates (ng g^{-1} day^{-1}) of white birch leaves and black spruce needles based on August 29, 2019 Hg concentrations.

Site	Average Atmospheric [Hg] (ng m^{-3})	MerPAS Hg uptake rate (ng g^{-1} day^{-1})	White birch Hg uptake rate (ng g^{-1} day^{-1})	Black spruce Hg uptake rate (ng g^{-1} day^{-1})
North	1.02	0.1128	0.1112	0.0226
East	0.68	0.0760	0.1419	0.0474
West	0.96	0.1064	0.1023	0.0210
South	0.97	0.1078	0.1155	0.0401
Tower Upper	0.87	0.0965	0.0985	0.0252
Tower Mid Upper	0.95	0.1051	0.1084	0.0262
Tower Mid Lower	0.95	0.1057	0.0845	0.0470
Tower Lower	0.92	0.1024		0.1567

Average atmospheric Hg concentrations over the period of deployment calculated from the MerPAS samplers ranged from 0.68 to 1.02 ng m^{-3} (Table 2.3). The East Site had the lowest average concentration (0.68 ng m^{-3}) while all the other sites' Hg concentrations were in a narrow range falling between 0.87 and 1.02 ng m^{-3}. This caused the uptake by the East Site MerPAS to be lower than the leaf uptake more frequently than the other sites although the leaf concentrations at the East Site were similar with the other leaves. Towards the end of the growing season the white birch leaves had similar uptake ranges to the uptake of the MerPASs, with every site other than the East Site having less than a 25 percent difference in uptake rate between the MerPAS and leaves (Table 2.3). During senescence and the decline in photosynthesis, this relationship broke down and the percent difference was greater in both yellow and green leaves at almost every site because Hg concentrations increased in the leaves. The black spruce Hg needle uptake rates were less than fifty percent lower than the MerPASs at almost every sampling time.

2.3.3 Foliage quality and mercury over the growing season

The foliar quality (%C, %N, C:N) differed over the growing season by tree type ($F_{2,7}$=110, P<0.001). In both black spruce needles and white birch leaves time influenced %N, %C, and C:N (black spruce: $F_{22,64}$=17.9, P<0.001; white birch $F_{36,208}$=14.7, P<0.001). Overall, %N by mass decreased over the growing season (black spruce: $F_{11,33}$=13.4, P<0.001; white birch $F_{12,72}$=24.9, P<0.001) (Fig. 2.3) while %C increased slightly (black spruce: $F_{11,33}$=25.2, P<0.001; white birch: $F_{12,72}$=35.1, P<0.001) (Fig. 2.4) and C:N increased (black spruce: $F_{11,33}$=10.3, P<0.001; white birch: $F_{12,72}$=22.0, P<0.001) (Fig. 2.5). The initial %N by mass in white birch leaves were greater (June 13 average 3.42%; June 20 average 2.69%) than in black spruce needles (June 20 average 2.48%), a trend that remained constant over the season. In white birch leaves this caused the C:N to increase initially but reach a plateau mid-season until senescence occurred (final two points of Fig. 2.5). A similar trend of increasing C:N was observed in black spruce needles but without senescence there was no clear change in September. Similar to the Hg concentrations, height had no influence on %N or %C by mass in leaves or needles (Table 2.2). While there was variation in %N and %C across the sites there were no consistent trends over time. Data has been compiled into averages ± SE in figures to show variability (Fig. 2.3, 2.4, 2.5).

Using the September green leaf values for Hg concentration, %N, %C, and C:N over the growing season in white birch leaves, %N was significantly negatively correlated with Hg (Fig. 2.6A) while %C was positively correlated with Hg (Fig. 2.6B) as was C:N with Hg. Black spruce needles did not exhibit the same trend: neither %N nor %C were significantly correlated with Hg and C:N was slightly significantly negatively correlated with Hg. See Table 2.2 for summary.
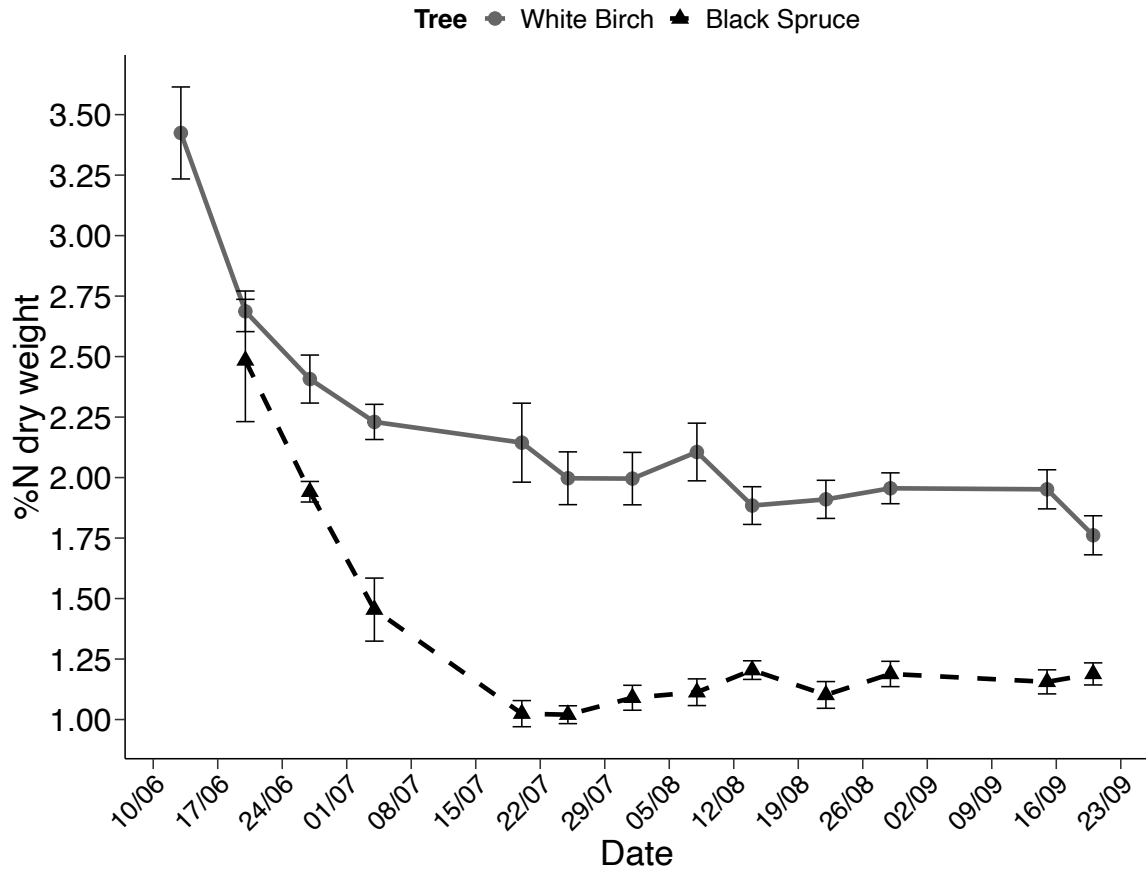
Figure 2.3 Percent nitrogen by mass over 2019 growing season in white birch leaves and black spruce needles. Points are mean ± SE (n=7 for white birch and n=8 for black spruce).

Figure 2.4 Percent carbon by mass over 2019 growing season in white birch leaves and black spruce needles. Points are mean ± SE (n=7 for white birch and n=8 for black spruce).
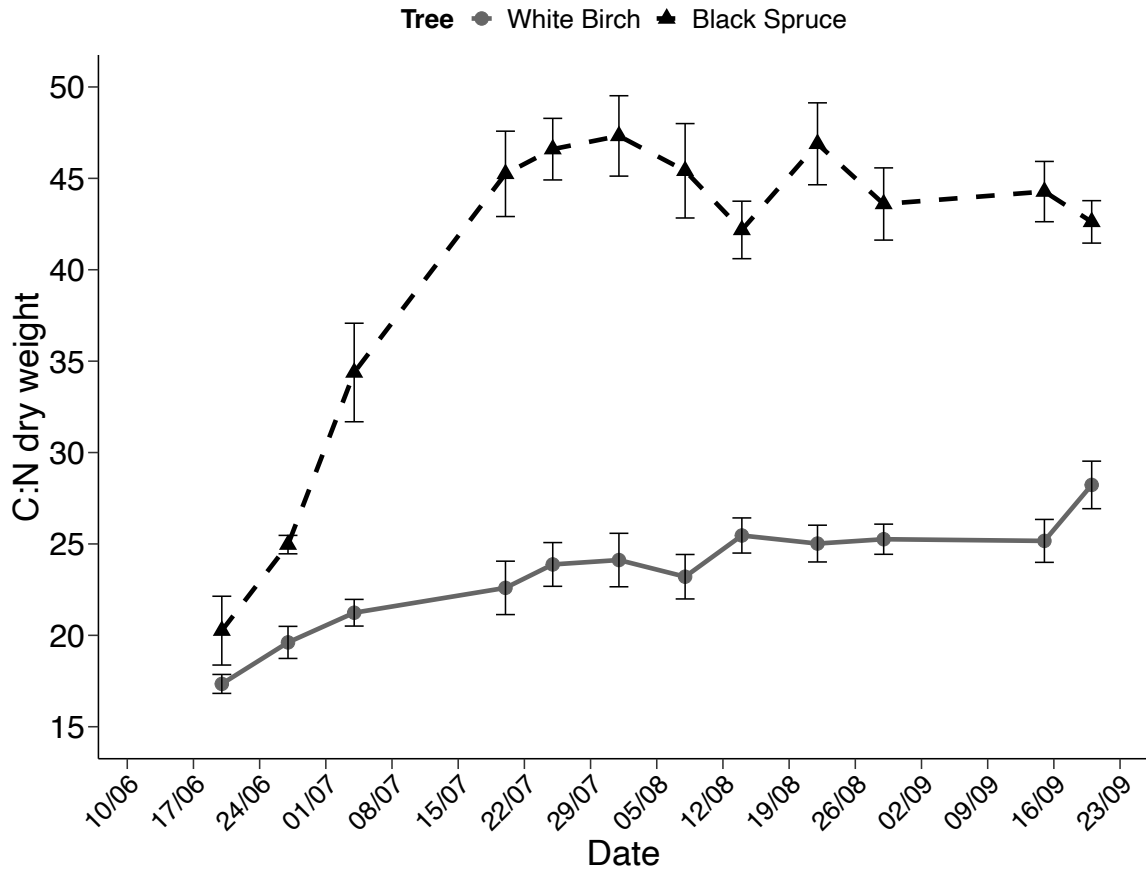
Figure 2.5 Carbon to nitrogen ratios over 2019 growing season in white birch leaves and black spruce needles. Points are mean ± SE (n=7 for white birch and n=8 for black spruce).
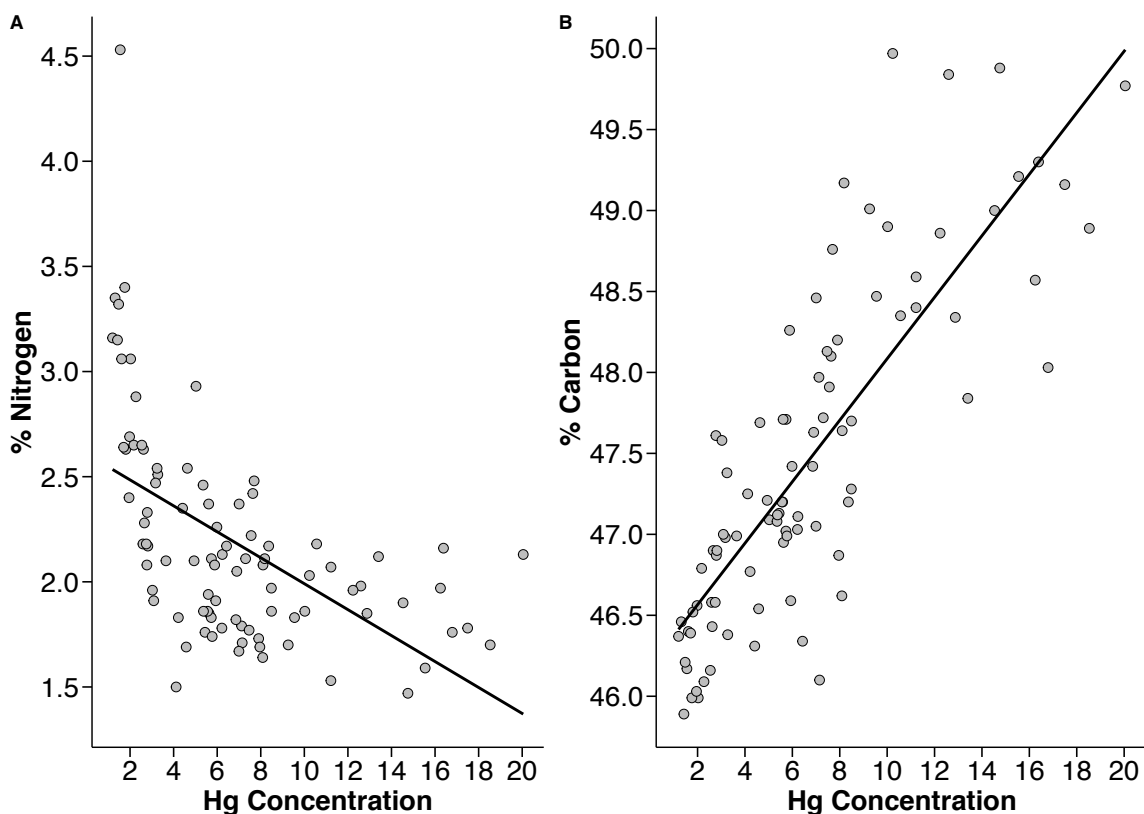
Figure 2.6 Foliage quality and mercury concentration over summer 2019 growing season in green white birch leaves. A: Hg concentration and percent nitrogen content by mass; B: Hg concentration and percent carbon content by mass.

2.3.4 The effect of senescence on mercury and foliage quality

While there was no statistically significant difference of Hg concentration in yellow, green, and fallen white birch leaves ($F_{1,10}$=3.72, P=0.066) there was a trend (Fig. 2.7A) that the yellow leaves had higher Hg concentrations (average yellow concentration 17.01±1.01 ng g^{-1}) than the green leaves (average Hg concentration = 15.09±0.72 ng g^{-1}). This trend was also consistent for falling leaves where I observed greater Hg concentrations (Table 2.3). The %N of the falling leaves were more variable than the on-tree leaves (both yellow and green) at the same time point, resulting in more varied C:N ratios. There was a significant difference for leaf stage of senescence (i.e. yellow, green, or litterfall) as a main effect in a MANOVA of %N, %C and C:N ($F_{3,18}$=116, P<0.001)

that was driven by %N ($F_{1,10}$=318, P<0.001) with green leaves having greater %N than yellow leaves (Fig. 2.7B). The %C in the leaves was not significantly different ($F_{1,10}$=2.36, P=0.138) but the C:N was ($F_{1,10}$=211, P<0.001), influenced by the difference of %N (Fig. 2.7B).
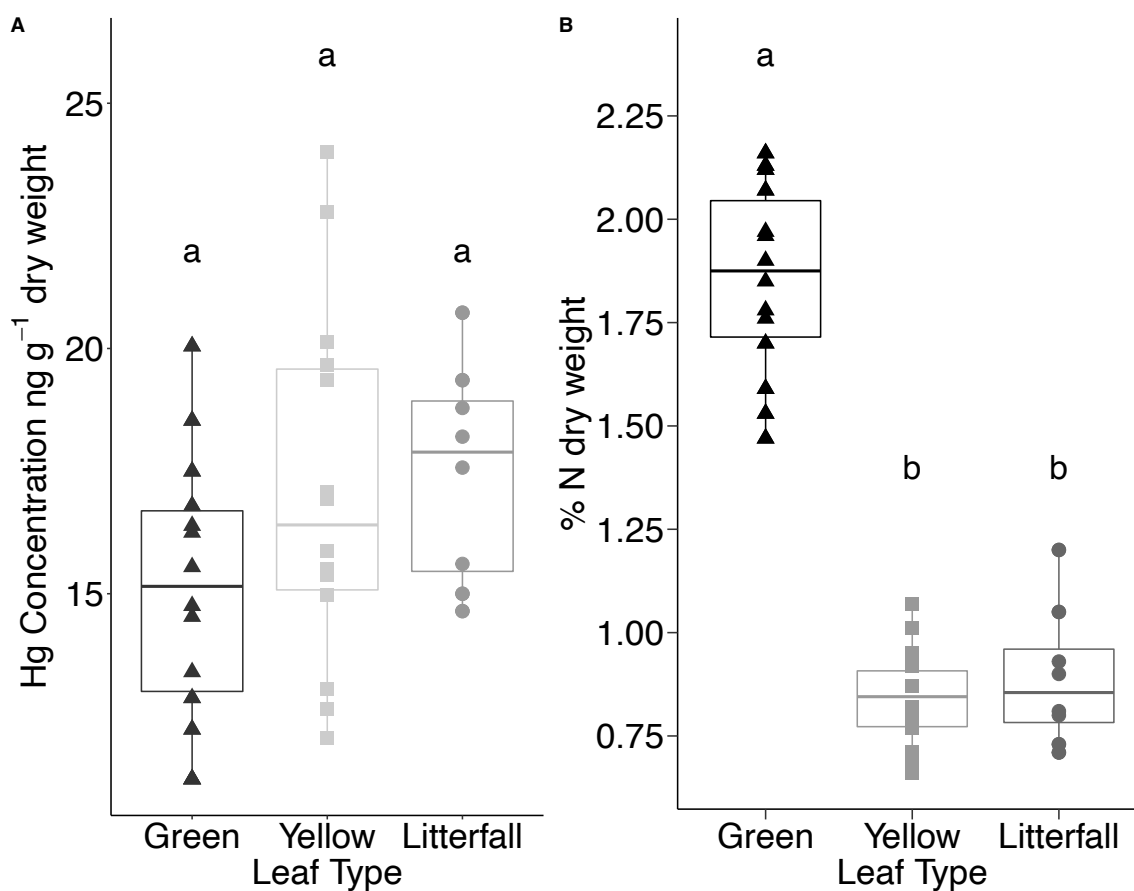
Figure 2.7 A: Mercury concentration (dry weight, ng g^{-1}) and B: percent nitrogen (by mass of dry weight) content of yellow, green, and fallen white birch leaves. Boxes display interquartile range, median (line in box), and whiskers are maximum and minimum values excluding outliers. Letters denote significant differences using Tukey post-hoc comparisons on a two-way ANOVA.

Table 2.4 Litterfall Hg concentrations (ng g^{-1}), %N and %C by mass, and C:N collected in litter traps 1 m above ground at base of tower in September and October 2019 (N=1) compared to September 20 2019 white birch leaves on tree (values are mean ±SE, n=7).

Date	[Hg] ng g^{-1}	%N	%C	C:N
September 20 green leaves	16.61 ± 0.77	1.76 ± 0.08	49.13 ± 0.23	28.23 ± 1.30
September 20 yellow leaves	19.77 ± 1.03	0.89 ± 0.05	49.92 ± 0.33	57.45 ± 3.80
September 17 litter	18.79	1.2	50.05	41.75
September 18 litter	19.35	1.05	50.37	48.10
September 19 litter	17.57	0.93	50.39	53.92
September 20 litter	18.20	0.90	50.58	55.94
October 6 litter	20.72	0.8	49.05	61.29

2.4 Discussion

2.4.1 Accumulation of mercury over the growing season in leaves and needles

The increase in Hg concentration in white birch leaves was relatively linear up to senescence. The mid-season decrease in Hg concentration in black spruce needles was likely a function of growth dilution as the needles grew at different rates over the sampling period while the white birch leaves stopped increasing in surface area by early July. Mercury concentrations in foliage have been found to differ between species and between conifer and deciduous tissues (e.g. Siwik *et al*., 2009, Barquero *et al*., 2019), consistent with my observed Hg concentrations that showed white birch leaves had higher Hg concentrations by the end of the growing season than the black spruce needles.

Whether foliar tissues reach Hg saturation is uncertain in the literature, but I did not find evidence to support this as concentrations continued to increase over the growing season. Ericksen *et al*. (2003) and Frescholtz *et al*. (2003) used mesocosm studies and found Hg concentrations of Hg in tree leaves leveled off after approximately three months. These studies also expressed Hg concentration on a mass by mass unit, which does not account for changes in surface area and how that may influence Hg concentration and distribution in foliar tissue. In total, the leaves in their studies were on the branch longer than at my study site and the leaves were exposed to higher atmospheric Hg concentrations, which could be factors in why I did not observe such a trend in white birch leaves. In the boreal forest the growing season is shorter than in many other regions of the world where Hg uptake has been researched (e.g. sub-tropical forests in China), and background concentrations are often greater (Zhou *et al*., 2019). There is conflicting evidence of Hg saturation in foliage although as studies in regions of China (Kang *et al*., 2019) and Spain (Barquero *et al*., 2019) with longer growing seasons and greater atmospheric Hg concentrations have not indicated saturation with greater final observed Hg concentrations in leaves.

2.4.2 Foliage as mercury passive air samplers

Considering growth dilution that occurs in both conifer and deciduous foliage, the magnitude of Hg uptake and overall increase in Hg observed in both needles and leaves is suggestive of active uptake processes. While Hg accumulates in foliage tissue over the growing season there is some Hg that is reemitted after it has been incorporated into the tissue (Graydon *et al.*, 2006, Yuan *et al.*, 2019). Both foliage types accumulated C and biomass over the growing season although growth was more noticeably for the conifer needles, which only reached full growth towards the end of August. Because the white birch leaves demonstrated uptake rates similar to the MerPAS, this growth coupled with unidentified reemissions of Hg, suggest there are active uptake processes or additional passive uptake processes (other than via the stomata). Other studies have found daily needle uptake rates to be significantly lower than deciduous leaves (e.g. Blackwell *et al.*, 2014, Blackwell *et al.*, 2015), consistent with my observations, although most studies that have investigated conifer needle concentrations have looked at more mature tissues. Barquero *et al.* (2019) suggest that uptake in pine needles, and likely other needles, involves sorption to the external part of the needle rather than primarily stomatal uptake. They suggest this makes needle Hg concentration more dependent on atmospheric concentrations.

Atmospheric Hg concentration, light exposure, and other meteorological factors (Stamenkovic *et al.*, 2008, Siwik *et al.*, 2009, Stamenkovic and Gustin, 2009, Esbrí *et al.*, 2016) have all been shown to influence Hg uptake in foliage. All of these factors vary both spatially and on short (hourly to daily) and long-time scales (seasonally to yearly). The main factors governing atmospheric $Hg(0)_g$ concentration differ depending on season. Esbrí *et al.* (2016) noted that for summer, solar radiation has the strongest impact. Because canopy shading influences light penetration, I expected a difference in Hg concentration in foliage between the different tower heights but observed no such trend. While I observed variation in both wind speed and light penetration with height, this did not clearly influence atmospheric Hg concentration or Hg accumulation in the foliage I measured. That said, the tree canopy continued approximately four meters above my highest sampling heightsuch that the highest samples experienced some shading.

Similarly, I did not see a clear gradient in atmospheric Hg concentrations from the MerPASs deployed at different heights.

The forest site was a pristine location and due to its remote location removed from any point Hg sources and large cities, it had lower than average atmospheric Hg concentrations (North American average background Hg concentration 1.2-1.3 ng m^{-3} [Zhang *et al.*, 2016]). A study found differences in Hg deposition on leaves in a forest canopy that was located in an urban environment with higher overall atmospheric Hg concentration as well as increased Hg(0)$_g$ and Hg(II)$_g$ compared to the rural environment they sampled at (Stupple, 2009). This research noted the higher Hg(0)$_g$ and Hg(II)$_g$ at the urban site contributed to elevated and more variable upper canopy Hg concentrations as well as increased Hg in throughfall (Stupple, 2009). This highlights the importance of understanding atmospheric concentrations and uptake patterns to determine Hg inputs into soils.

The accumulation rate differences between white birch leaves and the MerPASs Hg uptake suggest variability in uptake on even small spatial and temporal scales. While the Hg uptake rates (ng day^{-1}) in leaves varied depending on which sample date was used, Hg concentrations in white birch leaves before senescence began (after the leaves had been exposed to atmospheric Hg for several months) were relatively similar to the MerPAS uptake rate values. While white birch leaves do not act as precise PAS and it is likely there are additional, active uptake processes, the leaves could provide estimates of atmospheric concentrations at very broad sampling scales where deployment of MerPASs or active monitoring is not feasible. Similar to deploying MerPAS, investment of resources is comparably minor compared to active monitoring and to use leaves as indicators of atmospheric Hg, sampling would only require leaves before they changed color and an estimate of growing season length for analysis. As noted however, when considering the uptake rates with changing rates of growth over the season it lends support to active uptake processes in addition to passive uptake through the stomata, or additional passive uptake through alternative mechanisms. Further, when comparing uptake rates after the leaves had started to degrade (September) the Hg concentrations were higher and biased the uptake rates. As a result of the consistent growth and Hg

concentration variability the needles did not act as effective PAS at any point during their first growing season although further investigation of needles should be done to determine rates of uptake on more mature needles.

2.4.3 The role of senescence in the forest mercury cycle

During senescence the chloroplasts are some of the first organelles to breakdown (Lim *et al*., 2007), causing the leaves to turn color as the tree resorbs essential nutrients stored in the leaf tissue (Kikuzawa and Lechowicz, 2011). It is unknown what compounds Hg binds to within needles and leaves, but it is likely a range of compounds based on how Hg is released during decomposition (see Chapter 3). Considering overall differences in tissue composition the compounds Hg is bound to are likely different between conifer needles and deciduous leaves. This is further supported if the primary entry route of gaseous Hg differs between needles and leaves. While there were significant correlations between white birch Hg concentrations and %N, %C, and C:N, this was not the case for black spruce needles. This may be because of differences in uptake pathways or patterns as well as differences in composition between the needles and leaves. Based on the negative correlation with %N observed for white birch with Hg concentration, it is unlikely that Hg is associated with compounds that readily leave the leaf or needle over the growing season.

The last sampling day in August, before any leaves had turned yellow, the leaves were beginning to degrade in quality. This is the point at which Hg concentrations increased at a steeper rate until the leaves abscised and fell. This increase in Hg concentration is not due to a sudden influx of Hg that occurred towards the end of the growing season but instead to do with the resorption of nutrients that is occurring as the leaves start senescing (Makino and Osmond, 1991, Kikuzawa and Lechowicz, 2011). This is supported by my observed %N of leaves that declined significantly when the leaves turned color from green to yellow. This further supports that Hg is not associated with nutrients high in %N that are drawn back into the tree. Because the conifer needles did not senesce that year it is not possible to comment if a similar process would occur, although there was a similar decline in %N with time. Visual senescent stage (i.e. green versus yellow) for white birch leaves could be used as an important timing cue for when foliage collection should occur.

As I observed a clear difference in %N content between these stages, leaf quality may be an important determinant of Hg cycling in forests.

2.4.4 Climate change implications and conclusions

Deciduous leaves demonstrated greater uptake rates of Hg than new conifer needles and because they contribute to litterfall each year, this foliage type cycles Hg more rapidly from the atmosphere into soil systems. New conifer needles do not act as effective PASs and because of growth dilution, Hg uptake rates are difficult to determine. This complicates determining if there are additional, more active Hg uptake mechanisms and how much they contribute to Hg accumulation. It is also because of this dilution there was not a significant relationship with %N or %C over the growing season that could be related to Hg uptake. While uptake rates in black spruce needles after only one growing season were not similar to the MerPASs, multi-year studies should investigate uptake over the entire residence time of a needle on a branch. These data would contribute to passive versus non-passive uptake processes as the main growth phase of the needles would be complete. Deciduous leaves demonstrated Hg uptake rates similar to the MerPASs towards the end of the growing season. While there was variation, this study suggests white birch leaves could be used to monitor atmospheric Hg levels on a broad scale with close monitoring of the forest condition as the relationship broke down during senescence. The significant relationships between %N and Hg concentrations, and %C and Hg concentration in white birch leaves suggests that these could be important indicators as to if the leaves can be effective as the %N declined significantly with color change in the leaves, the same point at which the efficacy of the leaves as PASs stopped.

Projections of climate change in the southern boreal forest are expected to have increased temperatures as well as changing precipitation patterns (Soja *et al*., 2007). As these are both factors that can influence stomatal activity, Hg uptake will likely change with a changing climate. This makes research into partitioning of Hg uptake an important factor in predicting how uptake rates may change and if foliage can be used in the future effectively as indicators of atmospheric Hg. In addition, climate change is also projected to have an impact on tree species composition. There is an anticipated shift in deciduous tree species northward in the boreal forest (Cramer *et al*., 2001, McKenney *et al*., 2007,

2011) with climate warming. As deciduous and coniferous species uptake Hg at different rates, and primary production of forests has been linked to declining atmospheric Hg (Jiskra *et al*., 2018), this could have major implications for atmospheric Hg concentrations. In addition to differences in the amount of Hg sequestered by leaves each year, litter Hg inputs are different based on foliage type. Deciduous leaves drop every autumn in the boreal forest, causing an annual input of Hg while conifer needles drop on multiyear cycles. A shift to more deciduous tree cover would cause a change in litter input quantity and quality at large spatial scales. As deciduous leaves seem to cycle Hg more rapidly from the atmosphere to the soil this species composition change would have broad reaching implications for Hg soil inputs and subsequent downstream implications.

2.5   References

Arnold J., Gustin M.S., Weisberg P.J., 2018. Evidence for nonstomatal uptake of Hg by aspen and translocation of Hg from foliage to tree rings in Austrian pine. Environment Science & Technology 52, 1174–1182.

Assad, M., Parelle, J., Cazaux, D., Gimbert, F., Chalot, M., Tatin-Froux, F., 2016. Mercury uptake into poplar leaves. Chemosphere 146, 1–7.

Barquero, J. I., Rojas, S., Esbrí, J.M., Garcia-Noguero, E.M., Higueras, P., 2019. Factors influencing mercury uptake by leaves stone pine (*Pinus pinea* L.) in Almaden (central Spain). Environmental Science Pollution Research 26, 3129–3137.

Bishop, K.H., Lee, Y., Munthe, J., Dambrine, E., 1998. Xylem sap as a pathway for total mercury and methylmercury transport from soils to tree canopy in boreal forest. Biogeochemistry 40, 101–113.

Blackwell, B.D., Driscoll, C.T., Maxwell, J.A., Holsen, T.M., 2014. Changing climate alters inputs and pathways of mercury deposition to forested ecosystems. Biogeochemistry 119, 215–228.

Blackwell, B.D., Driscoll, C.T., 2015. Deposition of mercury in forests along a montane elevation gradient. Environment Science & Technology 49, 5363–5370.

Demers, J.D., Driscoll, C.T., Fahey, T.J., Yavitt, J.B., 2007. Mercury cycling in litter and soil in different forest types in the Adirondack region, New York, USA. Ecological Applications 17, 1341–1351.

Demers, J.D., Blum, J.D., Zak, D.R., 2013. Mercury isotopes in a forested ecosystem: implications for air-surface exchange dynamics and the global mercury cycle. Global Biogeochemical Cycles 27, 222–238.

Driscoll, C.T., Mason, R.P., Chan, H.M., Jacob, D.J., Pirrone, N., 2013. Mercury as a global pollutant: sources, pathways, and effects. Environment Science & Technology 47, 4967–4983.

Ericksen, J. A., Gustin, M.S., Schorran, D.E., Johnson, D.W., Lindberg, S.E., Coleman, J.S., 2003. Accumulation of atmospheric mercury in forest foliage. Atmospheric Environment 37, 1613–1622.

Esbrí, M.J., Martínez-Coronado, A., Higueras, P.L., 2016. Temporal variations in gaseous elemental mercury concentrations at a contaminated site: main factors affecting nocturnal maxima in daily cycles. Atmospheric Environment 125, 8–14.

Gan, S., Amasino, R.M., 1997. Making sense of senescence. Plant Physiology 113, 313–319.

Graydon, J.A., St. Louis, V.L., Lindberg, S.E., Hintelmann, H., Krabbenhoft, D.P., 2006. Investigation of mercury exchange between forest canopy vegetation and the atmosphere using a new dynamic chamber. Environment Science & Technology 40, 4680–4688.

Graydon, J.A., St. Louis, V.L., Hintelmann, H., Lindberg, S.E., Sandilands, K.A., Rudd, J.W.M., Kelly, C.A., Hall, B.D., Mowat, L.D., 2008. Long-term wet and dry deposition of total and methyl mercury in the remote boreal ecoregion of Canada. Environment Science & Technology 42, 8345–8351.

Grigal, D.F., 2002. Inputs and outputs of mercury from terrestrial watersheds: a review. Environmental Reviews 10, 1–39.

Frescholtz, T.F., Gustin, M.S., 2004. Soil and foliar mercury emission as a function of soil concentration. Water, Air, and Soil Pollution 155, 223–237.

Frescholtz, T.F., Gustin, M.S., Schorran, D.E., Fernandez, G.C.J., 2003. Assessing the source of mercury in foliar tissue of quaking aspen. Environmental Toxicology and Chemistry 22, 2114–2119.

Kang, H., Lui, X., Guo, J., Wang, B., Xu, G., Wu, G., Kang, S., Huang, J., 2019. Characterization of mercury concentration from soils to needle and tree rings of Schrenk spruce (*Picea schrenkiana*) of the middle Tianshan Mountains, northwest China. Ecological Indicators 104, 24–31.

Kikuzawa, K., Lechowicz, M.J., 2014. Ecology of Leaf Longevity, first ed. Springer Verlag, Tokyo.

Laacouri, A., Nater, E.A., Kolka, R.K., 2013. Distribution and uptake dynamics of mercury in leaves of common deciduous tree species in Minnesota, U.S.A. Environmental Science & Technology 47, 10462–10470.

Lim, P.O., Kim, H.J., Nam, H.G., 2007. Leaf senescence. Annual Review of Plant Biology. 58, 115–136.

Lindberg, S., Bullock, R., Ebinghaus, R., Engstrom, D., Feng, X., Fitzgerald, W., Pirrone, N., Pretsbo, E., Seigneur, C., 2007. A synthesis of progress and uncertainties in attributing the sources of mercury in deposition. Ambio 36, 19–32.

Makino, A. Osmond, B., 1991. Effects of nitrogen nutrition on nitrogen partitioning between chloroplasts and mitochondria in pea and wheat. Plant Physiology 96, 355–362.

McKenney, D.W., Pedlar, J.H., Lawrence, K., Campbell, K., Hutchinson, M.F., 2007. Potential impacts of climate change on the distribution of North American trees. Bioscience 57, 939–948.

McKenney, D.W., Pedlar, J.H., Rood, R.B., Price, D., 2011. Revisiting projected climate shifts in the climate envelopes of North American trees using updated general circulation models. Global Change Biology 17, 2720–2730.

McLagan, D.S., Mazur, M.E.E., Mitchell, C.P.J., Wania, F., 2016a. Passive air sampling of gaseous elemental mercury: a critical review. Atmospheric Chemistry and Physics 16, 3061–76.

McLagan D.S., Mitchell C.P.J., Huang H., Lei Y.D., Cole, A.S., Steffen, A., Hung, H., Wania, F., 2016b. A high-precision passive air sampler for gaseous mercury. Environmental Science Technology Letters 3, 24–29.

McLaughlin, J., 2009. Boreal mixed-wood watershed riparian zone cation-cycling during two contrasting climatic years. Soil Science Society of America Journal 73, 1408–1418.

Millhollen, A.G., Gustin, M.S., Obrist, D., 2006. Foliar mercury accumulation and exchange for three tree species. Environment Science & Technology 40, 6001–6006.

Moore, T.R., Trofymow, J.A., Taylor, B., Prescott, C., Camiré, C., Duschene, L., Fyles, J., Kozak, L., Kranabetter, M., Morrison, I., Siltanen, M., Smith, S., Titus, B., Visser, S., Wein, R., Zoltai, S., 1999. Litter decomposition rates in Canadian forests. Global Change Biology 5, 75–82.

Niu, Z., Zhang, X., Wang, Z., Ci, Z., 2011. Field controlled experiments of mercury accumulation in crops from air and soil. Environmental Pollution 159, 2684–2689.

Obrist, D., Johnson, D.W., Lindberg, S.E., Luo, Y., Hararuk, O., Bracho, R., Battles, J.J., Dail, D.B., Edmonds, R.L., Monson, R.K., Ollinger, S.V., Pallardy, S.G., Pregitzer, K.S., Todd, D.E., 2011. Mercury distribution across 14 U.S. forests. part I: spatial patterns of concentration in biomass, litter and soils. Environment Science & Technology 45, 3974–3981.

Parton, W., Silver, W.L., Burke, I.C., Grassens, L., Harmon, M. E., Currie, W.S., King, J.Y., Adair, E.C., Brandt, L.A., Hart, S.C., Fasth, B., 2007. Global-scale similarities in nitrogen release patterns during long-term decomposition. Science 315, 361–364.

Pinheiro, J., Bates, D., DebRoy, S., Sarkar, D., R Core Team. 2019. nlme: Linear and Nonlinear Mixed Effects Models. https://CRAN.R-project.org/package=nlme.

Rea, A.W., Lindberg, S.E., Scherbatskoy, T., Keeler, G.J., 2002. Mercury accumulation in foliage over time in two northern-hardwood forests. Water, Air, and Soil Pollution 133, 49–67.

Restrepo, A.R., Hayward, S.J., Armitage, J.M., Wania F., 2015. Evaluating the PAS-SIM model using a passive air sampler calibration study for pesticides. Environmental Science: Processes & Impacts 17, 1228−1237.

Richardson, J.B., Friedland, A.J., 2015. Mercury in coniferous and deciduous upland forests in northern New England, USA: Implications of climate change. Biogeosciences 12, 6737–6749.

Risch, M.R., DeWild, J.F., Gay, D.A., Zhang, L., Boyer, E.W., Krabbenhoft, D.P., 2017. Atmospheric mercury deposition to forests in the eastern USA. Environmental Pollution 228, 8–18.

Schroeder, W.H., Munthe, J., 1998. Atmospheric mercury – an overview. Atmospheric Environment 32, 809–822.

Siwik, E.I.H., Campbell, L.M., Mierle, G., 2009. Fine-scale mercury trends in temperate deciduous tree leaves from Ontario, Canada. Science of the Total Environment 407, 6275–6279.

Soja, A.J., Tchebakova, N.M., French, N.H.F., Flannigan, M.D., Shugart, H.H., Stocks, B.J., Sukhinin, A.I., Parfenova, E.I., Chapin III, F.S., Stackhouse Jr., P.W., 2007. Climate-induced boreal forest change: predictions versus current observations. Global and Planetary Change 56, 274–296.

Stamenkovic, J., Gustin, M.S., Arnone, J.A., Johnson, D.W., Larsen, J.D., Verburg, P.S.J., 2008. Atmospheric mercury exchange with a tallgrass prairie ecosystem housed in mesocosms. Science of the Total Environment 406, 227–238.

Stamenkovic, J., Gustin, M. S., 2009. Nonstomatal uptake versus stomatal uptake of atmospheric mercury. Environment Science & Technology 43, 1367–1372.

Stupple, G. W., 2009. Air Mercury Speciation, Foliar Uptake, and Wash-Off along an Urban-Rural Gradient. Master's thesis, University of Toronto, Toronto, Canada.

United Nations Environment Program, 2018. Global Mercury Assessment 2018. UNEP Chemicals Branch, Geneva, Switzerland, 1–62.

U.S. EPA. "Method 7473 (SW-846): Mercury in Solids and Solutions by Thermal Decomposition, Amalgamation, and Atomic Absorption Spectrophotometry," Revision 0: Washington, DC, 1998.

Yuan, W., Sommar, J., Lin, C., Wang, X., Li, K., Liu, Y., Zhang, H., Lu, Z., Wu, C., Feng, X., 2019. Stable isotope evidence shows re-emission of elemental mercury vapor occurring after reductive loss from foliage. Environment Science & Technology 53, 651−660.

Zhang, L., Wright, L.P., Blanchard, P., 2009. A review of current knowledge concerning dry deposition of atmospheric mercury. Atmospheric Environment 43, 5853–5864.

Zhou, J. Du, B., Shang, L., Wang, Z., Cui, H., Fan, X., Zhou, J. 2020. Mercury fluxes, budgets, and pools in forest ecosystems of China: A review. Critical Reviews in Environmental Science and Technology, 50, 1411-1450.

Zhang, Y., Jacob, D.J., Horowitz, H.M., Chen, L., Amos, H.M., Krabbenhoft, D.P., Slemr, F., St. Louis, V.L., Sunderland, E.M., 2016. Observed decrease in atmospheric mercury explained by global decline in anthropogenic emissions. Proceedings of the National Academy of Science 113, 526–531.

Chapter 3

3 Foliage type controls mercury release from forest litters via decomposition

3.1 Introduction

Forests have an important role in carbon (C) and nutrient cycling at local to global scales. Over the last twenty years research has increasingly highlighted the role of the terrestrial landscape and forests in biogeochemical cycling of non-nutrient elements, including mercury (Hg) (e.g. Grigal, 2002, Obrist *et al*., 2007). Mercury is emitted to, and circulated in, a large atmospheric pool dominated by gaseous elemental Hg (GEM, $Hg(0)_g$), with much smaller fractions of gaseous oxidized Hg (GOM, $Hg(II)_g$), and particle bound Hg (PBM, $Hg(II)_s$) (Schroeder and Munthe, 1998).

Mercury accumulates in both vegetation and soil of undisturbed forests (Stamenkovic and Gustin, 2009, Obrist *et al*., 2011, Demers *et al*., 2013). The forest canopy is a significant sink for atmospheric Hg because of the large surface area and high aerodynamic resistance (Zhang *et al*., 2009), and research has shown that much of this sequestration in vegetation is not solely due to surface deposition of $Hg(II)_g$ and $Hg(II)_s$ but also uptake processes including stomatal uptake of $Hg(0)_g$ (Stamenkovic and Gustin, 2009). Through stomatal uptake gaseous Hg is taken into the leaf when the stomata are open and incorporated into leaf tissues, predominantly in stomatal and epidermal cell walls (Millhollen *et al*., 2006, Stamenkovic and Gustin, 2009). Although oxidation and re-emission of tissue-bound Hg occurs, there is a net accumulation of Hg over the growing season (Grigal, 2002, Rea *et al*., 2002, Assad *et al*., 2016), and the accumulation rate varies among tree species (Graydon *et al*., 2008, Siwik *et al*., 2009). The continuous accumulation of Hg in leaves over the growing season and the large mass deposited to the forest floor annually makes litterfall a main input of Hg to forest soils (Demers *et al*., 2007, Graydon *et al*., 2008, Risch *et al*., 2017).

Coniferous needles generally have higher Hg concentrations as a result of the increased exposure time to the atmosphere (Niu *et al*., 2011, Blackwell and Driscoll, 2015), although deciduous species have been suggested to play a more active role in gaseous Hg

exchange, potentially due to greater stomatal conductance and/or larger leaf specific area, and as a result, accumulate Hg more rapidly (Millhollen *et al*., 2006). The Hg loading from litterfall in a forest is highly variable and generally lower in coniferous forests than deciduous forests due to greater annual litter mass inputs from deciduous species (Demers *et al*., 2007, Richardson and Friedland, 2015).

Following litterfall, litter decomposition is controlled by temperature, moisture, and species-level differences in litter quality (Berg *et al*., 1993, Moore *et al*., 1999, Parton *et al*., 2007, Cornwell *et al*., 2008). The fallen litter with associated Hg is then subject to decomposition although the specific processes (and their rates) that govern Hg release from litter and/or its incorporation into soil organic matter (SOM) are not described. Litter quality regulates decomposition rates and litter mass loss because it influences both microbial community composition, and how rapidly microorganisms decompose the litter (Taylor *et al*., 1989). Litter that tends to decompose at slower rates is commonly referred to as lower quality (from a microbial perspective) and is considered recalcitrant, while fast decomposing litters are referred to as higher quality, and considered more labile (Manzoni *et al*., 2010).

Dissolved organic matter (DOM) (i.e. organic molecules < 0.45 μm) is one product of decomposition and plays a major role in the transport of energy and pollutants in soil pore water and groundwater (Kalbitz *et al*., 2000). As Hg binds strongly to DOM (Grigal, 2002, Jiang *et al*., 2015), the production and release of DOM by litter decomposition would be expected to regulate rates of Hg release into soils. Given that deciduous leaves decompose more rapidly than conifer needles, I hypothesized that, upon senescence and litterfall in the autumn, deciduous leaf litter will release DOM and associated Hg via leachate into underlying soils more rapidly than coniferous litter. Similarly, because warmer temperatures stimulate microbial activity, I hypothesized that increasing temperature conditions during decomposing will release DOM and associated Hg via leachate more rapidly than litters decomposing at a cooler temperature. To investigate this senesced tree litter and soil was collected from the southern boreal forest in Ontario, Canada, and I conducted a laboratory-based mesocosm experiment to evaluate the role of

tree litter type and temperature on the release of DOM and Hg immediately after litterfall. The specific objectives of this study were to:

1) Determine the influence of litter type (conifer vs deciduous) on the release of Hg from litter into soil;

2) Determine the influence of temperature on the release of Hg from litter into soil;

3) Relate Hg concentrations in soil porewater with DOM quantity and quality.

3.2 Methods

3.2.1 Litter and soil collection

Tree litterfall and forest soil were collected near White River, Ontario in the mixed broad leaf deciduous and coniferous southern boreal forest (48°21'N, 85°21'W) during senescence in early October 2018. The dominant tree species in the forest stand are white birch (*Betula papyrifera*), balsam fir (*Abies balsamea*) and black spruce (*Picea mariana*); the stand is approximately 70 years old after regeneration following a fire and the soil is classified as Typic Haplorthod based on USDA-NRCS classification, common to the boreal forest under deciduous and coniferous tree stands (McLaughlin, 2009).

The litter and soil samples were collected within 200 meters of each other. The soil (top 5 cm mineral soil) was collected in three locations within the forest stand. At each location, the fresh litter layer on the surface was scraped off and the mineral soil was collected manually. Recently fallen deciduous litter (primarily white birch) was collected from the top of a moss layer that made it possible to separate recently fallen leaves from further decomposed litter. Recently fallen coniferous litter (primarily black spruce and jack pine (*Pinus banksiana*)) was collected under four trees, two black spruce and two jack pine. All sample collection was done with clean tools and powder-free nitrile gloves were worn. Samples were kept cool with icepacks in coolers and transported to the Biotron Institute for Experimental Climate Change (Biotron) at Western University where they were stored at 4 °C to minimize microbial activity before the experimental mesocosms were set up.

3.2.2 Litter and soil characterization

Clean tools and gloves were worn for all handling of soil and litter. The soils from the three sites were homogenized by hand and put through a 4 mm sieve while still damp. Prior to setting up the mesocosms I analyzed the soil and litter to determine soil texture, soil moisture content, percent C (%C) by mass of soil and litter, percent nitrogen (%N) by mass of soil and litter, and Hg concentration of the soil and litter. Prior to analysis, all litter was blotted to remove excess water and sorted to remove non-leaf or needle fragments. In addition, only similar-colored (yellow) white birch leaves were included in the experiment to control for differing stages of senescence that might affect Hg concentrations because preliminary analysis revealed Hg concentrations were significantly different based on leaf color (see Appendix B). Soil and litter samples were freeze dried then homogenized using a stainless-steel grinder or mortar and pestle before running total solid Hg, %C, and %N analyses.

Soil texture was determined by hand using the feel method (Thien, 1979) on field moist homogenized soil. Soil and litter moisture contents were determined gravimetrically for six replicates by placing 5 g of damp soil or litter in a 60 °C oven for 48 hours and comparing the mass before and after to analyze water loss. The moisture contents were determined with the equation:

$$\% \text{ Moisture} = ((wwt - dwt \text{ (g)} / dwt \text{ (g)}) \times 100$$

Moisture content calculations were used to provide dry weight equivalents for all soil and litter.

All leaves and needles were rinsed with 18.2 MOhm deionized water before analysis. To control for leaf to leaf variability, white birch leaves were cut in half, and half of each leaf was placed in the mesocosm experiment while the other half was analyzed for initial %C and %N by mass and Hg concentration such that a direct paired comparison could be made between initial litter values and changes due to treatment effects during the experiment. For coniferous litter samples, homogenized litter was weighed into aliquots for all mesocosms, and half of each aliquot was used for initial characterization of %C,

%N, and Hg, while the other half was used in the mesocosm experiment to allow for a more direct comparison of litter before and after mesocosm incubations. Similarly, soil samples were sieved and well homogenized before initial characterization and sub-sampled from each mesocosm. Percent C and N (by mass) in litter and soil were measured by purge and trap chromatography using an Elementar Isotope Cube® CNSHO elemental analyzer. After initial daily factor check using sulfanilamide, blanks, duplicates, and certified reference materials (CRM) were run every ten samples. The CRM for litter samples was Birch Leaf Standard (CatNo. B2166) and for soil samples Soil Standard Peaty (CatNo. B2176) was used. All duplicates and recovery values were within 20% and all reported percent differences were under 20%; if a sample exceeded these values the samples were further homogenized and re-run.

Mercury concentrations in the soil and litter were determined in the ISO 17025 accredited Analytical Services Laboratory in the Biotron using a Milestone® DMA-80 analyzer following standard method US EPA 7473 (1998) of Thermal Decomposition Atomic Adsorption (DMA). After calibration, blanks, duplicates, matrix spikes, matrix spike duplicates, and a CRM were run every ten samples. Marine sediment (PACS-3) was used as the CRM for litter and soil (National Resource Council Canada, 2018). Percent recovery was within 10% for initial check standards and 20% for matrix spikes and CRM in the sample runs. Reported percent differences for duplicates were all within 20%. If any checks failed these standards, samples were further homogenized and re-run. Mercury concentrations were analyzed as concentrations and also compared by determining the Hg:C (ng:g) ratio to standardize for % C in the litter and soil.

3.2.3 Mesocosm design

The experimental mesocosms (36 total) were 500 mL glass jars with lids. Each lid had a small hole in the top with a foam plug in it to allow for gas exchange but prevent particulate contamination. There were three litter treatments: coniferous litter (black spruce / jack pine); deciduous litter (white birch), and no litter which acted as the control. Each mesocosm received 21±0.1 g dry weight equivalent of field moist soil (approximately one third of the mesocosm by volume). A Rhizon® porewater sampler (pore size 0.15 μm, 5 cm long) was installed horizontally in each mesocosm under the

soil to non-destructively collect soil porewater. The coniferous treatment mesocosms received 3.8 g dry weight equivalent coniferous litter and the deciduous treatment received 1.8 g dry weight equivalent of leaves placed on top of the soil. With the addition of the litters each mesocosm was approximately half full (headspace = 250 mL). A thin layer of plastic mesh (1 mm^2 mesh size) separated the litter from the soil to facilitate removal and weighing of the litter from the mesocosms at the end of the experiment. The final mass of each assembled mesocosm was measured to monitor and maintain gravimetric moisture content over the experiment.

Mesocosms were incubated at two temperature treatments (12 °C, 16 °C), with each treatment consisting of six replicates (3 litters × 2 temperatures × 6 replicates = 36 total). The 12 °C temperature represents the average growing season temperature at the field sites where the samples were acquired (approx. 11.9 °C) (see Chapter 2, and McLaughlin, 2009). The 16 °C temperature value was chosen based on the Intergovernmental Panel on Climate Change (IPCC) (2013) projection of +4 °C increased (range 2.6 to 4.8, mean = 3.7) mean surface air temperature from climate warming scenario Representation Concentration Pathway (RCP) 8.5 at the end of the century for the boreal region. The temperatures were controlled in environmental growth chambers and all mesocosms were kept in darkness except during porewater sampling, moisture additions, and to change the mesocosm lids before respiration analysis.

3.2.4 Mesocosm sampling

Heterotrophic respiration (CO_2 flux) was used to estimate microbial activity in each mesocosm and was measured using a Licor® Infrared Gas Analyzer (IRGA LI-8100A) with a Multiplexer unit (LI-8150). These measurements were taken every two weeks in the dark within the environmental chambers. The headspace in each mesocosms was purged for accumulated CO_2 for 45 seconds prior to the measurement, and then the CO_2 concentration was measured from the soil for 90 seconds expressed as a flux as $\mu mol\ CO_2$ $m^{-2}s^{-1}$.

Porewater samples were taken every two weeks from the Rhizon samplers. The samples were analyzed alternating for dissolved organic carbon (DOC) and carbon quality

analyses or total mercury (THg). To sample porewater, a clean (20 mL) syringe was attached to the end of the Rhizon sampler and approximately 10 mL was extracted for analysis. Samples for DOC and carbon quality analyses were stored in clean glass bottles at 4 °C stored in darkness until analysis, or immediately frozen in acid washed 20 mL polyethylene vials for THg analysis. Initial masses of each mesocosm were maintained throughout the experiment with deionized water added following porewater sampling.

3.2.5 Physical and Chemical Analyses

The DOC concentrations in porewater were determined using the persulfate wet oxidation method on an Aurora® 1030W Total Carbon analyzer. After initial daily calibration of the instrument, blanks, duplicates, and standards were run every ten samples. All duplicates and recovery values were within 20% and all reported percent differences were <20%; if a sample exceeded these values the samples were further homogenized and re-run. Proxy measures of DOM quality to make indirect measures of DOM quality (Cory and McKnight, 2005) and indications of the humification, freshness, and source of DOM (Fellmen *et al*., 2010) were determined using fluorescence and absorbance spectrometry using a Horiba Aqualog® spectrometer. The porewater was analyzed using excitation and emission matrices focusing on three common indices: humification index (HIX), freshness index (BIX), and fluorescence index (FI), as well as specific ultraviolet absorption at 254 nm (SUVA$_{254}$) wavelength. The excitation wavelengths ranged from 240 to 600 nm with 8 nm increments and the emission wavelengths ranged from 210 to 620 nm with 5 nm increments, all with an integration time of 0.75 seconds. The matrices were then used to calculate the HIX, BIX and FI optical indices using R Software (base statistics package, R Core Team 2012) with the equations described by Fellman *et al*. (2010). Specific UV absorbance at 254 nm (SUVA$_{254}$) was used as a proxy for DOC aromaticity (Weishaar *et al*., 2009). All samples were diluted 1:20 with deionised water to minimize inner filtering effects, and all samples were normalized under water Raman peak at an excitation of 350 nm to account for variation in lamp intensity (Lawaetz and Stedmon, 2009). The final SUVA$_{254}$ values were calculated by dividing absorbance at 254 nm by the DOC concentration (mg L^{-1}) of the sample (×100).

The THg concentration of porewater samples were measured using Oxidation, Purge and Trap and Cold-Vapour Atomic Fluorescence Spectroscopy (CVAFS) on a Tekran® 2600 Total Hg following standard method US EPA 1631 (2002). Frozen samples were thawed rapidly in a warm water bath before being transferred to glass analytical vials and immediately oxidized with bromine monochloride (BrCl). Samples were left for 24 hours with an excess of BrCl before being sequentially reduced with hydroxylamine hydrochloride ($NH_2OH \cdot HCl$) and then stannous chloride ($SnCl_2$) before analysis. Samples were purged with nitrogen gas (N_2) to strip $Hg(0)_g$, where it was carried to a gold trap, then thermally desorbed and carried to another gold trap where it is again desorbed and carried to a CVFAS cell for detection. The instrument was calibrated daily before samples were run and appropriate method blanks, bottle blanks, duplicates, matrix spikes, matrix spike duplicates, and standards were run and within accepted range (under the reporting limit for method blanks and bottle blanks, within 80% recovery for matrix spikes, and 20 reported % difference for duplicates) otherwise the sample was rerun. Concentrations were corrected for method blanks that were run every ten samples.

After three months all mesocosms were destructively sampled. The litter in each mesocosm was carefully removed and weighed to determine mass loss (%) relative to starting mass using dry weight equivalents using the formula:

$$\% \ mass \ loss = ((initial \ dwt \ (g) - final \ dwt \ (g))/initial \ dwt \ (g))100$$

Total Hg concentration, %C and %N in soil and litter were analyzed using the same methods as for the initial characterization; C:N of both litter types and soil was calculated from %C and %N values.

3.2.6 Statistical analyses

Initial %C, %N, C:N, and Hg concentrations of litter (and soil for Hg) were compared using a one-way MANOVA and one-way ANOVA, respectively. I also examined these same variables using a two-way ANOVA with temperature and litter type as main effects to ensure there were no pre-existing (non-intentional) differences among the mesocosms placed into different temperature treatments. I also accounted for any initial conditions

and the temporal non-independence of sample analysis for %C, %N, C:N and Hg concentrations of litter (and soil for Hg) when assessing treatment variables using a two-way repeated measures (RM) multivariate ANOVA (MANOVA) and RM-ANOVA , respectively. A two-way ANOVA with temperature and litter type as main effects was used to analyze changes in decomposition (mass loss) of the litter following the three-month incubation period. A two-way RM-ANOVA was also used to examine changes in porewater over the experiment for heterotrophic respiration, Hg concentration, DOC content, and $SUVA_{254}$. Data was log_{10} transformed or Tukey transformed where necessary to normalize distribution, normal distributions were analyzed using residual histograms, QQ-plots and using Shapiro Wilks tests for normality. A two-way RM-MANOVA test was also used for analysis of the HIX, BIX, and FI. All pairwise significance tests were performed using Tukey post hoc tests where necessary. I ran Spearman's correlations on porewater data including DOC, EEMs, THg, and $SUVA_{254}$. Analyses were run using Statistica 7 (StatSoft. Inc., 2004) or the base statistics package in R Software (2019).

3.3 Results

The initial %C, %N by mass and C:N values all differed between coniferous and deciduous litter with coniferous litter having greater %C and lower %N values than deciduous litter that resulted in higher C:N for the coniferous litter (Figure 3.1 A-C)(all statistics P<0.001, d.f.=1, 20). Some initial differences existed among the coniferous litter aliquots prior to mesocosm initiation that led to 12 °C mesocosms receiving slightly, but significantly lower C:N litter (temperature $F_{3,18}$=3.31, P=0.044; temperature-by-litter interaction $F_{3,18}$=3.90, P=0.026). Because all deciduous litter was created from dividing individual leaves for initial and post experimental analysis the deciduous litter treatments were in a similar range before incubation between temperature treatments. Initial Hg concentrations were significantly greater in the soil compared to either litter types, and among litters, greater in coniferous than deciduous litter ($F_{1,22}$=22.8, P<0.001) for both raw values and when standardized for the %C in the litter (Table 3.1). Initial soil %C was 26.51 ± 0.11, 1.03 ± 0.004 %N, and had a C:N of 25.78 ± 0.05.
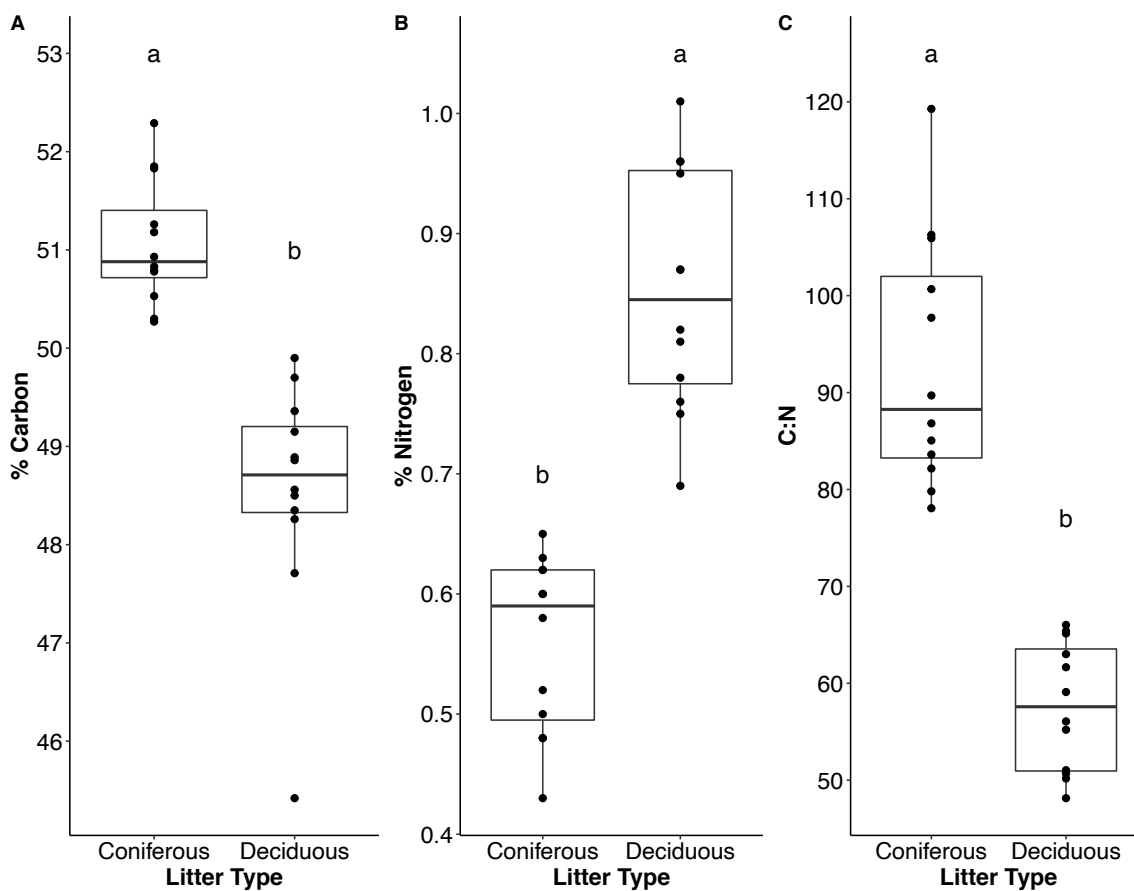
Figure 3.1 Initial litter quality (A-C: %C, %N, C:N) variables of coniferous (black spruce / jack pine) and deciduous (white birch) litters. Boxes display interquartile range, median (line in box), and whiskers are maximum and minimum values excluding outliers (any values over 1.5 times the interquartile range over the 75th percentile or under 1.5 times the interquartile range under the 25th percentile). Letters denote significant differences using Tukey post-hoc comparisons on a two-way ANOVA.

Table 3.1 Initial and final Hg concentrations (ng g^{-1}) and Hg to C (ng:g) ratios in mineral soil used in three month incubation experiment at two temperature treatments (12 °C and 16 °C). Soil was bare (control), under coniferous litter (black spruce/ jack pine), or under deciduous (white birch) litter. Values are means ± SE.

		Initial Hg (ng g^{-1})	Initial Hg:C (ng:g)	Final Hg (ng g^{-1})	Final Hg:C (ng:g)
Control	12 °C	121.47 ± 0.003	453.01 ± 20.89	133.09 ± 5.37	602.03 ± 51.40
	16 °C			135.15 ± 1.58	515.92 ± 31.56
Coniferous	12 °C	118.70 ± 0.003	472.80 ± 20.94	127.67 ± 1.38	545.16 ± 20.69
	16 °C			125.44 ± 3.57	496.67 ± 17.23
Deciduous	12 °C	117.52 ± 0.020	461.97 ± 28.21	126.09 ± 1.73	543.30 ± 28.87
	16 °C			127.15 ± 4.47	538.78 ± 34.82

3.3.1 Mass loss

Litter decomposition (expressed as % mass loss) was lowest in the deciduous litter (Litter: $F_{1,20}$=4.391, P=0.049) incubated at 12 °C (Temperature: $F_{1,20}$=4.80, P=0.041), where litter mass loss was approximately 10% less than in all other treatments (Figure 3.2). Coniferous litter mass loss was not significantly different between the temperature treatments leading to a significant litter × temperature interaction ($F_{1,20}$=10.8, P=0.004).
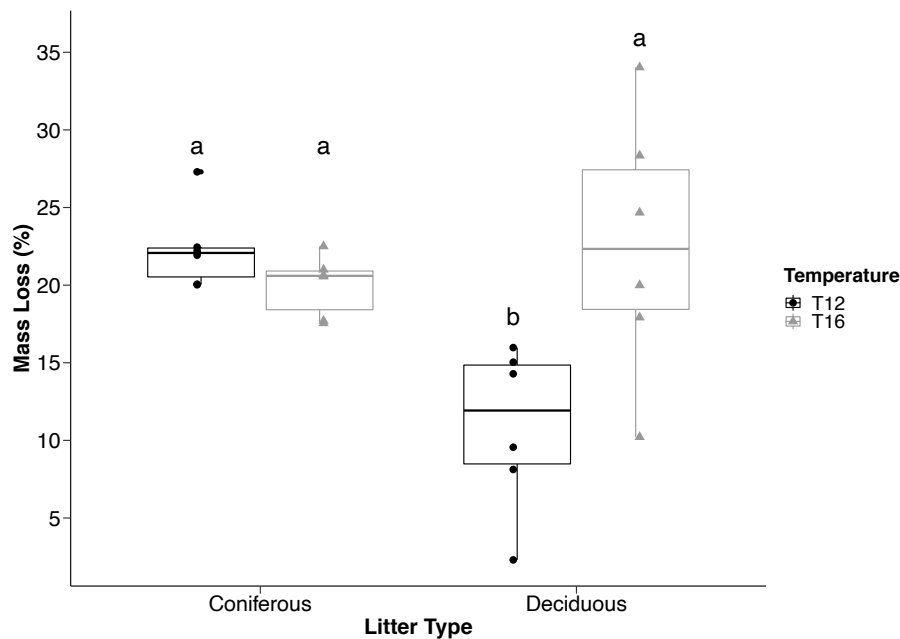
Figure 3.2 The percent mass loss (mean ± SE) of homogenized coniferous litter (black spruce/ jack pine) and deciduous litter (white birch) after three months of incubation at two temperature treatments (T12=12 °C and T16=16 °C). Letters denote significant differences using Tukey post-hoc comparisons on a two-way ANOVA. Boxes display interquartile range, median (line in box), and whiskers are maximum and minimum values excluding outliers (any values over 1.5 times the interquartile range over the 75th percentile or under 1.5 times the interquartile range under the 25th percentile).

3.3.2 Litter quality

The overall litter quality trends remained after three months incubation such that the coniferous litter had lower %N values and greater %C and C:N than the deciduous litter (Figure 3.4 A-C) that was consistent for both temperature incubation treatments (Appendix A). The %C and C:N values of both litter types decreased over time at both temperatures compared to initial values (Figure 3.3 A-C) (all Wilk's values significant $P<0.001$ except Litter × Temperature × Time interaction that was non-significant). There

was no significant effect of temperature treatment on post-incubation %C, %N, or C:N values, however C:N showed significant Litter × Temperature interaction ($F_{1,20}$=17.7, P<0.001) where C:N was greater in 16 °C mesocosms compared to 12 °C mesocosms for conifer litter, but the opposite trend was observed in deciduous litter. These differences were driven by small, but significant differences in %N ($F_{1,20}$=16.9, P=0.001), where increases in litter %N were greater in the deciduous litter after incubation at 16 °C than 12 °C, and the opposite trend emerged for the coniferous litter with greater final %N at 12 °C (approximately 0.75%) than 16 °C (approximately 0.70%).
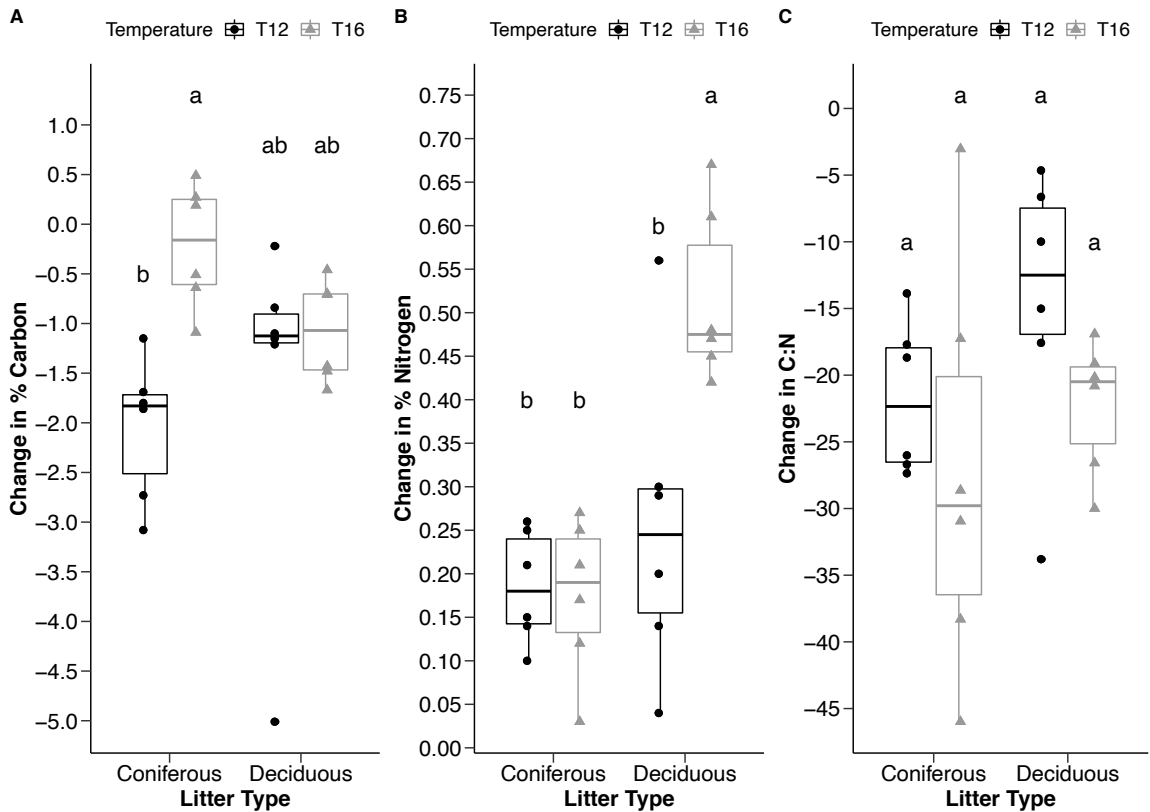
Figure 3.3 Changes in litter quality for coniferous litter (black spruce/ jack pine) and deciduous litter (white birch) values after three-month incubation (A-C: %C, %N, C:N ratios) at two temperature treatments (T12=12 °C and T16=16 °C). Letters denote significant differences using Tukey post-hoc comparisons. Boxes display interquartile range, median (line in box), and whiskers are maximum and minimum values excluding outliers (any values over 1.5 times the interquartile range over the 75th percentile or under 1.5 times the interquartile range under the 25th percentile).
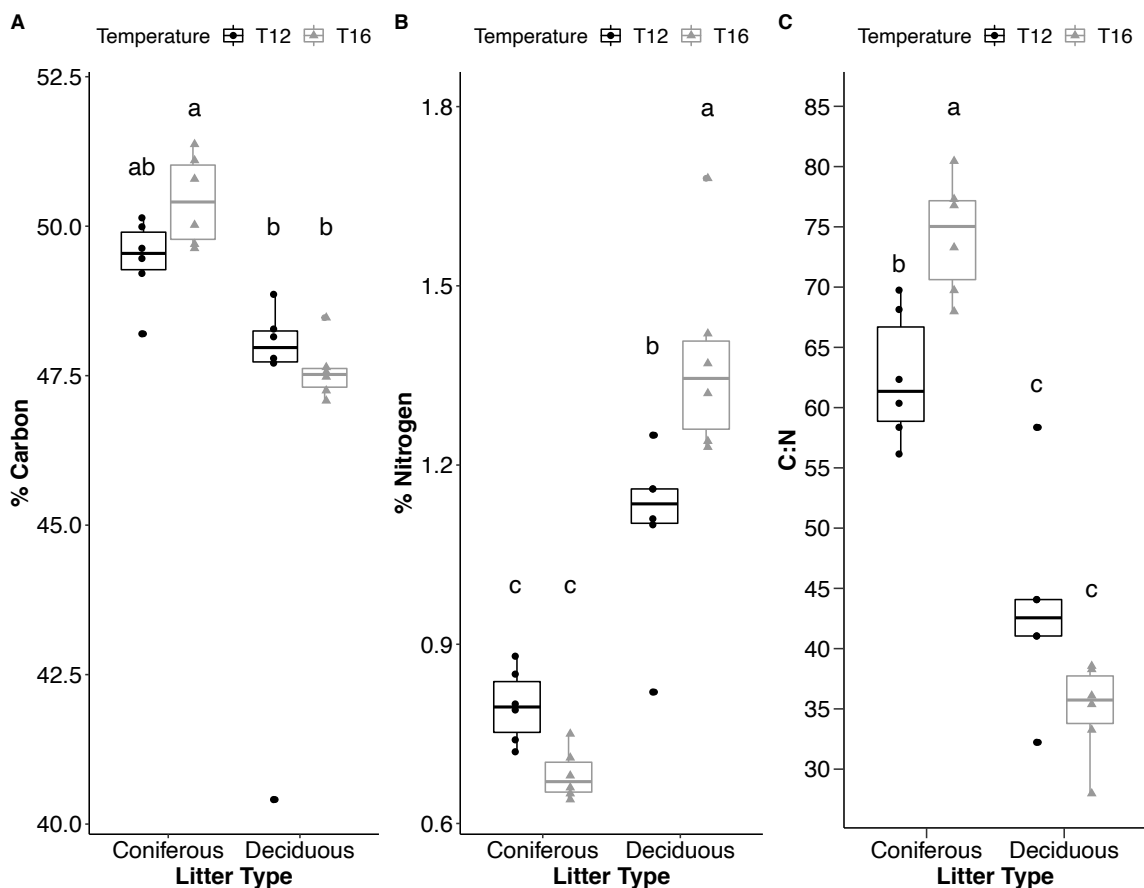
Figure 3.4 Final litter quality variables for coniferous litter (black spruce/ jack pine) and deciduous litter (white birch) values after three-month incubation (A-C: %C, %N, C:N ratios) at two temperature treatments (T12=12 °C and T16=16 °C). Letters denote significant differences using Tukey post-hoc comparisons. Boxes display interquartile range, median (line in box), and whiskers are maximum and minimum values excluding outliers.

3.3.3 Mercury in litter and soil

After three months incubation, the final litter Hg concentrations and Hg:C were higher than the initial concentrations for both litter types at 12 °C, and for the deciduous litter at 16 °C (Table 3.2). The final Hg concentration in conifer needles at 16 °C was slightly lower than the initial Hg concentration while there appears to be a dramatic increase in conifer needles at 12 °C, which corresponds to the greater change in %C observed in at

this temperature. The final Hg concentrations and Hg:C were not significantly different for coniferous litter at 16 °C to the initial values (Table 3.2), but final Hg concentrations and Hg:C were still higher in 12 °C coniferous litter than both deciduous litters (Table 3.2). Final soil Hg concentrations and Hg:C increased across treatments with time ($F_{1,30}$=35.0, P<0.001) regardless of litter type or if no litter was added, and neither temperature ($F_{1,30}$=0.06, P=0.801) nor litter type ($F_{2,30}$=2.32, P=0.115) influenced the final Hg concentrations (Table 3.1). There was no significant main effect of Temperature or Litter on final Hg:C in litter but there was an interaction of Litter and Temperature ($F_{1,20}$=6.07, P=0.023) whereby the Hg:C was greater at 16 °C for deciduous but lower for coniferous litter and coniferous litter had greater Hg:C at 12 °C.

Table 3.2 Initial and final Hg concentrations (ng g^{-1}) and Hg to C (ng:g) ratios in coniferous (black spruce/ jack pine) and deciduous (white birch) litter before and after three month decomposition incubation at two temperature treatments (12 °C and 16 °C). Values are means ± SE.

		Initial Hg (ng g^{-1})	Initial Hg:C (ng:g)	Final Hg (ng g^{-1})	Final Hg:C (ng:g)
Coniferous	12 °C			53.90 ± 2.04	109.05 ± 4.15
		37.59 ± 2.7	70.63 ± 4.55		
	16 °C			35.31 ± 0.99	69.99 ± 1.84
Deciduous	12 °C			36.13 ± 3.60	85.01 ± 16.82
		23.85 ± 0.99	49.52 ± 2.15		
	16 °C			42.93 ± 1.99	90.28 ± 4.44

3.3.4 Porewater carbon

The dissolved organic carbon (DOC) content was generally greater at 16 °C than 12 °C across all treatments and sampling times (Temperature: $F_{1,30}$=123, P<0.001), and generally increased over the three porewater sampling periods (Time: $F_{2,60}$=29.29, P<0.001). Deciduous litter treatments also had generally greater overall DOC

concentrations ($F_{2,30}$=8.30, P=0.001) than control and coniferous treatments (Figure 3.4). The increase under both 16 °C and over time was particularly pronounced in the control (no litter) treatments, as well as the coniferous litter treatments, but increases over time were less pronounced or not apparent for the control and conifer treatments at 12 °C (Time × Temperature: $F_{2,60}$=14.7, P<0.001). Mesocosms with coniferous litter had DOC concentrations that remained relatively steady (approximately 260 mg L^{-1}) under 12 °C. Additionally, the deciduous litter treatment displayed a different pattern over time from the other two treatments; while 16 °C still showed significantly greater DOC values, mesocosms with deciduous litter had the greatest DOC concentrations during the second sampling period (six weeks) for both 12 °C and 16 °C incubation temperatures (Time × Litter: $F_{4,60}$=16.0, P<0.001).
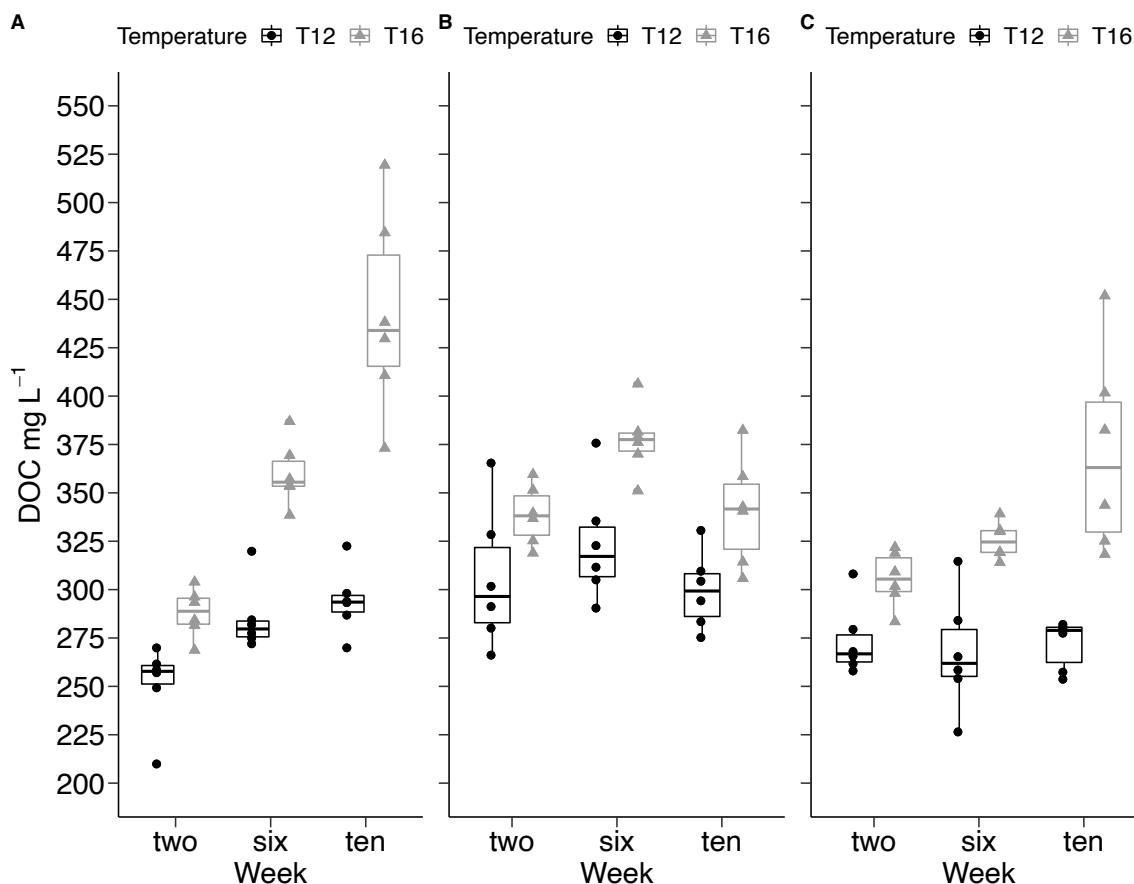
Figure 3.5 Trends in dissolved organic carbon content (mg L^{-1}) in organic soil porewater over three-month incubation at two temperature treatments (T12=12 °C and T16=16 °C). Treatments from left to right: control (A; no litter), deciduous litter (B; white birch), and coniferous litter (C; black spruce / jack pine). Boxes represents interquartile range, median (line in box), and whiskers are maximum and minimum values excluding outliers. Measurements were taken once per month.

3.3.5 Porewater mercury

The concentration of Hg in porewater varied with litter type ($F_{2,30}$= 24.2, P<0.001), temperature ($F_{1,30}$= 21.7, P<0.001), and also changed over time across treatments ($F_{2,60}$=25.4, P<0.001). The Hg concentrations tended to be greater in16 °C treatments. While all treatments started in a similar range of Hg (approx. 150 ng L^{-1}), the control and coniferous litter Hg concentrations did not change greatly over the experiment, and even

slightly decreased with time (Figure 3.6). While the deciduous litter had similar initial and final Hg porewater concentrations, the concentration dramatically increased after eight weeks incubation at both temperatures, coinciding with a peak in DOC concentration (Figure 3.5B). Porewater Hg was significantly positively correlated with FI (R=0.25, P<0.001), such that the decrease in Hg over time (except at eight weeks for deciduous litter) was correlated with decreasing FI that suggests an increasing proportion of more aromatic, plant and soil derived DOM. There was also a significant positive correlation between porewater Hg and DOC (R=0.16, P<0.001), as there was a peak in both DOC and Hg midway through the experiment for deciduous litters at both temperatures. No other porewater chemical proxies were significantly correlated with porewater Hg.
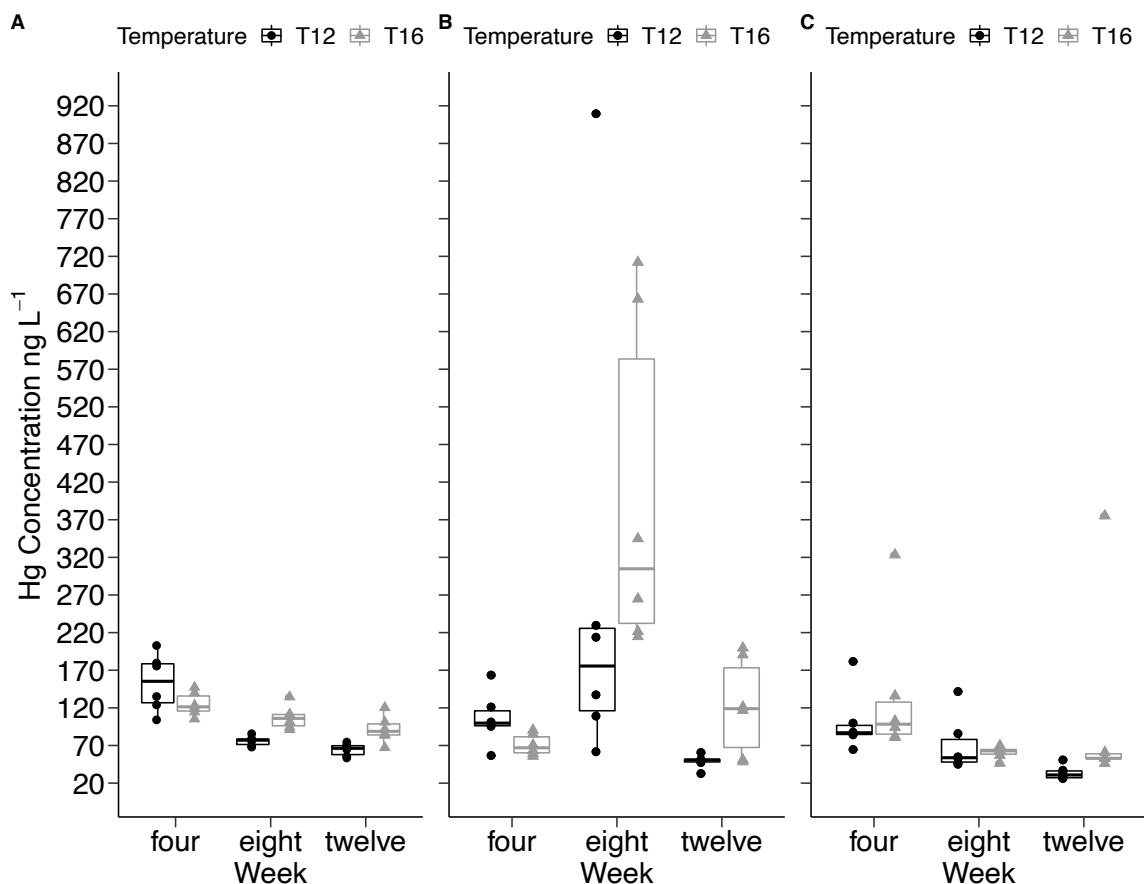
Figure 3.6 Trends in soil porewater Hg concentrations (ng L^{-1}) over three-month incubation at two temperature treatments (T12=12 °C and T16=16 °C). Treatments from left to right: control (A; no litter), deciduous litter (B; white birch), and coniferous litter (C; black spruce/ jack pine). Boxes represents interquartile range, median (line in box), and whiskers are maximum and minimum values excluding outliers. Measurements were taken once per month.

3.3.6 Porewater dissolved organic matter proxies

Specific UV absorbance at 254 nm (SUVA$_{254}$), used as an indicator of aromatic carbon content, generally increased over time across treatments (F$_{2,50}$=35.2, P<0.001) indicating an increase in recalcitrant carbon compounds in the DOC (Figure 3.7A-C). Temperature was not significant as a main effect (F$_{1,25}$=2.78, P=0.108) on SUVA$_{254}$ values, although SUVA$_{254}$ values were greater in the 16 °C incubation of the coniferous litter compared to

the 12 °C (Temperature × Litter: $F_{2,50}=5.71$, P=0.009) (Temperature × Time: $F_{2,50}=3.83$, P=0.024) (Figure 3.7C). Litter was also not significant as a main effect on $SUVA_{254}$ values ($F_{2,25}=2.65$, P=0.090), likely because the values are normalized for DOC content that varied based on litter type.
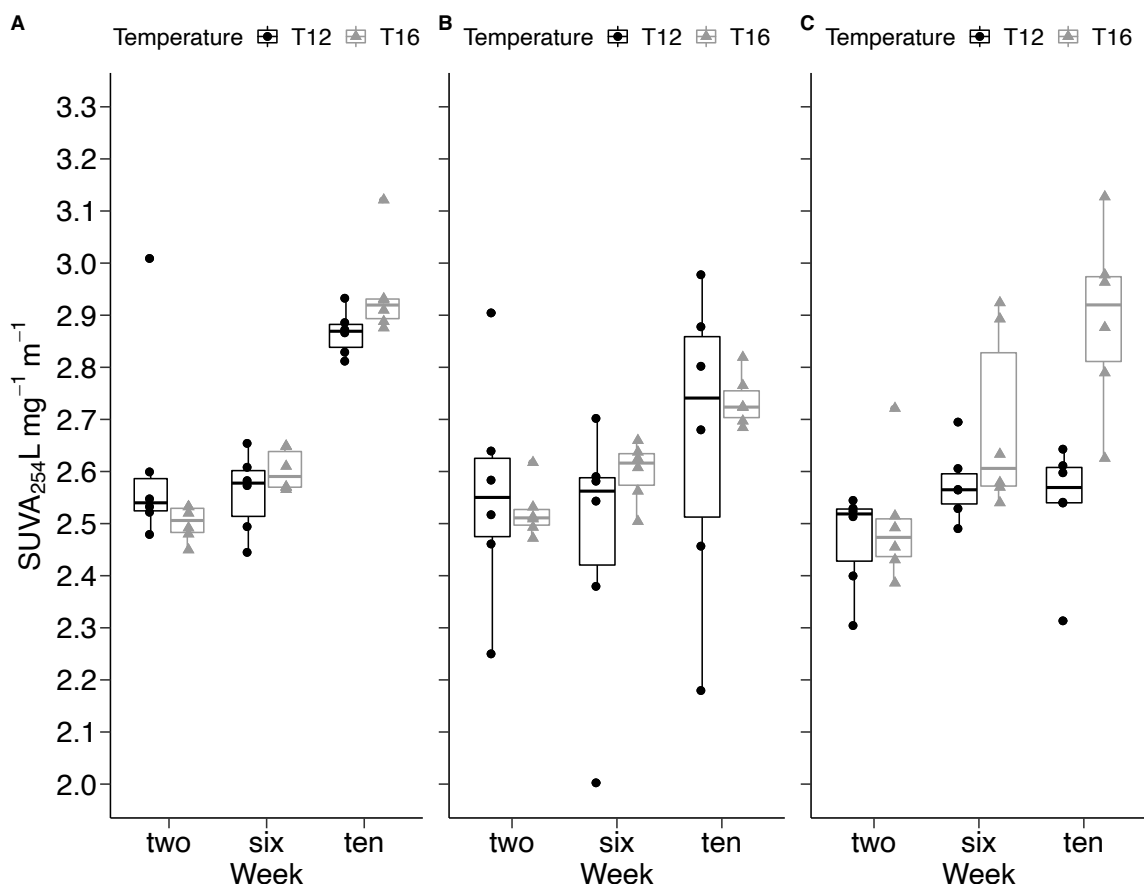
Figure 3.7 Trends in porewater carbon quality measured by specific ultraviolet absorbance at the wavelength 254 nm ($SUVA_{254}$) over three-month incubation at two temperature treatments (T12=12 °C and T16=16 °C). Treatments from left to right: control (A; no litter), deciduous litter (B; white birch), and coniferous litter (C; black spruce/ jack pine). Boxes represents interquartile range, median (line in box), and whiskers are maximum and minimum values excluding outliers. Measurements were taken once per month.

The humification index (HIX), freshness index (BIX), and fluorescence index (FI) determined litter type to be a significant determinant of DOM quality in porewater ($F_{6,46}$=9.02, P<0.001) with litter trends becoming more apparent over time ($F_{6,20}$=40.6, P<0.001) (Figure 3.8-3.10). Temperature did not significantly affect these indices ($F_{3,23}$=2.60, P=0.077), although individual indices showed temperature effects. The HIX values did not follow the same pattern as the other indices across litter treatments, rather HIX values increased steadily in the control at both temperatures (indicating more humified carbon), but values peaked midway through the experiment and then declined for both litter treatments (Figure 3.8A-C). Temperature did not have any clear relationship with the HIX; HIX values under conifer litter tended to be greater incubated at 16 °C compared to 12 °C, while HIX values tended to be lower at 16 °C compared to 12 °C in the deciduous mesocosms.

The BIX and FI values decreased with incubation time across treatments (Figure 3.9, Figure 3.10) with slight plateaus after the second sample for the two litter treatments compared to the control mesocosms (Time × Litter: $F_{4,48}$=3.69, P=0.011). Values for BIX and FI were lower at 16 °C for the control and coniferous litter mesocosms but were not significantly different between the two temperature treatments for mesocosms with deciduous litter (Time × Temperature: $F_{2,24}$=1.01, P=0.379). These decreasing FI values suggest more aromatic carbon (terrestrially sourced) released in DOM porewater with time, while decreasing BIX values suggests more DOM derived from decomposition processes over time.
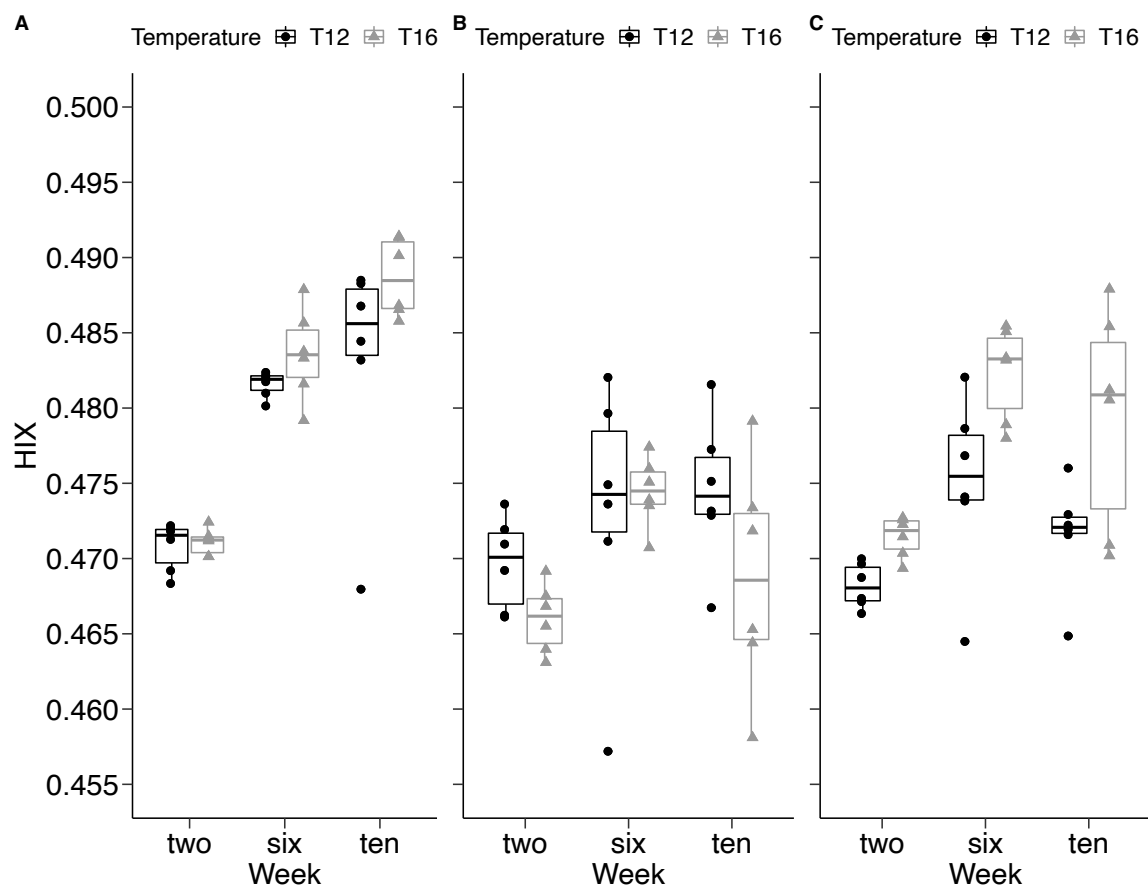
Figure 3.8 Trends in humification index (HIX) values in organic soil porewater over three-month incubation at two temperature treatments (T12=12 °C and T16=16 °C). Treatments from left to right: control (A; no litter), deciduous litter (B; white birch), and coniferous litter (C; black spruce/ jack pine). Boxes represents interquartile range, median (line in box), and whiskers are maximum and minimum values excluding outliers. Measurements were taken once per month.
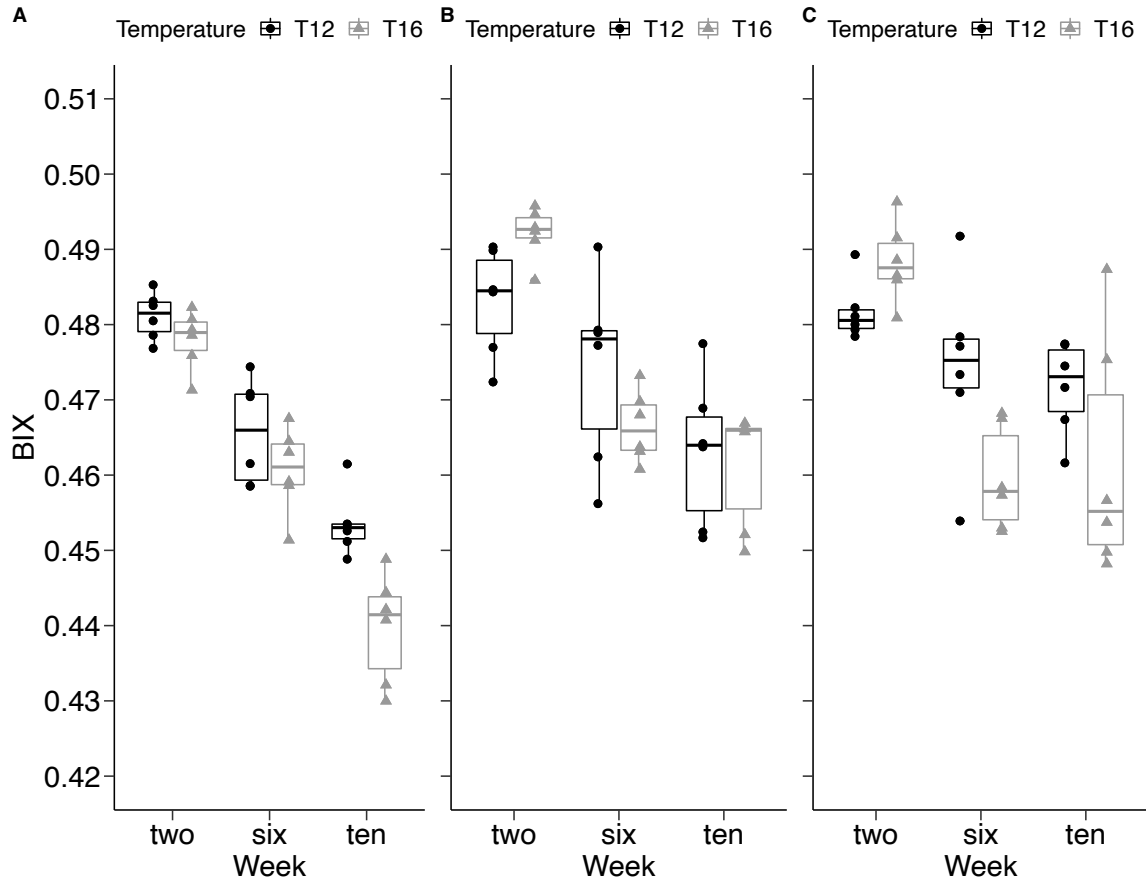
Figure 3.9 Trends in freshness index (BIX) values from organic soil porewater over three-month incubation at two temperature treatments (T12=12 °C and T16=16 °C). Treatments from left to right: control (A; no litter), deciduous litter (B; white birch), and coniferous litter (C; black spruce/ jack pine). Boxes represents interquartile range, median (line in box), and whiskers are maximum and minimum values excluding outliers. Measurements were taken once per month.
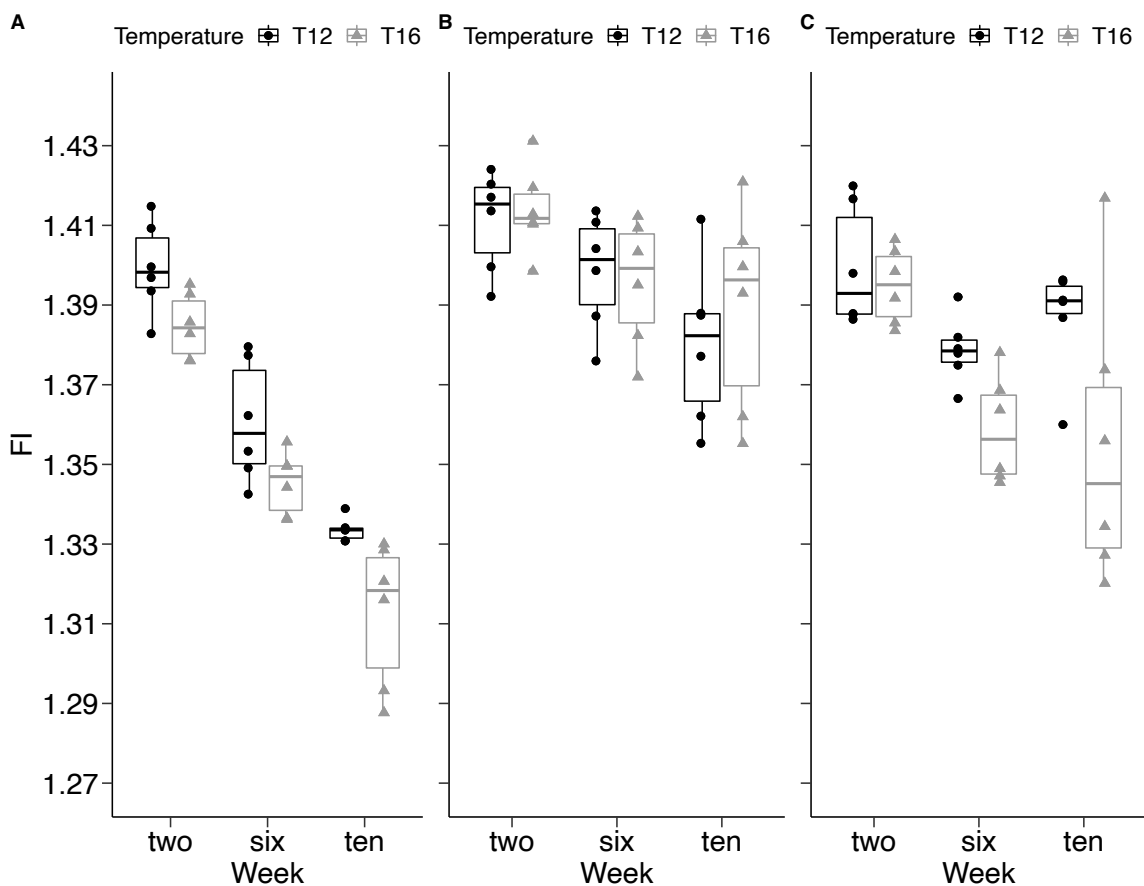
Figure 3.10 Trends in fluorescence index (FI) values in organic soil porewater over three-month incubation at two temperature treatments (T12=12 °C and T16=16 °C). Treatments from left to right: control (A; no litter), deciduous litter (B; white birch), and coniferous litter (C; black spruce/ jack pine). Boxes represents interquartile range, median (line in box), and whiskers are maximum and minimum values excluding outliers. Measurements were taken once per month.

3.3.7 Respiration

Heterotrophic respiration (CO_2 flux) was greatest in the coniferous litter treatment ($F_{2,30}$=20.1, P<0.001) (Figure 3.11C), and decreased with time across all treatments ($F_{5,150}$=131, P<0.001) although it seemed to plateau for the litter treatments in the last two measurements. The decrease in respiration over time was more pronounced in the conifer and deciduous litter treatments compared to the no litter control mesocosms (Litter ×

Time, $F_{10,50}=7.73$, P<0.001), but litter treatments did not show differences in respiration between incubation temperatures ($F_{1,30}=0.795$, P=0.380) (Figure 3.11B-C). However, respiration was greater at 16 °C than 12 °C for the control mesocosms (Figure 3.11A), leading to a significant temperature-by-litter interaction ($F_{2,30}=4.2741$, P=0.023).
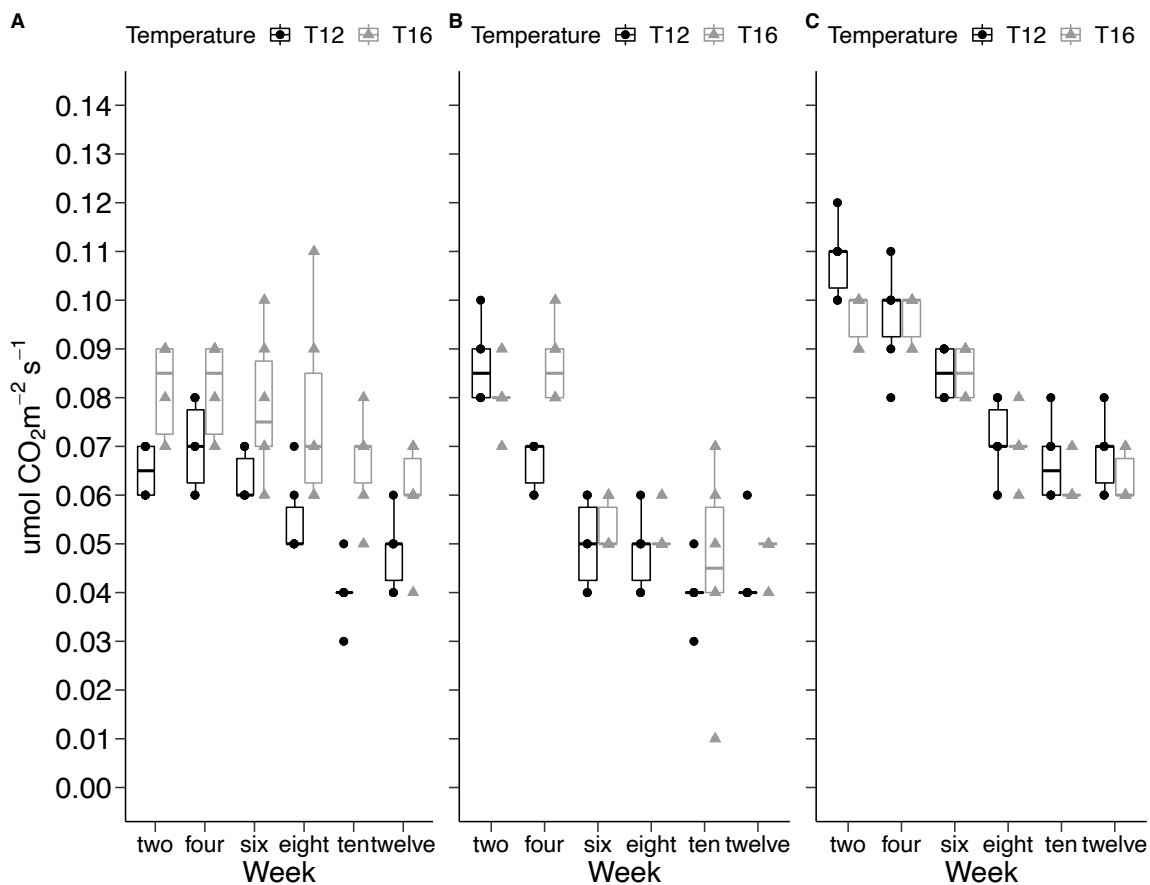
Figure 3.11 Heterotrophic respiration (CO_2) flux of organic soil and litter layer over three-month incubation at two temperature treatments (12 °C and 16 °C; T12 and T16). Treatments from left to right: control (A; no litter), deciduous litter (B; white birch), and coniferous litter (C; black spruce/ jack pine). Data points overlap in each panel (n=6). Boxes represents interquartile range, median (line in box), and whiskers are maximum and minimum values excluding outliers. Measurements were taken every two weeks.

3.4 Discussion

This study suggests that decompositional release of Hg from plant litters depended more on plant litter type rather than on abiotic factors (i.e. temperature) that regulate decomposition rates. Peak concentrations of Hg in porewater were associated with key decomposition products, namely DOC, and the DOM indicators of the source of DOM also suggested that Hg is linked to fresh decomposition products (i.e. FI values). Litter type had a strong influence on DOM quality, and therefore dictates decomposition rates and carbon accumulation in forest soils at local spatial scales (Cornwell *et al*., 2008).

The C:N of plant litter has long been used as an indicator of litter quality in the decomposition literature (Manzoni *et al*., 2010, Reich, 2014). Deciduous leaves (including white birch) with lower C:N ratio also generally have more labile sources of C compared to conifer needles (including black spruce / jack pine). Taken together, lower C:N ratios and more easily degradable C compounds as seen in the deciduous litter should decompose more rapidly, but in this study the deciduous litter was not significantly more decomposed (% mass loss) than the conifer litter treatment by the end of the incubation. Despite this I still observed the highest porewater Hg concentrations in the deciduous litter treatments. While %C, %N, and C:N ratios provide valuable information on the quality of the litter they do not identify the nature of the organic matter, which is important for controlling litter decomposition and Hg release rates. For instance, lignin is resistant to enzymatic breakdown, meaning litters with higher lignin content, such as coniferous needles, generally decompose more slowly than litters with lower lignin content (Taylor *et al*., 1989, Cornwell *et al*., 2008).

While increases in porewater Hg with deciduous litter were observed, patterns and values for coniferous litter and control soils were similar, suggesting the porewater Hg was derived from the underlying soil in the coniferous treatments, and not the litter. Furthermore, initial porewater Hg concentrations across all treatments were similar, also likely reflecting Hg derived from the soil. Previous studies have highlighted that forest floor Hg is strongly correlated with soil carbon stocks (Schwesig *et al*., 1998, Obrist *et al*., 2011), with highest Hg concentrations found in surface organic horizons (Juillerat *et al*., 2012), while studies of soil profiles have shown Hg concentrations to be fairly stable

in the mineral horizons at depths < 20 cm (Du *et al.*, 2019). The concentrations of Hg in the soil were within a similar range for other reported Hg concentrations in organic forest soils in North America (Juillerat *et al.*, 2012, Blackwell *et al.*, 2014, Oswald *et al.*, 2014, Blackwell and Driscoll, 2015) as were the Hg concentrations in the white birch leaves (Bushey *et al.*, 2008, Juillerat *et al.*, 2012, Blackwell and Driscoll, 2015) and conifer needle mix (Hall and St. Louis, 2004, Graydon *et al.*, 2006, Blackwell *et al.*, 2014, Blackwell and Driscoll, 2015).

As with mass loss of litter, I expected temperature to be a main determinant for heterotrophic respiration (Karhu *et al.*, 2014), which was the case for bare soil, but when litter was added to the mesocosms any clear effect of temperature disappeared. The lack of temperature response in respiration for the litter treatments may have arisen due to changes in the distribution of moisture in the soil profile caused by the litter layers. Specifically, the white birch leaves created a 'mat' like surface on the soil while the upper leaves remained dry. That said, no differences in moisture loss were noted in weekly watering to maintain gravimetric moisture content between the no litter and litter treatments. Another factor to consider is carbon use efficiency (CUE) of the microbial community that may have led to greater respiration rates under coniferous litter because conifer needles require more energy to decompose (i.e., low CUE), resulting in higher metabolic losses and greater CO_2 flux. Differences in microbial CUE may also explain why increased respiration was not reflected in DOC concentrations in the conifer treatment (Frey *et al.*, 2013), and ultimately lower levels of Hg release from less accessible compounds for the microbial community (Sollins *et al.*, 1996). Both litter quality and temperature as decomposition rate-controlling variables also influence the microbial community (Wardle *et al.*, 2004). While I did not explicitly manipulate the microbial community, it is possible that changes in the structure of the microbial community occurred under the different litter addition treatments, especially if there were shifts in soil pH during mesocosm incubation (Sleutel *et al.*, 2012). However, how this could translate into differences in or controls on Hg release from litter is unknown. Thorough homogenization of the soils did remove the possibility that a microbial home field advantage (where litters decompose more rapidly under the tree they fell from

compared to other environments) (Gholz *et al.*, 2001, Ayres *et al.*, 2009) contributed to the results.

While it is not certain the exact compounds the Hg bind to in plant litter, this work suggests that moderately recalcitrant C compounds are the main source of Hg released from litter. First, the flush of porewater Hg in the deciduous litter was associated with high DOC concentration, yet, despite the coniferous litter having greater starting Hg concentrations, I did not observe a flush of porewater Hg from this litter, suggesting the Hg is also bound to more recalcitrant compounds. The correlated peaks in Hg concentration, DOC concentration, and the HIX in the deciduous litter porewater midway through the experiment indeed suggests Hg release from white birch leaves is associated with mid-level recalcitrant C compounds, specifically aromatic compounds (measured by proxy using $SUVA_{254}$, which increased steadily over time). Furthermore, this increase in Hg, HIX, and DOC also followed a significant decline in BIX, suggesting the Hg is not associated with readily flushed (labile) C compounds that would have been released very early in the incubation. While Hg bound in coniferous litter did not readily enter the porewater over the three months I observed, this also suggests the Hg may be bound to the more recalcitrant C compounds that take longer to break down.

To date there has not been much research linking DOM quality via fluorescence spectroscopy and Hg but it has been recently noted that examining optical properties of DOM provides more insight on the sources and fate of Hg than just DOC concentrations which have traditionally been examined (Jiang *et al.*, 2017, Lescord *et al.*, 2018). While there was a significant correlation between DOC and Hg in the porewater it gives limited information on the compounds Hg is associated with. The significant correlation between FI and porewater Hg however indicates Hg is released along with greater aromatic compounds that lower FI values indicate. Jiang *et al.* (2017) used fluorescence analyses to trace the origin of Hg in freshwater lakes in China and concluded the composition and reactivity of DOM is a major determinant for mobility and transformation of Hg more so than just DOC content. Similarly, Lescord *et al.* (2018) also examined DOM quality and its relation to methylmercury (MeHg) concentrations in water and biota and concluded DOM analysis is important for understanding DOM-Hg biogeochemistry.

If litter-bound Hg is associated with more recalcitrant compounds, then this is also potentially linked to a longer residence time in the soil. There are few studies on Hg retention times in forest soils and much of the research done has been in tropical, sub-tropical (e.g. Ma *et al*., 2017, Du *et al*., 2019) and temperate forests (e.g. Demers *et al*., 2007, Juillerat *et al*., 2012), rather than the boreal forest (but see Hintelmann *et al*., 2002). Additionally, studies are often in areas of higher than average background concentrations like many sub-tropical forests in China (Du *et al*., 2019, Zhou *et al*., 2019). These forests vary widely in climates, species composition, and soil attributes all of which impact Hg cycling. The Canadian boreal forest is characterized by colder, drier conditions than those in sub-tropical forests of China for example, where much of Hg forest cycling research has taken place. Because climate exerts a major control on decomposition, it is not surprising carbon stocks in forests soils across the globe vary widely, which influence Hg storage and release.

The controls on decomposition ultimately also control potential Hg outflow to aquatic systems (Ravichandran, 2004). Rates of decomposition are expected to increase with increasing temperatures due to climate change (Trumbore, 1997). Although the temperature treatment did not clearly demonstrate this through % mass loss or respiration, DOC output was generally higher in the warmer treatments as were Hg concentrations. In addition to potential changes in Hg caused by increased rates of decomposition under warming, climate change is anticipated shift deciduous tree species northward in the boreal forest (Cramer *et al*., 2001, McKenney *et al*., 2007, 2011), which would fundamentally change litter quality inputs to forest soils. Lastly, climate change is also expected to change rates of Hg deposition and partitioning on inputs to forest soils from throughfall and litterfall (Blackwell *et al*., 2014). Taken together, changes to both litter quantity, litter quality and potential increases in litter Hg concentrations will have cascading effects on decomposition rates and the potential to change the dynamics and partitioning of terrestrial Hg cycling.

3.5   References

Ayres, E., Steltzer, H., Simmons, B.L., Simpson R.T., Steinweg, M., Wallenstien, M.D., Mellor, N., Parton, W.J., Moore, J.C., Wall, D.H., 2009. Home-field advantage

accelerates leaf litter decomposition in forests. Soil Biology and Biochemistry 41, 606–610.

Assad, M., Parelle, J., Cazaux, D., Gimbert, F., Chalot, M., Tatin-Froux, F., 2016. Mercury uptake into poplar leaves. Chemosphere 146, 1–7.

Berg, B., Berg, M.P., Bottner, P., Box, E., Breymeyer, A., Calvo De Anta, R., Couteaux, M., Escuardo, A., Gallardo, A., Kratz, W., Madeira, M., Mälkönen, E., McClaugherty, C., Meenetemeyer, V., Muñoz, F., Piussi, P., Remacle, J., Virzo De Santo, A., 1993. Litter mass loss rates in pine forests of Europe and eastern United States: some relationships with climate and litter quality. Biogeochemistry 20, 127–159.

Blackwell, B.D., Driscoll, C.T., Maxwell, J.A., Holsen, T.M., 2014. Changing climate alters inputs and pathways of mercury deposition to forested ecosystems. Biogeochemistry 119, 215–228.

Blackwell, B.D., Driscoll, C.T., 2015. Deposition of mercury in forests along a montane elevation gradient. Environment Science & Technology 49, 5363–5370.

Bushey, J.T., Nallana, A.G., Montesdeoca, M.R., Driscoll, C., 2008. Mercury dynamics of a northern hardwood canopy. Atmospheric Environment 42, 6905–6914.

Cornwell, W.K., Cornelissen, J.H.C., Amatangelo, K., Dorrepaal, E., Eviner, V.T., Godoy, O., Hobbies, S.E., Hoorens, B., Kurokawa, H., Pérez-Harguindeguy, N., Quested, H.M., Santiago, L.S., Wardle, D.A., Wright, I.J., Aerts, R., Allison, S.D., Van Bodegom, P., Brovkin, V., Chatain, A., Callaghan, T.V., Díaz, S., Garnier, E., Gurvich, D.E., Kazakou, E., Klein, J.A., Read, J., Reich, P.B., Soudzilovskaia, N.A., Viaeretti, M.V., Westoby, M., 2008. Plant species traits are the predominant control on litter decomposition rates within biomes worldwide. Ecology Letters 11, 1065–1071.

Cory, R.M., McKnight, D.M., 2005. Fluorescence spectroscopy reveals ubiquitous presence of oxidized and reduced quinones in dissolved organic matter. Environment Science & Technology 39, 8142–8149.

Cramer, W., Bondeau, A., Woodward, F.I., Prentice, I.C., Betts, R.A., Brovkin, V., Cox, P.M., Fisher, V., Foley, J.A., Friend, A.D., Kuckarik, C., Lomas, M.R., Ramankutty, N., Sitch, S., Smith, B., White, A., Young-Molling, C., 2001. Global response of terrestrial ecosystem structure and function to CO_2 and climate change: Results from six dynamic global vegetation models. Global Change Biology 7, 357–373.

Demers, J.D., Driscoll, C.T., Fahey, T.J., Yavitt, J.B., 2007. Mercury cycling in litter and soil in different forest types in the Adirondack region, New York, USA. Ecological Applications 17, 1341–1351.

Demers, J.D., Blum, J.D., Zak, D.R., 2013. Mercury isotopes in a forested ecosystem: Implications for air-surface exchange dynamics and the global mercury cycle. Global Biogeochemical Cycles 27, 222–238.

Driscoll, C.T., Mason, R.P., Chan, H.M., Jacob, D.J., Pirrone, N., 2013. Mercury as a global pollutant: sources, pathways, and effects. Environment Science & Technology 47, 4967–4983.

Du, B., Zhou, J., Zhou, L., Fan, X., Zhou, J., 2019. Mercury distribution in the foliage and soil profiles of a subtropical forest: process for mercury retention in soils. Journal of Geochemical Exploration 205, 106337.

Fellman, J.B., Hood, E., Spencer, R.G.M., 2010. Fluorescence spectroscopy opens new windows into dissolved organic matter dynamics in freshwater ecosystems: a review. Limnology and Oceanography 55, 2452–2462.

Frey, S.D., Lee, J., Melillo, J.M., Six, J., 2013. The temperature response of soil microbial efficiency and its feedback to climate. Nature Climate Change 3, 395–398.

Gholz, H.L., Wedin, D.A., Smitherman, S.M., Harmon, M.E., Parton, W.J., 2000. Long-term dynamics of pine and hardwood litter in contrasting environments: toward a global model of decomposition. Global Change Biology 6, 751–765.

Graydon, J.A., St. Louis, V.L., Hintelmann, H., Lindberg, S.E., Sandilands, K.A., Rudd, J.W.M., Kelly, C.A., Hall, B.D., Mowat, L.D., 2008. Long-term wet and dry deposition of total and methyl mercury in the remote boreal ecoregion of Canada. Environment Science & Technology 42, 8345–8351.

Graydon, J.A., St. Louis, V.L., Lindberg, S.E., Hintelmann, H., Krabbenhoft, D.P., 2006. Investigation of mercury exchange between forest canopy vegetation and the atmosphere using a new dynamic chamber. Environment Science & Technology 40, 4680–4688.

Grigal, D.F., 2002. Inputs and outputs of mercury from terrestrial watersheds: a review. Environmental Reviews 10, 1–39.

Hall, B.D., St. Louis, V.L., 2004. Methylmercury and total mercury in plant litter decomposing in upland forests and flooded landscapes. Environment Science & Technology 38, 5010–5021.

Hintelmann, H., Harris, R., Heyes, A., Hurley, J.P., Kelly, C.A., Krabbenhoft, D.P., Lindberg, S., Rudd, J.W.M., Scott, K.J., St. Louis, V.L., 2002. Reactivity and mobility of new and old mercury deposition in a boreal forest ecosystem during the first year of the METAALICUS study. Environment Science & Technology 36, 5034–5040.

IPCC. Climate Change 2013: The Physical Science Basis. Contribution of Working Group I to the Fifth Assessment Report of the Intergovernmental Panel on Climate Change. Cambridge University Press, Cambridge, United Kingdom and New York, USA, 2013, pp. 1535.

Jiang, T., Skyllberg, U., Bjorn, E., Green, N.W., Tang, J., Wang, D., Gao, J., and Li, C., 2017. Characteristics of dissolved organic matter (DOM) and relationship with

dissolved mercury in Xiaoqing River-Laizhou Bay Estuary, Bohai Sea, China. Environmental Pollution 223, 19–30.

Jiang, T., Skyllberg, U., Wei, S., Wang, D., Lu, S., Jiang, Z., Flanagan, D.C., 2015. Modeling the structure-specific kinetics of abiotic, dark reduction of Hg(II) complexed by O/N and S functional groups in humic acids while accounting for time-dependent structural arrangement. Geochimica et Cosmochimica Acta 154, 151–167.

Juillerat, J.I., Ross, D.S., Bank, M.S., 2012. Mercury in litterfall and upper soil horizons in forested ecosystems in Vermont, USA. Environmental Toxicology and Chemistry 31, 1720–1729.

Kalbitz, K., Solinger, S., Park, J., Michalzik, B., Matzner, E., 2000. Controls on the dynamics dissolved organic matter in soils: A review. Soil Science 165, 277–304.

Karhu, K., Auffret, M.D., Dungait, J.A.J., Hopkins, D.W., Prosser, J.I., Singh, B. K., Subke, J., Wookey, P.A., Årgen, G.I., Sebastià, T., Gouriveau, F., Bergkvist, G., Meir, P., Nottingham, A.T., Salinas, N., Hartley, I.P., 2014. Temperature sensitivity of soil respiration rates enhanced by microbial community response. Nature 513, 81–84.

Lescord, G.L., Emilson, E.J.S., Johnson, T.A., Branfireun, B.A., Gunn, J.M., 2018. Optical properties of dissolved organic matter and their relation to mercury concentrations in water and biota across a remote freshwater drainage basin. Environment Science & Technology 52, 3344–3353.

Lindberg, S., Bullock, R., Ebinghaus, R., Engstrom, D., Feng, X., Fitzgerald, W., Pirrone, N., Pretsbo, E., Seigneur, C., 2007. A synthesis of progress and uncertainties in attributing the sources of mercury in deposition. Ambio 36, 19–32.

Ma, M., Du, H., Wang, D., Sun, T., Sun, S., Yang, G., 2017. The fate of mercury and its relationship with carbon, nitrogen and bacterial communities during litter decomposing in two subtropical forests. Applied Geosciences 86, 26–35.

Manzoni, S., Trofymow, J.A., Jackson, R.B., Porporato, A., 2010. Stoichometric controls on carbon, nitrogen, and phosphorous dynamics in decomposing litter. Ecological Monographs 80, 89–106.

McKenney, D.W., Pedlar, J.H., Lawrence, K., Campbell, K., Hutchinson, M.F., 2007. Potential impacts of climate change on the distribution of North American trees. Bioscience 57, 939–948.

McKenney, D.W., Pedlar, J.H., Rood, R.B., Price, D., 2011. Revisiting projected climate shifts in the climate envelopes of North American trees using updated general circulation models. Global Change Biology 17, 2720–2730.

McLaughlin, J., 2009. Boreal mixed-wood watershed riparian zone cation-cycling during two contrasting climatic years. Soil Science Society of America Journal 73, 1408–1418.

Millhollen, A.G., Gustin, M.S., Obrist, D., 2006. Foliar mercury accumulation and exchange for three tree species. Environment Science & Technology 40, 6001–6006.

Moore, T.R., Trofymow, J.A., Taylor, B., Prescott, C., Camiré, C., Duschene, L., Fyles, J., Kozak, L., Kranabetter, M., Morrison, I., Siltanen, M., Smith, S., Titus, B., Visser, B., Wein, R., Zoltai, S., 1999. Litter decomposition rates in Canadian forests. Global Change Biology 5, 75–82.

Niu, Z., Zhang, X., Wang, Z., Ci, Z., 2011. Field controlled experiments of mercury accumulation in crops from air and soil. Environmental Pollution 159, 2684–2689.

Obrist, D., 2007. Atmospheric mercury pollution due to losses of terrestrial carbon pools? Biogeochemistry 85, 119–123.

Obrist, D., Johnson, D.W., Lindberg, S.E., Luo, Y., Hararuk, O., Bracho, R., Battles, J.J., Dail, D.B., Edmonds, R.L., Monson, R.K., Ollinger, S.V., Pallardy, S.G., Pregitzer, K.S., Todd, D.E., 2011. Mercury distribution across 14 U.S. forests.

part I: spatial patterns of concentration in biomass, litter and soils. Environment Science & Technology 45, 3974–3981.

Oswald, C., Heyes, A., Branfireun, B.A., 2014. Fate and transport of ambient mercury and applied mercury isotope in terrestrial upland soils: insights from the METAALICUS watershed. Environment Science & Technology 48, 1023–1031.

Parton, W., Silver, W.L., Burke, I.C., Grassens, L., Harmon, M. E., Currie, W.S., King, J.Y., Adair, E.C., Brandt, L.A., Hart, S.C., Fasth, B., 2007. Global-scale similarities in nitrogen release patterns during long-term decomposition. Science 315, 361–364.

Ravichandran, M., 2004. Interactions between mercury and dissolved organic matter – a review. Chemosphere 55, 319–331.

Rea, A.W., Lindberg, S.E., Scherbatskoy, T., Keeler, G.J., 2002. Mercury accumulation in foliage over time in two northern mixed-hardwood forests. Water, Air, and Soil Pollution 133, 49–67.

Reich, P.B., 2014. The world-wide "fast-slow" plant economics spectrum: A traits manifesto. Journal of Ecology 102, 275–301.

Richardson, J.B., Friedland, A.J., 2015. Mercury in coniferous and deciduous upland forests in northern New England, USA: implications of climate change. Biogeosciences 12, 6737–6749.

Risch, M.R., DeWild, J.F., Gay, D.A., Zhang, L., Boyer, E.W., Krabbenhoft, D.P., 2017. Atmospheric mercury deposition to forests in the eastern USA. Environmental Pollution 228, 8–18.

Schroeder, W.H., Munthe, J., 1998. Atmospheric mercury – an overview. Atmospheric Environment 32, 809–822.

Schwesig, D., Ilgen, G., Matzner, E., 1998. Mercury and methylmercury in upland and wetland acid forest soils of a watershed in NE-Bavaria, Germany. Water, Air, and Soil Pollution 113, 141−154.

Sleutel, S., Bouckaert, L., Buchan, D., Van Loo, D., Cornelis, W.M., Sanga, H.G., 2012. Manipulation of the soil pore and microbial community structure in soil mesocosm incubation studies. Soil Biology and Biogeochemistry 45, 40−48.

Siwik, E.I.H., Campbell, L.M., Mierle, G., 2009. Fine-scale mercury trends in temperate deciduous tree leaves from Ontario, Canada. Science of the Total Environment 407, 6275–6279.

Sollins, P., Homann, P., Caldwell, B.A., 1996. Stabilization and destabilization of soil organic matter: mechanisms and controls. Geoderma 74, 65–105.

Stamenkovic, J., Gustin, M.S., 2009. Nonstomatal uptake versus stomatal uptake of atmospheric mercury. Environment Science & Technology 43, 1367–1372.

Taylor, B.R., Parkinson, D., Parsons, W.F.J., 1989. Nitrogen and lignin content as predictors of litter decay-rates – a microcosm test. Ecology 70, 97–104.

Thien, S.J., 1979. A flow diagram for teaching texture by feel analysis. Journal of Agronomic Education 8, 54−55.

Trumbore, S.E., 1997. Potential responses of soil organic carbon to global environmental change. Proceedings of the National Academy of Science of the United States of America 94, 8284−8291.

U.S. EPA. "Method 7473 (SW-846): Mercury in Solids and Solutions by Thermal Decomposition, Amalgamation, and Atomic Absorption Spectrophotometry," Revision 0: Washington, DC, 1998.

U.S. EPA. "Method 1631: Mercury in Water by Oxidation, Purge and Trap, and Cold Vapor Atomic Fluorescence Spectrometry," Revision E: Washington, DC, 2002.

Wardle, D.A., Bardgett R.D., Klironomos J.N., Setälä H., van der Putten W.H., Wall D.H., 2004. Ecological linkages between aboveground and belowground biota. Science 304, 1629–1633.

Weishaar, J.L., Aiken, G.R., Bergamaschi, B.A., Fram, M.S., Fujii, R., Mopper, K., 2003. Evaluation of specific ultraviolet absorbance as an indicator of the chemical composition and reactivity of dissolved organic carbon. Environment Science & Technology 37, 4702–4708.

Wright, P.L., Zhang, L., Marsik, F.J., 2016. Overview of mercury dry deposition, litterfall, and throughfall studies. Atmospheric Chemistry and Physics 16, 13399−13416.

Yuan, W., Sommar, J., Lin, C., Wang, X., Li, K., Liu, Y., Zhang, H., Lu, Z., Wu, C., Feng, X., 2019. Stable isotope evidence shows re-emission of elemental mercury vapor occurring after reductive loss from foliage. Environment Science & Technology 53, 651−660.

Zhang, L., Wright, L.P., Blanchard, P., 2009. A review of current knowledge concerning dry deposition of atmospheric mercury. Atmospheric Environment 43, 5853–5864.

Zhou, J. Du, B., Shang, L., Wang, Z., Cui, H., Fan, X., Zhou, J., 2020. Mercury fluxes, budgets, and pools in forest ecosystems of China: a review. Critical Reviews in Environmental Science and Technology, 50, 1411-1450.

Chapter 4

4   Discussion

4.1   Carbon and mercury cycles in the boreal forest

As the fate of mercury (Hg) in forests is linked to carbon (C), the controls that govern C cycling also regulate Hg cycling. Conifer and deciduous tree types differ in C cycling from foliage growth through to decomposition of litter with differing photosynthetic capacities, leaf longevities, and decomposition rates (Tuomi *et al*., 2009, Kikuzawa and Lechowicz, 2014). In this thesis I demonstrate that foliage type and environmental conditions regulate Hg cycling in the boreal forest from accumulation in foliage over a growing season into senescence (Chapter 2) to its release from forest litter into the soil pool (Chapter 3).

The boreal zone regulates climate and plays a significant role in biogeochemical cycles including both C and Hg (Brandt, 2009). While this forest zone is understudied regarding Hg cycling relative to other forest types, its expanse across the world makes it necessary to understand global Hg cycling as well as the processes and mechanisms occurring within it. This zone is also projected to experience more pronounced effects of climate warming (Price *et al*., 2013), so understanding the role of environmental conditions on Hg cycling is critical to forecast how global Hg cycles will change.

Many factors influence litter inputs in a forest such as time post disturbance and species composition, primarily conifer versus deciduous tree types (Chen *et al*., 2017). Litter quality, while playing an important role in controlling decomposition rates at the forest stand level, can also be considerably variable within a forest stand. I observed high variability in the decomposition of white birch (*Betula papyrifera*) leaves (both % mass loss and DOC content of white birch porewater), that could account for the high variability in Hg concentration in porewater during a peak observed midway through my experimental incubation (Chapter 3). There was no trend between mass loss and Hg concentration in porewater although the porewater Hg concentrations were measured throughout the experiment and were similar to the first sampling concentration after the

peak while mass loss was only measured at the end. Wardle *et al*. (2004) notes that heterogeneity in tree stand composition can dictate a 'patchy distribution' of litter quality that affects soil organisms within forest soils and can result in variable decomposition rates in nearby areas (Saetre and Bååth, 2000). I homogenized the soil carefully so patchy distribution of soil organisms was likely not present in the mesocosms that could contribute differences in decomposition stage. Still, this suggests Hg release even with similar litters in a natural system can vary both spatially and temporally. Litter quality, considered using carbon to nitrogen ratios, demonstrated the white birch litter was more nutrient rich (i.e. lower C:N driven by greater %N). Despite this difference in quality, the leaf litter did not decompose significantly more than the conifer needles, possibly due to differences in moisture distribution, but still released more Hg over this short time scale.

From the steep increase in Hg concentrations in white birch leaves at the end of the growing season associated with senescence (Chapter 2), to the increase in Hg concentrations post incubation (Chapter 3) it is clear that the quality of litter, both %C, %N, C:N, as well as moisture content, degradation stage, and foliage type, must be considered when examining Hg concentrations. The increase in Hg content in litter observed in Chapter 3 post incubation is most likely a function of mass loss of C. Because it was not possible to mass balance the C and Hg in each mesocosm I can only speculate as to why concentrations increased in both soil and litter. Other studies conducted in field conditions (Hall and St. Louis, 2004, Demers *et al*., 2007) have also observed an increase in litter Hg concentrations with decomposition but suggested potential translocation of Hg from soil to litter. Hall and St. Louis (2004) noted precipitation events as a potential pathway for Hg to translocate from soils to litter. The mesocosm system I used did not have precipitation events, although moisture levels were maintained through weekly additions of moisture added to the mesocosms from above in a squeeze bottle over the litter, mimicking rainfall. It is unlikely this could have facilitated the Hg transfer as there was no opportunity for movement of water other than vertical percolation whereas different slopes in natural systems and other weathering could contribute to greater variation in moisture distribution in a field setting. Additionally, in field experiments there are more sources of potential Hg inputs such as throughfall that were not present in the controlled mesocosms.

Loss of C in the litter post incubation is clear based on the %C decreases I observed contributing to overall mass loss of litter. The mass loss of C is also what drives the %N values to increase despite there being no inputs of N to the system. A similar effect may occur with Hg concentrations as there were no inputs of Hg to the mesocosms, although the increases in Hg concentration tissues with decomposition requires further research and careful mass balance. Ma *et al*. (2017), working in subtropical forests, also observed an increase in Hg concentration and N content as decomposition increased, and suggested a biotic mechanism was responsible for the increases such as immobilization of N as Hg binds strongly with organic matter (i.e. C compounds).

During decomposition, labile C compounds are preferentially released from litter before the more recalcitrant C compounds that Hg may be bound to. As conifer needles are more recalcitrant litter overall, this could suggest the Hg is bound to different compounds in each litter type or associated with compounds that are being selectively persevered. Based on the positive correlation between DOC content and Hg concentration, more rapid decomposition would result in more Hg bound to DOM that has the potential to leave the forest ecosystem as a main control on the amount of Hg that can be exported from soils into aquatic systems is decomposition of soil organic matter (Ravichandran, 2004). A similar effect of different Hg concentrations based on leaf color and degradation stage was observed in Chapter 2 (and see Appendix B) whereby Hg concentrations increased as the leaves degraded and turned yellow in color suggesting Hg is bound to C compounds not resorbed during senescence.

Conifer dominated forest stands have been observed to have greater Hg concentrations in litter horizons (Demers *et al*., 2007, Obrist *et al*., 2012). However, because conifer needles fall on varying multi-year cycles this does not necessarily translate into greater Hg inputs overall (Demers *et al*., 2007). The extent to which forest type influences soil overall Hg pools is not well understood. Both Demers *et al*. (2007) and Obrist *et al*. (2012) observed significantly greater Hg concentrations in the litter O_a horizon under conifer stands, but the trend was not consistent moving to deeper horizons and Obrist *et al*. (2012) concluded this was due to higher Hg concentrations in needles from longer exposure time. Richardson and Friedland (2015) assert that vegetation type, specifically

coniferous versus deciduous, controls Hg concentration in upper organic horizons while soil conditions control mineral horizon Hg concentrations. My results suggest vegetation type is a main control of how Hg cycles in forest systems. The forest soil Hg concentrations I measured were in a similar range to other North American forest soils but because I sampled from a mixed forest stand and homogenized the soil, I did not observe any foliage type differences.

4.2   Importance of timing for mercury sampling

While the Hg loading from litterfall every year is variable considering environmental conditions and atmospheric Hg concentrations it is important to consider the timing of sampling before drawing wider conclusions for sampling of foliage tissues. As both chapters demonstrated changing Hg concentrations in foliage tissues with time, it is important that sampling be as consistent as possible. Studies have observed Hg accumulation in the canopy (e.g. Siwik *et al*., 2007) consistent with my results for the birch leaves, but most studies collect only a few sampling points with gaps of weeks or months between each sample, or have been conducted in laboratory-based environments (e.g. Ericksen *et al*., 2003, Frescholtz *et al*., 2003). Depending on when these sampling events occur could bias estimations. As demonstrated in Chapter 2, the onset of senescence caused a more dramatic increase of Hg concentration in both leaves and needles. As the timing of these degradative processes changes annually it is important to consider the forest and leaf stage when sampling.

While conifer needles generally have a greater Hg concentration when they fall as litter, as observed in the initial Hg concentrations in Chapter 3, it takes years for the needle to accumulate this Hg and only contribute to litterfall on multiyear cycles. Deciduous leaves are more commonly investigated regarding Hg uptake (but see Barquero *et al*., 2019), which have clearer on-tree timelines. Previous Hg uptake rates in conifer needles have been calculated from fallen needles divided by the estimated time on the tree however, needles drop on multiyear cycles, and there can be great variability within a species dictated by factors such as climate and latitude (Reich *et al*., 1996). For example, when collecting fresh foliage Blackwell and Driscoll (2015) counted nodes on stems to indicate different growing seasons and noted stems had at least three nodes while some had up to

seven representing a large variation in exposure time. This method, however, was not possible for litterfall analysis, so all needles were assumed to be three years old, conservatively biasing their estimates (Blackwell and Driscoll, 2015). Similarly, Kang *et al*. (2019) estimated needle age based on appearance and used the arithmetic average of four years to calculate needle Hg concentrations. As the black spruce needle Hg concentrations did not clearly increase in the first growing season I observed, assuming linear uptake of Hg can bias litterfall Hg estimations when needle drop and longevity is known to be variable (Reich *et al*., 1996). Variable needle retention also complicates carbon cycling models (Reich *et al*., 2014), further obscuring extrapolations for Hg accumulation.

Litterfall, while comprising a main input of Hg into forests (Grigal, 2002, Rea *et al*., 2002, Assad *et al*., 2016), does not have standard sampling protocols either. Working with data collected with the National Atmospheric Deposition Program Mercury Deposition Network, Risch *et al*. (2017) used consistent sampling methods to collect litterfall over six years, the longest standard litterfall sampling collection program at the time. Their sample collection began each year when leaves began to fall in autumn and the contents from litter traps were collected every four weeks for eight to sixteen weeks depending when litterfall was complete. These methods provided a relatively consistent and straightforward approach to litterfall to be able to compare litterfall Hg concentrations across a wide range of spatial and temporal scales. However, these methods are not consistent across studies reporting Hg litterfall collection. Blackwell and Driscoll (2015) for example, left litterfall traps deployed over two years collecting the only litter twice. While it is not feasible to collect litter on broad scales with high frequency, during the interim of litter being collected the litter quantity and quality can change. As I observed in Chapter 3, C was immediately flushed from deciduous litter and a spike in Hg occurred not long after. Litter collected in a trap is generally kept off the ground and less susceptible to decomposition both from mechanical and microbial action, but leaching is free to occur.

4.3 Climate change implications on mercury cycling in forests

Climate change will alter C and Hg cycling across spatial and temporal scales. At a global scale, greenhouse gas emissions and Hg emissions dictate future cycling patterns. Vegetation acts a significant sink for both C and Hg and has an important role in both complex biogeochemical cycles. Vegetation, and specifically the boreal forest that covers approximately 270 million hectares (Brandt *et al*., 2013), plays a major role in the cycles of C and Hg. A shift in tree species composition, projected as a result of climate change (Parmesan and Yohe, 2003), will then have major ramifications of Hg and C cycling at local and global scales.

There are many factors that determine the future of carbon emissions to the atmosphere, and as a result, the rate and severity of climate change (Collins *et al*., 2013). Similarly, there are many uncertainties around the future of Hg emissions, the effects of which will be compounded by climate change altering global atmospheric circulation patterns (Krabbenhoft and Sunderland, 2013). While Hg emission projections cite the future of Asia's energy sector as a main determinant, even with a significant reduction or halt to anthropogenic Hg emissions, Hg will continue to circulate in the atmosphere (Streets *et al*., 2009, Amos *et al*., 2013). Amos *et al*. (2013) estimated that up to 60% of current atmospheric deposition comes from re-emitted Hg from surface reservoirs, demonstrating the importance of understanding Hg biogeochemistry regardless of future Hg emissions projections.

A changing climate will also cause endogenous plant processes to change, which could disturb Hg accumulation mechanisms. For example, stomata act as a main pathway for foliage to uptake Hg, in addition to assimilating C. Stomata are critically important for regulating gas exchange between a leaf's interior and the atmosphere, most importantly carbon dioxide (CO_2) and water. As a result, stomata influence photosynthesis, nutrient exchange and availability, drought tolerance, hydrology, etc. (see Buckley *et al*., 2017 for review). There are many factors that control stomatal conductance including environmental signals such as temperature (Urban *et al*., 2017), light intensity and atmospheric CO_2 concentrations, as well as endogenous factors like plant hormones

(Hetherington and Woodward, 2003). Many of these environmental signals, notably temperature, light intensity, and CO_2 concentration, also have been noted to influence Hg uptake as well as Hg distribution in the atmosphere (Graydon *et al*., 2006). As a result of these changes in gas exchange, and Hg entry into the tissue, will change. Further, CO_2 concentrations have been found to covary with $Hg(0)_g$ lending support to vegetation acting as a global pump (Jiskra *et al*., 2018). Warmer temperatures and changing moisture regimes will alter stomatal control and as a result, foliar Hg uptake and assimilation.

Climate change also forecasts shifts in species composition, notably a shift northward for deciduous species in the boreal forest (McKenney *et al*., 2011; Figure 4.1) as plant hardiness zones shift (McKenney *et al*., 2014). This would cause a major shift in litter inputs both in quality and quantity, broadly changing Hg residence times in forests. My results suggest deciduous trees cycle Hg through forests more quickly than conifer species, influencing overall catchment Hg cycles.

Below ground systems are similarly impacted by climate change. Global soil carbon cycles are changing, with soil C being lost with warming temperatures (Bellamy *et al*., 2005, Crowther *et al*., 2016), and as the fate of Hg cycling in forests is linked to C, the controls that govern soil C cycling also impact Hg cycling. There are innumerable factors that control overall C decomposition on both global and local scales and within these there are complex links between above ground and below ground processes and communities (Wardle *et al*., 2004). Latitude and climate play major roles in C cycling by dictating species composition, growing season length, broad scale patterns of decomposition (McGuire *et al*., 2002, Cornwell *et al*., 2008), but short-term environmental conditions also majorly influence C cycles by controlling things like plant growth and timing of senescence (Lim *et al*., 2007). The influence and importance of each of these factors is not understood for Hg there is great uncertainty surround the future of terrestrial Hg cycling (Obrist *et al*., 2018). Climate change will also have major implications on hydrology (Trenberth *et al*. 2003), which is a major determinant of Hg transport in forests (Oswald *et al*., 2014).
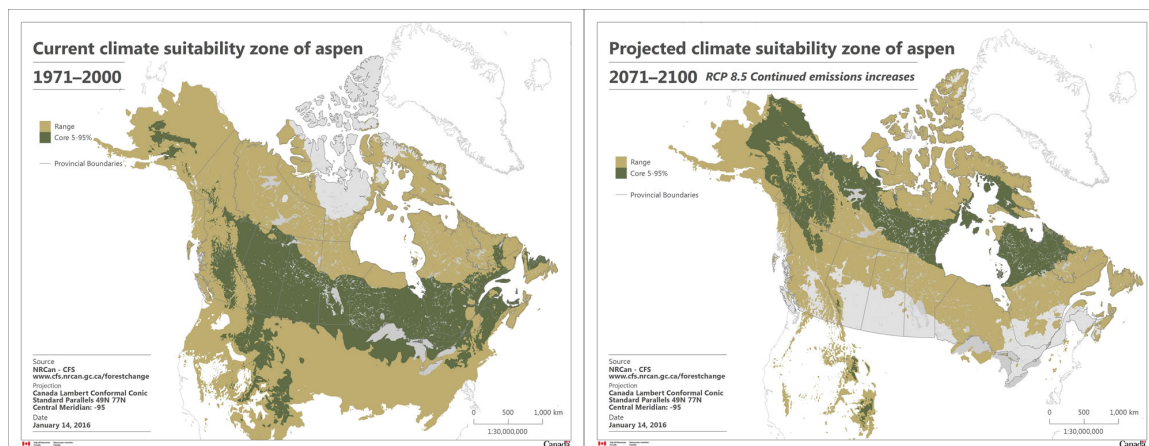
Figure 4.1 Current observed (1971-2000; left) and projected (2071-2100; right) climate suitability zones for Trembling Aspen (*Populus tremuloides*) in Canada based on scenario Representation Concentration Pathway 8.5 from IPCC assuming carbon emissions continue. Figure used with permissions from Natural Resources Canada, 2016 based on McKenney *et al*., 2011, 2014.

4.4   Study limitations and future directions

My results highlight the need for further research comparing Hg accumulation in conifer and deciduous trees. The solar radiation sensors and anemometers used in Chapter 2 on the tower showed different environmental conditions based on height but despite these differences I observed no trend of Hg accumulation by height or atmospheric Hg concentration. Because of the inherent variation in environmental conditions I observed, as well as other factors I did not measure (e.g. temperature gradient, humidity gradient) it is not possible to determine if there were no trends observed because of one or a combination of those factors. A laboratory-based growth study could control for light conditions (see Stamenkovic and Gustin, 2009) on foliar tissue but replication of forest conditions in a laboratory setting is nearly impossible. Further observation of Hg concentrations at different heights in the forest however, with active or passive Hg air monitoring, would contribute to understanding factors controlling Hg accumulation. In other forests with different canopy structures perhaps there would be a clear atmospheric Hg gradient, which would likely contribute to accumulation differences in foliar tissues.

With the onset of senescence leaves experience photodegradation because of reduced chlorophyll pigment that helps to filter light from leaf tissue that is damaging to leaf tissues (Hollósy, 2002). Light is also understood to be responsible for photoreduction and subsequent volatilization of Hg (Schroeder and Munthe, 1998), which can occur from leaf tissue (Yuan *et al*., 2019). In a preliminary experiment to this work, I observed different Hg concentrations in fallen White birch leaves that were different colors (Appendix B), although replicating this (Chapter 2) did not yield a statistically significant result. Fallen green, yellow, and brown leaves, representing a visual gradient of chlorophyll loss, were collected at the same time and the green leaves had higher Hg concentration than the yellow leaves. The brown leaves showed the greatest Hg concentration however this is likely due to preferential loss of other compounds in the leaf as it degrades further. Based on these data and the relationship between chlorophyll, light, and Hg, I hypothesized that with the onset of senescence Hg is volatilized from leaf tissues before litterfall occurs. To test this, I set up shade cloths at the end of August 2019 (approximately 50% and 100% reduction in PAR) at the upper tower level to see how Hg concentrations would change during senescence without direct exposure to light. However, the experiment was not successful, as I suspect the shading triggered senescence early and sped up the tissue degradation, and when I returned in mid-September most of the leaves had severely degraded in quality and abscised from the branch; of the remaining on-branch leaves I did not observe a trend in Hg concentration based on light exposure. A more controlled, high intensive sampling version of this experiment could better test this hypothesis. Shading of plants or trees in a laboratory-based setting would provide greater control on environmental conditions and sampling availability or a field-based experiment that sampled more frequently immediately after the shading was set up would also provide field-based conditions of light permeation.

One major challenge in studying Hg and decomposition in mesocosm incubation experiments is accounting for the artificial conditions. While it is true for all laboratory-based studies that draw conclusions about real world conditions, it is difficult to mimic field-like conditions that can play a major role in decomposition. For example, one of the first stages of decomposition is mechanical degradation largely facilitated by soil fauna and weathering, was not feasible to include in the mesocosm study. Similarly, the

flushing of DOM and associated Hg from litter and SOM would be largely controlled by precipitation events that vary in severity, duration, and frequency. While there was periodic removal of DOM (and associated Hg) from the porewater sampling in field conditions the DOM-Hg complexes would flow out of the system on a more regular basis influenced by precipitation and hydrology. A similar, field-based observational study using lysimeters to collect soil porewater in the autumn would provide field conditions and real time flushing of DOM for analysis.

Future research should also examine decomposition of forest litter and Hg on a longer time scale. While I observed an increase in Hg concentrations midway through the incubation from the deciduous leaves, I did not observe such an event for conifer needles. It remains unclear if this is because the Hg is released more slowly, consistently throughout decomposition or if a spike would have occurred after the three-month incubation period. An incubation of six or nine months would provide further insight into Hg release via leachate in both litter types and whether there is a peak in Hg release in coniferous litter or if it is a steadier release, and whether there are multiple peaks with deciduous litter. Additionally, incubation on different substrates would provide insight into DOM quality changes with Hg release. Using a substrate such as sterile sand or artificial soils under the litter would reduce any 'swamping' effects of the forest soil I likely observed in Chapter 3. Future research is also needed to understand Hg retention in forest soils with changing precipitation regimes. Additional research should also focus on identifying compounds Hg binds to in foliage to predict release and subsequent export or retention in soils and compare between deciduous and coniferous species.

Finally, it is unclear how representative white birch and black spruce (with jack pine in Chapter 3) are for their foliage type (deciduous and coniferous, respectively). While the use of only three species limits data extrapolation to the boreal forest as a whole or to other species, these are common species across the boreal forest and fall within the genera of cold-tolerant trees noted to characterize the boreal zone (Brandt *et al*., 2013). As noted in Chapter 3, there have been observations of Hg concentrations in all three species in other studies (white birch: Bushey *et al*., 2008, Juillerat *et al*., 2012, Blackwell and Driscoll 2015; black spruce and jack pine: Hall and St. Louis, 2004, Graydon *et al*.,

2006, Blackwell *et al*., 2014, Blackwell and Driscoll, 2015), which were similar both to the concentrations I observed but also to other deciduous and coniferous species sampled in the areas of those studies. Additionally, all three of these species are expected to have range shifts with climate change (McKenney *et al*., 2007, 2011).

4.5   Conclusions and significance

Overall, both the field-based study observing Hg accumulation (Chapter 2) and the laboratory incubation mesocosm experiment (Chapter 3) revealed foliage type — both fresh and as litter — to influence Hg cycling in forest ecosystems. Deciduous foliage moves Hg through the ecosystem more quickly by accumulating more atmospheric Hg over a single growing season, has a larger input of litter onto the forest floor annually, and then enters the soil pool more rapidly via decomposition. Conifer needles did not accumulate Hg at the same rate and over one growing season did not accumulate as much Hg as the leaves but experienced growth more consistently over their first growing season. White birch leaves had Hg uptake rates similar to those of PASs before senescence began and could be used on a broad scale for atmospheric Hg monitoring, but new conifer needles did not act as effective PASs. Further, the Hg that the conifer needles accumulate over one summer does not enter the soil pool that year but instead the needles, and associated Hg, fall on multi-year cycles. Once deposited to the ground, deciduous litter demonstrated a more rapid release of Hg via leachate than conifer needles in the incubation experiment.

Projected changes to climate will be gradual and communities, both above and below ground, will respond over time but the scales of these changes are unclear. While there remains a large knowledge gap around terrestrial Hg cycling, this research can contribute to better predictions of recovery times for contaminated lake fisheries and catchments. Understanding how Hg moves in forests and the influence of forest type will contribute to better understanding of the potential Hg that could be transported out of forest soils. The study site in Chapter 2, and the litter and soil collection site in Chapter 3, is directly upslope from several boreal peatlands that have demonstrated Hg methylation. The DOM bound Hg entering the soil pool in the forest has potential then to flow out from my study site to these sites of methylation. There are many factors that control the Hg outflow from

upland sites, the main one being hydrology that is largely catchment specific (Oswald *et al*., 2014).

Downstream from forests, particularly in aquatic environments and the noted peatlands, methylation can occur. Through this process methylmercury (MeHg) is produced, which is a potent neurotoxin that can bioaccumulate and biomagnify in the food chain and can pose severe health risks for both humans and wildlife (Mergler *et al*., 2007). There has been much research done further downstream from forests (as opposed to within forests) focusing on methylmercury concentrations in fish (Harris *et al.*, 2007), as this is a common exposure source for humans to high MeHg concentrations. Research has also examined Hg concentrations in terrestrial environments such as high elevation montane forests, and in a range of species including insects, salamanders, and birds (Cristol *et al*., 2008, Rimmer *et al*., 2010). Experimental data using enriched stable isotopes has demonstrated that methylation of Hg is proportional to Hg inputs into the system (Harris *et al*., 2007). So, understanding the controls on release of Hg from forest soils will contribute to better predictions on the recovery time of contaminated watersheds and how future Hg cycles will be impacted by climate change.

4.6   References

Amos, H.M., Jacob, D.J., Streets, D.G., Sunderland, E.M., 2013. Legacy impacts of all-time anthropogenic emissions on the global mercury cycle, Global Biogeochemical Cycles, 27, 410–421.

Assad, M., Parelle, J., Cazaux, D., Gimbert, F., Chalot, M., Tatin-Froux, F., 2016. Mercury uptake into poplar leaves. Chemosphere 146, 1–7.

Barquero, J.I., Rojas, S., Esbrí, J.M., Garcia-Noguero, E.M., Higueras, P. 2019. Factors influencing mercury uptake by leaves stone pine (*Pinus pinea* L.) in Almaden (central Spain). Environmental Science and Pollution Research 26, 3129–3137.

Bellamy, P.H., Loveland, P.J., Bradley, R.I., Lark, R.M., Kirk, G.J.D., 2005. Carbon losses from all soils across England and Wales 1978–2003. Nature 437, 245–248.

Blackwell, B.D., Driscoll, C.T., 2015. Deposition of mercury in forests along a montane elevation gradient. Environment Science & Technology 49, 5363–5370.

Blackwell, B.D., Driscoll, C.T., Maxwell, J.A., Holsen, T.M., 2014. Changing climate alters inputs and pathways of mercury deposition to forested ecosystems. Biogeochemistry 119, 215–228.

Brandt, J.P., 2009. The extent of the North American boreal zone. Environmental Reviews 17, 101–161.

Brandt, J.P., Flannigan, M.D., Maynard, D.G., Thompson, I.D., Volney, W.J.A., 2013. An introduction to Canada's boreal zone: ecosystem processes, health, sustainability, and environmental issues. Environmental Reviews 21, 207–226.

Buckley, T.N., 2017. Modelling stomatal conductance. Plant Physiology 174, 572–582.

Bushey, J.T., Nallana, A.G., Montesdeoca, M.R., Driscoll, C., 2008. Mercury dynamics of a northern hardwood canopy. Atmospheric Environment 42, 6905–6914.

Chen, H.Y.H., Brant, A.N., Seedre, M., Brassard, B.W., Taylor, A.R., 2017. The contribution of litterfall to net primary production during secondary succession in the boreal forest. Ecosystems 20, 830–844.

Collins, M., Knutti, R., Arblaster, J., Dufresne, J.L., Fichefet, T., Friedlingstein, P., Gao, X., Gutowski, W.J., Johns, T., Krinner, G., Shongwe, M., Tebaldi, C., Weaver, A.J., Wehner, M.F., Allen, M.R., Andrews, T., Beyerle, U., Bitz, C.M., Bony, S., Booth, B.B.B., 2013. Long-term Climate Change: Projections, Commitments and Irreversibility. In T.F. Stocker, D. Qin, G.K. Plattner, M.M.B. Tignor, S.K. Allen, J. Boschung, A. Nauels, Y. Xia, V. Bex, P.M. Midgley (Eds.), Climate Change 2013 - The Physical Science Basis: Contribution of Working Group I to the Fifth Assessment Report of the Intergovernmental Panel on Climate Change, 1029–1136. (Intergovernmental Panel on Climate Change). Cambridge University Press.

Cornwell, W.K., Cornelissen, J.H.C., Amatangelo, K., Dorrepaal, E., Eviner, V.T., Godoy, O., Hobbies, S.E., Hoorens, B., Kurokawa, H., Pérez-Harguindeguy, N., Quested, H.M., Santiago, L.S., Wardle, D.A., Wright, I.J., Aerts, R., Allison, S.D., Van Bodegom, P., Brovkin, V., Chatain, A., Callaghan, T.V., Díaz, S., Garnier, E., Gurvich, D.E., Kazakou, E., Klein, J.A., Read, J., Reich, P.B., Soudzilovskaia, N.A., Viaeretti, M.V., Westoby, M., 2008. Plant species traits are the predominant control on litter decomposition rates within biomes worldwide. Ecology Letters 11, 1065–1071.

Cristol, D.A., Brasso, R.L., Condon, A.M., Fovargue, R.E., Friedman, S.L., Hallinger, K.K., Monroe, A.P., White, A.E., 2008. The movement of aquatic mercury through terrestrial food webs. Science 320, 335.

Crowther T.W., Todd-Brown, K.E.O., Rowe, C.W., Wieder, W.R., Carey, J.C., Machmuller, M.B., Snoek, B.L., Fang S., Zhou, G., Allison, S.D., Blair, J.M., Bridgham, S.D., Burton, A.J., Carrillo, Y., Reich, P.B., Clark, J.S., Classen, A.T., Dijkstra, F.A., Elberling, B., Emmett, B.A., Estiarte, M., Frey, S.D., Guo, J., Harte, J., Jiang, L., Johnson, B.R., Kröel-Dulay, G., Larsen, K.S., Laudon, H., Lavallee, J.M., Luo, Y., Lupascu, M., Ma, L.N., Marhan, S., Michelsen, A., Mohan, J., Niu, S., Pendall, E., Peñuelas, J., Pfeifer-Meister, L., Poll, C., Reinsch. S., Reynolds, L.L., Schmidt, I.K., Sistla, S., Sokol, N.W., Templer, P.H., Treseder, K.K., Welker, J.M. Bradford, M.A., 2016. Quantifying global soil carbon losses in response to warming. Nature 540, 104–108.

Demers, J.D., Driscoll, C.T., Fahey, T.J., Yavitt, J.B., 2007. Mercury cycling in litter and soil in different forest types in the Adirondack region, New York, USA. Ecological Applications 17, 1341–1351.

Ericksen, J. A., Gustin, M.S., Schorran, D.E., Johnson, D.W., Lindberg, S.E., Coleman, J.S., 2003. Accumulation of atmospheric mercury in forest foliage. Atmospheric environment 37, 1613–1622.

Frescholtz, T.F., Gustin, M.S., Schorran, D.E., Fernandez, C.J., 2003. Assessing the source of mercury in foliar tissue of quaking aspen. Environmental Toxicology and Chemistry 22, 2114–2119.

Graydon, J.A., St. Louis, V.L., Lindberg, S.E., Hintelmann, H., Krabbenhoft, D.P., 2006. Investigation of mercury exchange between forest canopy vegetation and the atmosphere using a new dynamic chamber. Environment Science & Technology 40, 4680–4688.

Grigal, D.F., 2002. Inputs and outputs of mercury from terrestrial watersheds: A review. Environmental Reviews 10, 1–39.

Harris, R.C., Rudd, J.W.M., Amyot, M., Babiarz, C.L., Beaty, K.G., Blanchfield, P.J., Bodaly, R.A., Branfireun, B.A., Gilmour, C.C., Graydon, J.A., Heyes, A., Hintelmann, H., Hurley, J.P., Kelly, C.A., Krabbenhoft, D.P., Lindberg, S.E., Mason, R.P., Paterson, M.J, Podemski, C.L., Tate, M.T., 2007. Whole-ecosystem study shows rapid fish-mercury response to changes in mercury deposition. Proceedings of the National Academy of Sciences 104, 16586–16591.

Hall, B.D., St. Louis, V.L., 2004. Methylmercury and total mercury in plant litter decomposing in upland forests and flooded landscapes. Environment Science & Technology 38, 5010–5021.

Hetherington, A.M., Woodward, F.I., 2003. The role of stomata in sensing and driving environmental change. Nature 424, 901–908.

Hollósy, F., 2002. Effects of ultraviolet radiation on plant cells. Micron 33, 179–197.

Jiskra, M., Sonke, J.E., Obrist, D., Bieser, J., Ebinghaus, R., Lund Myhre, C., Pfaffhuber, K., Wängberg, I., Kyllönen, K., Worthy, D., Martin, L., Labuschagne, C., Mkololo, T., Ramonet, M., Magand, O., Dommergue, A., 2018. A vegetation control on seasonal variations in global atmospheric mercury concentrations. Nature Geoscience 11, 244–250.

Juillerat, J.I., Ross, D.S., Bank, M.S., 2012. Mercury in litterfall and upper soil horizons in forested ecosystems in Vermont, USA. Environmental Toxicology and Chemistry 31, 1720–1729.

Kang, H., Lui, X., Guo, J., Wang, B., Xu, G., Wu, G., Kang, S., Huang, J., 2019. Characterization of mercury concentration from soils to needle and tree rings of Schrenk spruce (*Picea schrenkiana*) of the middle Tianshan Mountains, northwest China. Ecological Indicators 104, 24–31.

Kikuzawa, K., Lechowicz, M.J., 2014. Ecology of Leaf Longevity, first ed. Springer Verlag, Tokyo.

Krabbenhoft, D.P., Sunderland, E.M., 2013. Global change and mercury. Science 341, 1457.

Lim, P.O., Kim, H.J., Nam, H.G., 2007. Leaf senescence. Annual Review of Plant Biology. 58, 115–136.

Ma, M., Du, H., Wang, D., Sun, T., Sun, S., Yang, G., 2017. The fate of mercury and its relationship with carbon, nitrogen and bacterial communities during litter decomposing in two subtropical forests. Applied Geosciences 86, 26–35.

McGuire, A.D., Wirth, C., Apps, M., Beringer, J., Clein, J., Epstein, H., Kicklighter, D.W., Bhatti, J., Chapin III, F.S., de Groot, B., Efremov, D., Eugster, W., Fukuda, M., Gower, T., Hinzman, L., Huntley, B., Jia, G.J., Kasischke, E., Melillo, J., Romanovsky, V., Shvidenko, A., Vaganov, E., Walker, D., 2002. Environmental variation, vegetation distribution, carbon dynamics and water/energy exchange at high latitudes. Journal of Vegetation Science 13, 301–314.

McKenney, D.W., Pedlar, J.H., Lawrence, K., Campbell, K., Hutchinson, M.F., 2007. Potential impacts of climate change on the distribution of North American trees. Bioscience 57, 939–948.

McKenney, D.W., Pedlar, J.H., Lawrence, K., Papadopol, P., Campbell, K., Hutchinson, M.F., 2014. Change and evolution in the plant hardiness zones of Canada. Bioscience 64, 341–350.

McKenney, D.W., Pedlar, J.H., Rood, R.B., Price, D., 2011. Revisiting projected climate shifts in the climate envelopes of North American trees using updated general circulation models. Global Change Biology 17, 2720–2730.

Mergler, D., Anderson, H.A., Chan, L.H.M., Mahaffey, K.R., Murray, M., Sakamoto, M., Stern, A.H., 2007. Methylmercury exposure and health effects in humans: a worldwide concern. Ambio 36, 3–11.

Natural Resources Canada. 2016. Distribution of Tree Species, Canada's Plant Hardiness. https://www.nrcan.gc.ca/climate-change/impacts-adaptations/climate-change-impacts-forests/forest-change-indicators/distribution-tree-species/17778

Obrist, D., Johnson, D.W., Edmonds, R.L., 2012. Effects of Vegetation type on mercury concentrations and pools in two adjacent coniferous deciduous forests. Journal of Plant Nutrition and Soil Science 175, 68–77.

Oswald, C., Heyes, A., Branfireun, B.A., 2014. Fate and transport of ambient mercury and applied mercury isotope in terrestrial upland soils: insights from the METAALICUS watershed. Environment Science & Technology 48, 1023–1031.

Parmesan, C., Yohe, G., 2003. A globally coherent fingerprint of climate change impacts across natural systems. Nature 421, 37–42.

Price, D.T., Alfaro, R.I., Brown, K.J., Flannigan, M.D., Fleming, R.A., Hogg, E.H., Girardin, M.P., Lakusta, T., Johnston, M., McKenney, D.W., Pedlar, J.H., Stratton, T., Sturrock, R.N., Thompson, I.D., Trofymow, J.A., Venier., L.A., 2013. Anticipating the consequences of climate change for Canada's boreal forest ecosystems. Environmental Reviews 21, 322–65.

Ravichandran, M., 2004. Interactions between mercury and dissolved organic matter – a review. Chemosphere 55, 319–331.

Rea, A.W., Lindberg, S.E., Scherbatskoy, T., Keeler, G.J., 2002. Mercury accumulation in foliage over time in two northern mixed-hardwood forests. Water, Air, and Soil Pollution 133, 49–67.

Reich, P.B., Koike, T., Gower, S.T., Schoettle, S.W., 1995. Causes and consequences of variation in conifer leaf life span. In: Ecophysiology of Coniferous Forests, 225–254.

Reich, P.B., Rich, R.L., Luc, X., Wang, Y., Oleksyn, J., 2014. Biogeographic variation in evergreen conifer needle longevity and impacts on boreal forest carbon cycle projections. Proceedings of the National Academy of Sciences, 111, 13703–13708.

Richardson, J.B., Friedland, A.J., 2015. Mercury in coniferous and deciduous upland forests in northern New England, USA: implications of climate change. Biogeosciences 12, 6737–6749.

Rimmer, C.C., Miller, E.K., MacFarland, K.P., Taylor, R.J., Faccio, S.D., 2010. Mercury bioaccumulation and trophic transfer in the terrestrial food web of a montane forest. Ecotoxicology 19, 697–709.

Risch, M.R., DeWild, J.F., Gay, D.A., Zhang, L., Boyer, E.W., Krabbenhoft, D.P., 2017. Atmospheric mercury deposition to forests in the eastern USA. Environmental Pollution 228, 8–18.

Saetre, P., Bååth, E., 2000. Spatial variation and patterns of soil microbial community structure in a mixed spruce–birch stand. Soil Biology and Biochemistry 32, 909–917.

Schroeder, W.H., Munthe, J., 1998. Atmospheric mercury – an overview. Atmospheric Environment 32, 809–822.

Siwik, E.I.H., Campbell, L.M., Mierle, G., 2009. Fine-scale mercury trends in temperate deciduous tree leaves from Ontario, Canada. Science of the Total Environment 407, 6275–6279.

Stamenkovic, J., Gustin, M.S., 2009. Nonstomatal uptake versus stomatal uptake of atmospheric mercury. Environment Science & Technology 43, 1367–1372.

Streets., D.G., Zhang, Q., Wu, Y., 2009. Projections of global mercury emissions in 2050. Environment Science & Technology 43, 2983−2988.

Trenberth, K.E., Dai, A., Rasmussen, R.M., Parsons, D.B., 2003. The changing character of precipitation. Bulletin of the American Meteorological Society 84, 1205–1217.

Tuomi, M., Thum, T., Järvinen, H., Fronzek, S., Berg, B., Harmon, M., Trofymow, J.A., Sevanto, S., Liski, J., 2009. Leaf litter decomposition—estimates of global variability based on Yasso07 model. Ecological Modelling 220, 3362–3371.

Urban, J., Ingwers, M.W., McGuire, M.A., Teskey, R.O., 2017. Stomatal conductance increases with rising temperature. Plant Signaling & Behaviour 12, e1356534.

Wardle, D.A., Bardgett R.D., Klironomos J.N., Setälä H., van der Putten W.H., Wall D.H., 2004. Ecological linkages between aboveground and belowground biota. Science 304, 1629–1633.

Yuan, W., Sommar, J., Lin, C., Wang, X., Li, K., Liu, Y., Zhang, H., Lu, Z., Wu, C., Feng, X., 2019. Stable isotope evidence shows re-emission of elemental mercury vapor occurring after reductive loss from foliage. Environment Science & Technology 53, 651−660.

Appendices

Appendix A: Repeated measures multivariate analysis of variance results and multivariate analysis of variance results for changes in (final – initial) %C, %N, and C:N ratios of coniferous (black spruce and jack pine) and deciduous (white birch) litter measured before and after three-month incubation at two temperature treatments (12 °C and 16 °C).

		Litter		Temperature		Litter × Temperature	
		F	P	F	P	F	P
%C	Initial	44.0	**0.000**	0.71	0.409	1.88	0.185
	Final	15.4	**0.000**	1.53	0.230	0.04	0.840
%C	Change	0.230	0.637	8.08	**0.010**	2.56	0.125
%N	Initial	75.6	**0.000**	1.80	0.197	3.16	0.091
	Final	109	**0.000**	5.40	0.106	16.8	**0.001**
%N	Change	18.9	**0.000**	7.06	**0.015**	8.23	**0.010**
C:N	Initial	106	**0.000**	5.82	**0.026**	7.15	**0.015**
	Final	146	**0.000**	0.436	0.516	17.7	**0.000**
C:N	Change	2.21	0.153	2.625	0.121	0.06	0.809

Appendix B: Mercury (ng g^{-1}) concentrations of senesced white birch litter collected October 2018. Visually sorted into color groups green, yellow, and brown. Leaves were oven dried at 60 °C for 48 hours before homogenization and analysis following US EPA 7473. Letters denote significant differences based on one-way ANOVA and Tukey post-hoc comparisons using leaf color as main effect (F$_{2,8}$=33.4, P<0.001)

	Green	Yellow	Brown
Hg ng g^{1}	27.52	19.37	45.53
	28.07	19.49	59.22
	26.43	17.25	44.58
Average	**27.34^{b}**	**18.7^{b}**	**49.78^{a}**

Curriculum Vitae

Name: Madelaine Anderson

Post-secondary Education and Degrees:
University of British Columbia
Vancouver, British Columbia, Canada
2013-2017 BSc. Hons.

University of Western Ontario
London, Ontario, Canada
2018—present MSc. Environment & Sustainability

Honors and Awards:
Biology Graduate Travel Award
University of Western Ontario
2019, 2020

Environment and Sustainability Collaborative
Program Graduate Travel Award
University of Western Ontario
2019

Go Global International Learning Programs Award
University of British Columbia
2016

Indigenous Entrance Scholarship
University of British Columbia
2013

Related Work Experience
Teaching Assistant Environmental Biology (Biology 2485)
University of Western Ontario
2019, 2020

Teaching Assistant Ecology (Biology 2483)
University of Western Ontario
2018, 2019

Conferences:

Anderson, M.J.R., Lindo, Z., Branfireun, B.A. 2019. Mercury's Journey from Litter to Soils in the Boreal Forest. Canadian Society of Ecology and Evolution. Fredericton, NB. [Standard Talk].